Fresh water and sediment dynamics in the catchment of Lac at Bonaire.

MSc Thesis - Hydrology and Quantitative Water Management

Lotte Hobbelt

Fresh water and sediment dynamics in the catchment of Lac at Bonaire.

MSc Thesis - Hydrology and Quantitative Water Management

Lotte Hobbelt
Reg.nr.: 890103341010
Maart 2014

Supervisors:

Roel Dijksma	(Hydrology and Quantitative Water Management Group, Wageningen University)
dr. Saskia Keesstra	(Soil Physics and Land Management Group, Wageningen University)
Sabine Engel	(STINAPA, Bonaire)

Abstract

Deterioration of mangrove forests is occurring globally. The loss of mangrove habitats causes a decline in fishery resources, livelihood and biodiversity loss. Deterioration is also been seen in the mangrove forest of Lac Bay on Bonaire. Especially at the landside of the mangroves hyper saline conditions are found and *Rhizophora* mangles as well as *Avicennia germinans* trees are dying. The deterioration of the mangroves at the landside is partly compensated by expansion of the mangroves at the sea side. The main causes for the seaward shift seem to be, 1) less fresh water inflow during rainy season, 2) increased sediment transport towards Lac, 3) reduced interaction (tidal flow) between sea side and land side. This project has focussed on the dynamics of the fresh water fluxes toward the mangroves and the associated sediment transport. During two major rain events water discharge and sediment transport was measured for two catchments. Based on these measurements the total runoff amount and amount of sediments transported during the rainy season was determined. It can be concluded that runoff have brought only relatively minor quantities of fresh water to Lac. However, extreme events or extreme annual rainfall sums (1980, 1981, 1985, 1988, 2004, 2005) might have caused extreme runoff amounts and in addition extreme sediment load transports toward the mangrove system. Along with the deterioration of the channels and the associated water circulation, this might have caused root smothering and mangrove die off. This mangrove die off is probably strengthened by a relatively dry period with relatively less freshwater transport by surface runoff toward the mangrove system which enhances the hyper saline waters in the back of the system. Although deterioration of the landscape occurs since the 17th century, due to cutting down forests and overgrazing by goats and sheep's, heavy rainfall events will not only lead to an increase in water supply but also to more extreme sediment transport rates toward the mangrove system. In addition, also removal of dams would cause an increase in surface runoff towards the mangrove system and an increase in sediment transport. Monitoring rainfall, surface runoff, and sediment transport over a large number of years together with monitoring the growth and the health of the mangrove forest would give more insight in how the mangrove systems reacts on hydrological changes over a number of years.

Preface

The presented report is a Master's thesis within the discipline of hydrology and quantitative water management written at Wageningen University in The Netherlands under the supervision of Roel Dijksma, Saskia Keesstra and Sabine Engel. Field work has been conducted in Bonaire (Netherlands Antilles) from 1st October 2012 until 19th January 2013 in co-operation with Stichting Nationale Parken Bonaire (STINAPA).

I would like to thank STINAPA for providing housing and transportation, Ramon de Leon and Sabine Engel for taking such good care of us, and Iris, Tatiana, Vinni and Geert who gave me a wonderful time on Bonaire. I would especially like to thank my supervisor Roel Dijksma. He did not only guide me through the research, but also provided a sympathetic ear for my own personal difficulties. The wonderful time on Bonaire, was followed by a very difficult period. Due to this period I will always have some mixed feelings about Bonaire, despite the beauty of the island.

Table of contents.

1 Introduction

1.1 Problem description

Deterioration of mangrove forests is occurring globally (Valiela *et al.*, 2001; Saenger *et al.,* 1983; Spalding *et al.,* 1997*),* with a loss of at least 35% in the past two decades (Valiela *et al.*, 2001). Mangrove forests have a high importance for the sustainability of coastal zones (Valiela *el al.*, 2001), protection of shorelines against extreme weather events (Teas, 1977; Ewel *et al.,* 1998) and interception of land derived nutrients, pollutions and suspended sediments before they reach the deeper water (Marshall, 1994; Rivera-Monroy and Twilley, 1996; Tam and Wong, 1999). Thereby it has essential ecological functions, like nurseries for coastal fish and shellfish, habitats for a diversity of species, but also a recreational function. Significant reduction and deterioration of these mangrove forests will therefore have consequences and means a loss of important contributions to subsistence uses and ecological, economic, and conservation functions. (Valiela *et al*., 2001)

This research focuses on the catchment of the mangrove forest of Lac Bay on Bonaire. The bay is the main mangrove area for Bonaire and provides several key ecological functions. Besides the function of protecting the reefs of the east coast by entrapping nutrients and sediments, it also has an important nursery function for many important reef species, it serves as roosting area for birds and it is a foraging area for i.a. turtles on the sea grass beds (Augustinus, 2005; Debrot *et al.*, 2010). Based on its nature values the Lac has been designated as a legally protected Ramsar site (STINAPA Bonaire, 2003) and identified as a IUCN IBA (Important Bird Area) (Wells and Debrot, 2008). Nagelkerken *et al.* (2000) has studied the coherence between mangroves, sea grass beds and coral reef in the Lac Bay. Mangrove roots and sea grass are important nursery systems for juvenile coral reef fish. Nagelkerken *et al.* (2000) showed that if nursery systems do not work properly, the amount of adult fishes on the reefs will decrease. In accordance, Mumby *et al.* (2004) showed that mangroves are unexpectedly important, serving as an intermediate nursery habitat that may increase the chance of survival of young fish.

However, deterioration of the mangrove forest in Lac Bay occurs. Already in 1969 Wagenaar Hummelink and Roos reported that changes in and mortification of the mangroves system had taken place over the last hundreds of years. Especially at the landside of the mangroves *Rhizophora mangle* as well as *Avicennia germinans* trees are dying. The deterioration of the landside is partly compensated by expansion of the mangroves at the sea side (Wagenaar Hummelink and Roos, 1969). The expansion takes place on former halimedabanks (shallow bank at the edge of the basin) where Rhizophora seedlings develop into new mangrove forest (Van

Moorsel and Meijer, 1993). Over the last decade's 60 ha (40%) of the mangrove system of Lac have died. On the seaside approximately 60 ha of new mangrove forest developed. This implies that the total area of the mangrove is constant. Lott (2001) considered that from a conservation perspective it is important to 'become aware, that dynamics, or changes in an ecosystem, are parts of the normal functioning of the system'. However, as Debrot *et al.* (2010) mentioned: 'The main problem is that in the case of Lac, free expansion of mangroves seaward has essentially reduced the effective surface area of the lagoon by 82 ha during a 35 year period (average: 2.34 ha per year)'. Thereby, the fast seaward shift has not only consequences on the biodiversity of the trees but also on the diversity of animal and fish species.

The mangrove system of Lac is different to mangrove systems on other islands or in other countries, since there is hardly any fresh water supply by rivers. Fresh water supply is important for the development and vitality of the mangroves (Augustinus, 2005). Mixing freshwater with denser saline coastal waters creates pressure gradients, which drive gravitational circulations, and enhance the flushing of a system (Kjerfve, 1990). Refreshment of the landside waters in Lac is dependent on fresh water fluxes caused by rainfalls and sea water circulation. However, fresh water fluxes only occur when rainfall exceeds evapotranspiration. This only occurs a few months a year during the rainy season (November until January). At present day, dams and roads block the fresh water inflow to the mangroves (Wagenaar Hummelinck and Roos, 1969; Debrot *et al*, 2012). The sea water circulation is both driven by feeder channels and sheet flow through the forest, but the feeder channels are most important in draining water and removing of salt from the landside waters of the mangrove (Van Loon, 2005). However, these channels are filled up by fresh sediments and overgrown with mangrove trees (*Rhizophore mangle*). The filling up of the channels and creeks seems to be caused by an increase in sediment transport towards Lac. The highly accelerated rate of filling in may be caused by excessive grazing and poor land-use practices (Debrot *et al.*, 2010). This increase in sediment towards Lac might also have negative influence to sea grass beds and mangrove trees. Sea grasses may survive temporary inundations of sediment for several months, but not for long periods. In South Australia (Neverauskas, 1988) and Queensland (Kirkman, 1978) smothering of sea grass by large amounts of sediment was observed. In addition, Ellison (1998) mentioned that excess input of sediments can cause dead of mangrove trees due to root smothering. Wagenaar Hummelink and Roos (1969) pinpointed also the filling in of sediments from the hinterlands as an important cause for mortalities of the mangroves and triggers the migration of the mangroves seaward.

Summarized, the main causes for the seaward shift seem to be:

1) Less fresh water inflow during rainy season.

2) Increased sediment transport towards Lac.
3) Reduced interaction (tidal flow) between sea side and land side.

This research, as part of a larger project, will focus on the dynamics of the fresh water fluxes toward the mangroves and the associated sediment transport.

Already a lot of research has been conducted in the mangroves of Lac. The first large research in Lac was done by Wagenaar Hummelinck and Roos in 1969, predominantly focusing on Lac maintenance. Environmental and ecological changes in Lac are well described by i.a. Lott (2001) and Moorsel and Meijer (1993). Although a hydrological investigation is done of Bonaire's water system in 2005, quantitative data of the Lac catchment, in terms of precipitation distribution, fresh water fluxes and sediment fluxes into Lac, is hardly available. In addition, insight in constructions that influence water flow, such as dams and wells, is not available yet. Also the spatial sensitivity on erosion is not known. To come up with a solution for the mangroves mortality and mangrove seaward shift quantitative and qualitative data of precipitation, fresh water fluxes and sediment fluxes are required.

1.2 Objectives

Research question:

What are the dynamics of the fresh water fluxes towards the Lac mangrove system in the Lac catchment and the associated sediment transport?

Purpose:

Define the catchment area and get more insight in the dynamics of fresh water fluxes and sediment fluxes towards the mangrove forest. Using the results, an attempt is made to formulate suggestions for adjustments to improve the mangrove ecosystem.

Sub questions:

Precipitation and evapotranspiration

- What is the rainfall intensity in the Lac catchment?
- What is the spatial distribution of precipitation in the Lac catchment?
- What is the temporal distribution of the precipitation in the Lac catchment?

- ***Precipitation and evapotranspiration***
- What is the amount of fresh water that reaches the mangrove system? (per event and during the rainy season (November-January) of 2012/2013)

- What is the temporal runoff pattern in the Lac catchment?

Sediment transport

- What is the total sediment load transported to the mangrove system? (per event and during the rainy season (November-January) of 2012/2013)
- What is the temporal sediment transport pattern in the Lac catchment?
- What are the sediment transport rates at the outlet of the catchment?
- What are the sediment sources in the catchment and what is the main sediment source (road material, catchment sediments) transported to the mangroves?

Wells and dams

- Where are the wells and dams located in the catchment?
- How much water can be stored behind the dams?
- What is the temporal variation in storage behind the dams?

Mitigation strategies

- How can we increase the fresh water flux into the mangroves?
- What is the influence of the dams and roads on the fresh water flux into the mangroves?
- How can we decrease the sediment load into the mangroves?

1.3 Outline

The first part of this thesis is a short description of the research area. The thesis proceeds with a description of methods. Subsequently, presented results are analysed and the defined research questions are answered. Then a discussion is given summarizing drawn conclusions in a synthesis. The thesis ends with the most important conclusions drawn from the study, followed by recommendations for further research in the Lac region.

2 Study area

Bonaire is located in the southern Caribbean (12°10'N, 68°15'W) approximately 100 km north of Venezuela (figure 1). Bonaire is a crescent shaped island, oriented NW-SE, circa 40 km long and 8-15 km wide, with a land area of 288 km^2. Bonaire is a special municipality within the Netherlands since October 2010, with approximately 13.000 permanent inhabitants.

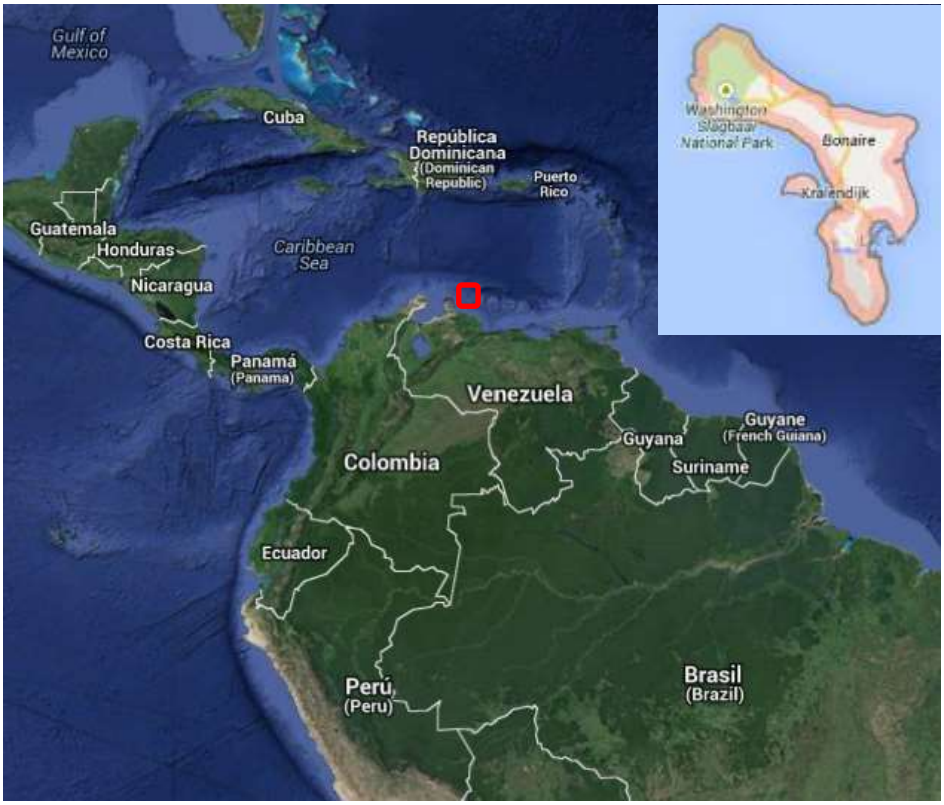

Figure 1 *Location of Bonaire. Upper right corner: Map of Bonaire (after Google Maps 2013).*

The southern part (south of the capital Kralendijk) is rather flat with maximum elevations of 25m above sea level. In contrast with the southern part the northern part is more hilly with elevations up to 241m above sea level (Mt. Brandaris)(figure 2).

The geology of Bonaire is complex (figure 3), with the core of the island consisting of strongly folded and faulted rocks of volcanic Cretaceous origin (145-65 Ma before present). Tectonic movements during and after this period shaped the region, which highly folded the strata. The basement of Bonaire, the so called Washikemba formation, emerged during this period. This formation mainly consist of volcanites as basalt, porphyrite, andesite and dacite flows and intrusions (Borst and de Haas, 2005).

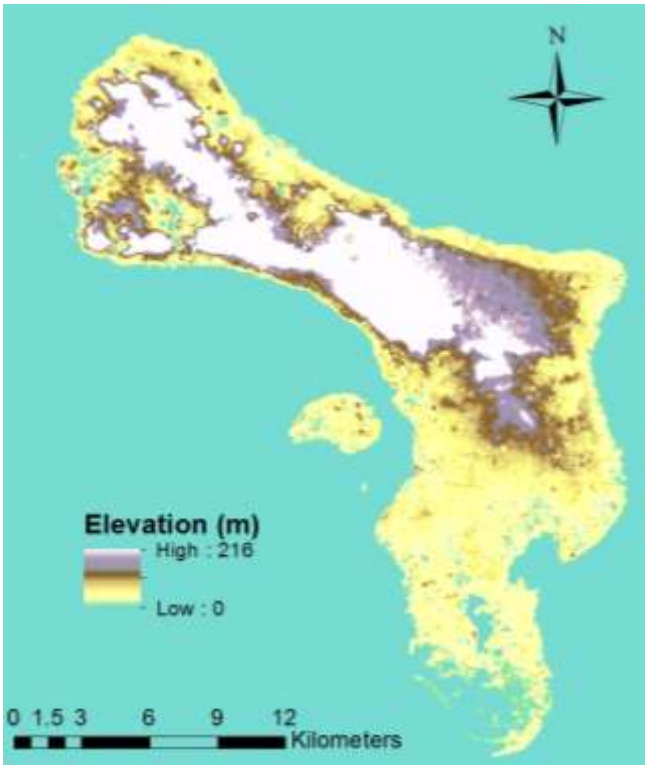

Figure 2 *Elevation map of Bonaire.*

Around 70-60 Ma before present, the volcanic arc of which the ABC-islands (Aruba, Bonaire and Curaçao) are part of, collided with the northern margin of the South-American continent. This collision caused uplift and folding, faulting and metamorphism of the rocks. The exhuming rocks may have been deposited as pebbles in the Rincon Formation that overlies the Washikemba Formation (van der Lelij *et al*., 2010). This Rincon Formation consist of limestone's, calcareous sandstones and marls (Borst and de Haas, 2005). Deposition of conglomerates and limestone took place during Eocene (58-35Ma before present), followed by limestone deposition in Neogene (24-1.8Ma before present) and Quaternary (1.8Ma before present - present) (van der Lelij *et al.,* 2010; Pijpers, 1933). The Soebi Blanco Formation is a 400m thick formation consisting fluvial sandstones and conglomerates which is probably older than the Rincon Formation and younger than Eocene (Borst and the Haas, 2005). During Quaternary the islands were subjected to discontinuous vertical uplift, which caused erosion and denudation. Due to glacial and interglacial periods sea levels dropped and rose respectively. The combination of change in sea level and slow vertical uplift caused the forming and accumulation of limestone terraces out of coral reefs (Alexander, 1961). During the periods with low sea levels terraces were formed and in periods of relative sea level rise the terraces emerged. Although sea level rose again, the terrace remained above sea level due to tectonic uplift. The terraces which are cut into the limestone can be divided in upper, middle and lower terraces, of which the upper is the oldest.

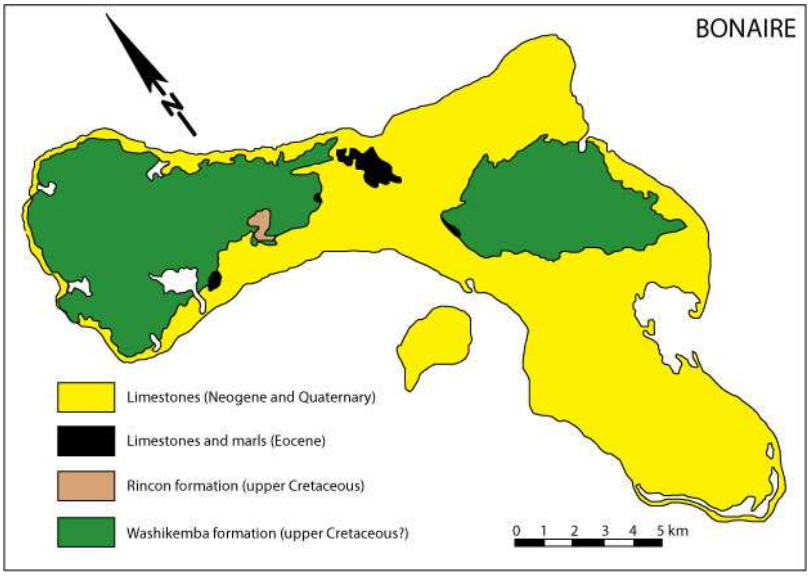

Figure 3 *Geological map of Bonaire*

Bonaire is dry with an average annual rainfall of 470 mm falling mostly in the period October until January and can be characterized by a semi-arid climate according to the Köppen classification. In 2005, Borst and De Haas set up a water balance for the whole island. On average 5% (6.5 million m^3/year) of the annual precipitation of 470 (135 million m^3/year) mm recharges the groundwater and 10% (13 million m^3/year) runs off to the sea, with an annual potential evapotranspiration of 2600 mm and an actual evapotranspiration of 400 mm (115 million ^{3}/year). Due to the dry conditions, the vegetation is mainly xeromorphic with many areas dominated by columnar cactus intermixed with low scrubs and large expanses of land with bare soil. Virtually all trees on the island were removed in the early nineteenth century and woody vegetation continued to be cut for charcoal production into the twentieth century. Grazing animals were introduced by 1700 and have significantly altered the vegetation. Free roaming goats and donkeys have continued to have an impact in many areas even to the present day. (Wells and Debrot, 2008)

Lac Bay is located on the southeast coast of Bonaire and is the greatest lagoon in the Netherlands Antilles. The soil texture found in the bay ranges from loam to clay (Van Kekem *et al*., 2006). The lagoon is surrounded by mangrove forest which is dominated by two mangrove species, the *Avicennia germinans* and *Rhizophora mangle.* Dead mangrove trees can be found especially at the landside of the mangrove forest. In this area, Awa Lodo di San José and Awa Lodo di Chicho (figure 5 and 6) changed to large shallow hyper saline waters. The deterioration of the landside is partly compensated by expansion of the mangroves at the sea side. The strongest expansion is seen between Boca Chikitu and Boca Fogon and between Boca di Coco and Puitu (figure 5 and 6) (Wagenaar Hummelink and Roos, 1969). The expansion takes place on former halimedabanks

(shallow bank at the edge of the basin) where Rhizophora seedlings develop into new mangrove forest (Van Moorsel and Meijer, 1993). The Lac area, including the mangrove area, has a length of approximately 3.9 km north-south and 3.0 km east-west, with an overall standing water surface area of approximately 7.5 km (van Moorsel en Meijer 1993). The watersheds of Lac Bay are shown in figure 4. The vegetation in these watersheds mainly consist of a mixture of cactus plants, low scrubs and bare soils.

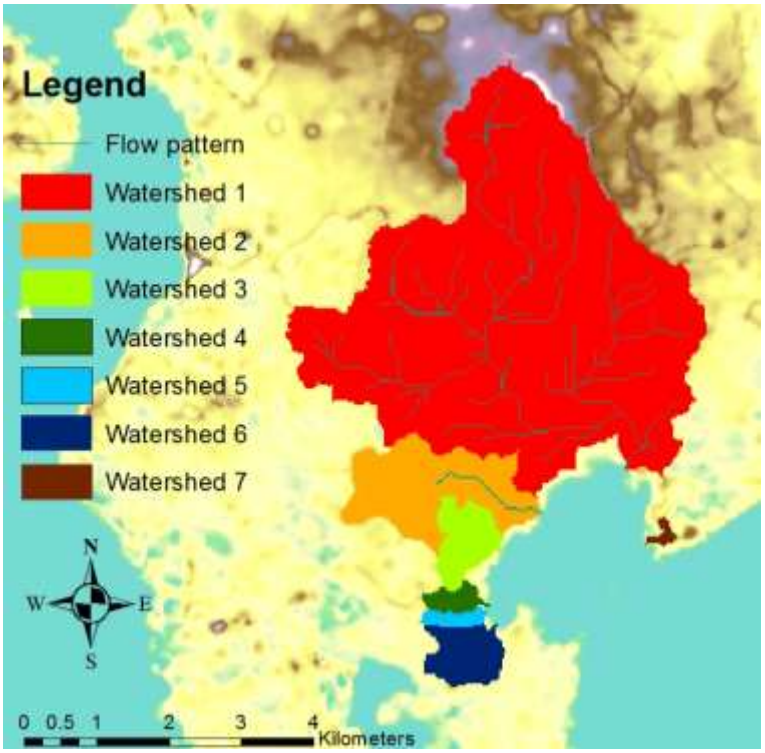

Figure 4 *Watersheds of Lac Bay*

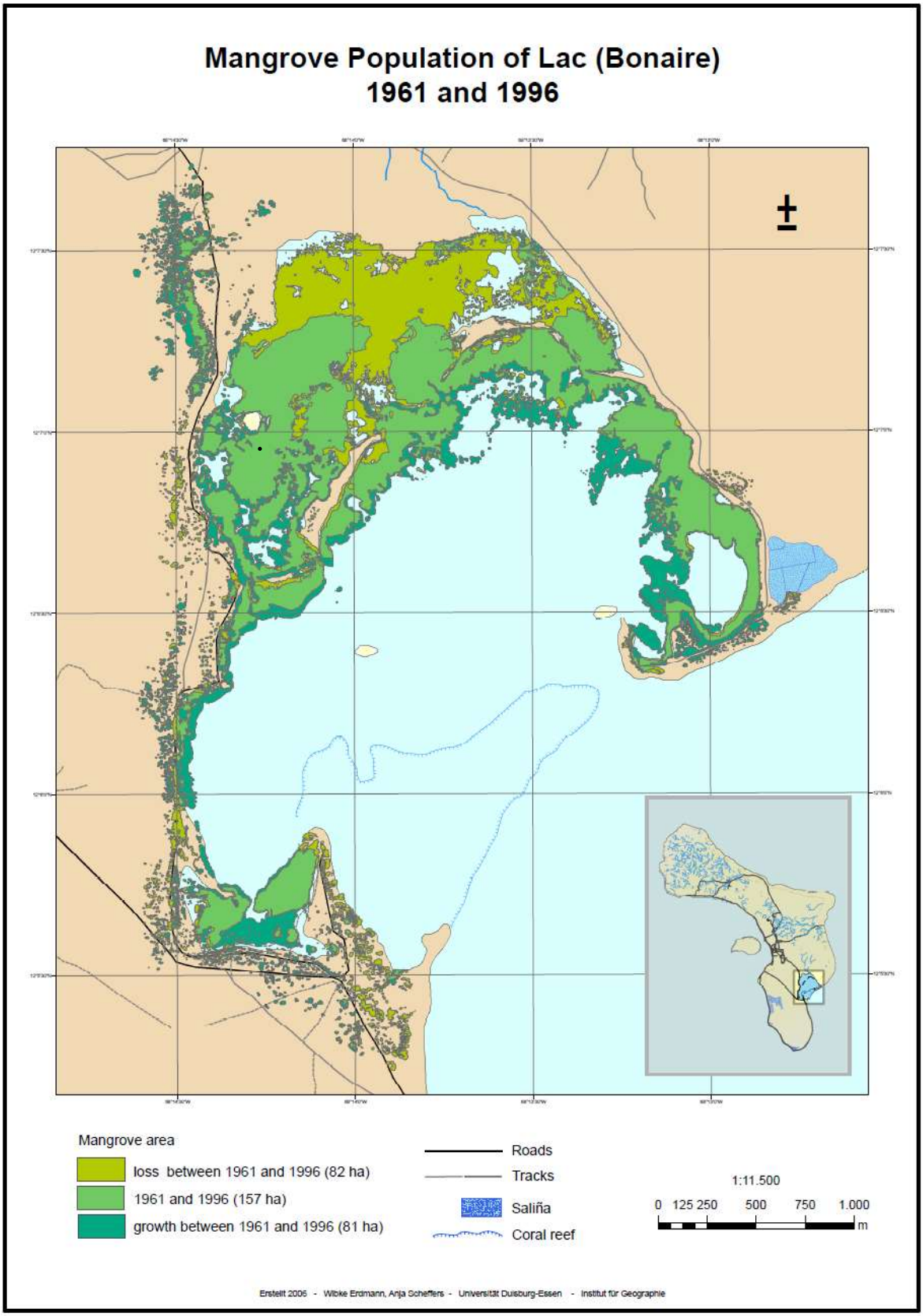

Figure 5 *The loss of mangroves in Lac has been balanced by new growth during a 35 year period (Erdmann and Scheffers, 2006).*

Figure 6 *Overview map of Lac Bonaire, with naming for the different areas.*

3 Methods

3.1 Rainfall

Rainfall is measured using a tipping bucket rain gauge (from October 17, 2012, 6.00 PM until January 29, 2013, 12.00 PM) and eight handmade rain gauges (from October 10, 2012 until January 18, 2013) (until October 30 nine handmade rain gauges). Both, the tipping bucket and rain gauges, were placed on those locations were high obstacles like cacti, bushes, trees and buildings could have hardly any influence on the measurement. The distance to an obstacle was at least 4 times the height of the obstacle.

Figure 7 shows a tipping bucket rain gauge together with a schematic representation. The tipping bucket used in this research had a resolution of 0.2 mm with an accuracy of 1% and a temporal resolution of 5 minutes. This means that the bucket tips after 0.2 mm of rainwater is collected in the bucket and that the amount of tips is registered every 5 minutes.

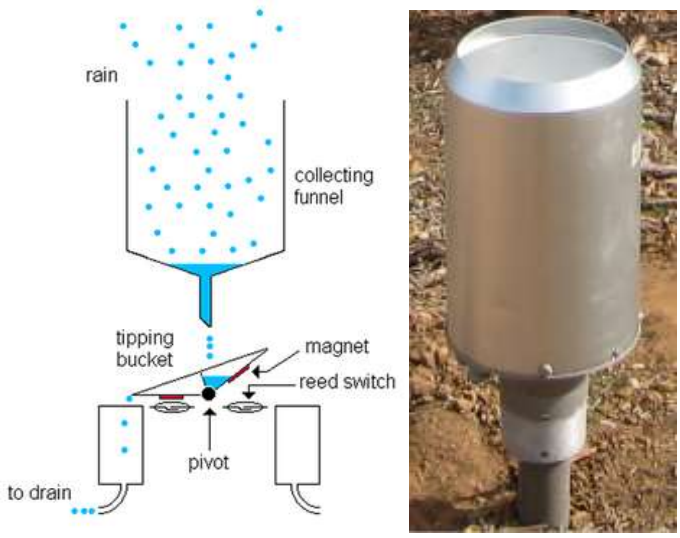

Figure 7 *Tipping bucket rain gauge. Schematic representation on the left side.*

The handmade rain gauge is made of a funnel connected with a 4 L container using a hose (figure 8). In order to minimize the water splashing effect, the funnel was placed minimal 40 cm above the soil surface. Also the vertical upper edge of the funnel minimizes a measurement error as a consequence of water splashing. In order to avoid significant evaporation a white container was used, which was buried half into the ground. The latest also ensures a more stable structure during strong winds. Besides that a table tennis ball was put in each funnel, which allowed the water to flow into the container but prevented evaporation. To ensure that the water only enters the container through the funnel a plastic bag was attached at the flask-hose assembly.

Figure 8 *Handmade rain gauge.*

The rainfall collected by the handmade rain gauge was measured by weighing, using a scale with an accuracy of 1 g. The water weight was determined as follows:

$$Waterweight[g] = weight\ (container + water)[g] - \ weight\ (container)[g]$$

The following formula is used to determine the rainfall sum over a certain period for a certain handmade rain gauge:

$$Rainfall\ Sum[mm] = \frac{water\ weight\ [g]*1000}{funnel\ area\ [mm^2]} \qquad (1)$$

In order to get insight in the spatial distribution of rainfall the rainfall sums are interpolated. In this research it is assumed that points closer to each other are more alike than points farther apart. The inverse distance weighting method is therefore used to interpolated the rainfall sums, which assumes that each measured point has a local influence that diminishes with distance (ArcGIS 9.2 Desktop Help, 2007).

The following formula is used to interpolate over a certain area.

$$P_i = \ \sum_{n=1}^{N}(w(\frac{1}{d_n})^2 * P_n) \qquad (2)$$

With:

P_i : Predicted value in point with no observation

P_n : Observation value

d_n : Distance between observation point and the point to be predicted

W : Factor

N : Number of observations

This inverse distance weighting interpolation technique is also used to determine the total rainfall amount fallen the catchment areas over a certain period. Since not all rain gauges are emptied at the same time, the time period over which the rainfall sum is measured differs. To determine the rainfall sum for a certain day on the location of the tipping bucket, the time period of the closest rain gauge is used.

3.2 Runoff

In order to determine the amount of fresh water flowing into the mangrove system divers were installed. These divers measure the pressure which can be converted to groundwater level. The water levels are used to calculate the discharge towards the mangrove system. The divers had a temporal resolution of 5 minutes.

The divers are placed in pvc pipes (piezometers) which were inserted into the ground (figure 9). In the lower part of the pipes small holes were made, allowing water to flow into the pipe when the water levels in the gullies rose. This lower part was wrapped with stockings which protected the diver for clogging by sediment. The diver was fixed with fishing line to the top of the piezometer.

To determine the water column above the diver the following formula is used:

$$Water\ column\ [cm] = P_{diver} - P_{baro} \qquad (3)$$

With:

P_{diver} : Measured pressure diver [cmH_2O]

P_{baro} : Measured pressure baro diver[cmH_2O]

To get the water column above the soil surface the distance between soil surface and measuring point is subtracted from the water column (see figure 10). The distance between soil surface and measuring point is added to the water column, when the diver hangs above the soil surface.

Calibration of the water levels was not possible, since no manual and automatically measurements were done at the same time.

Figure 9 *Piezometer*

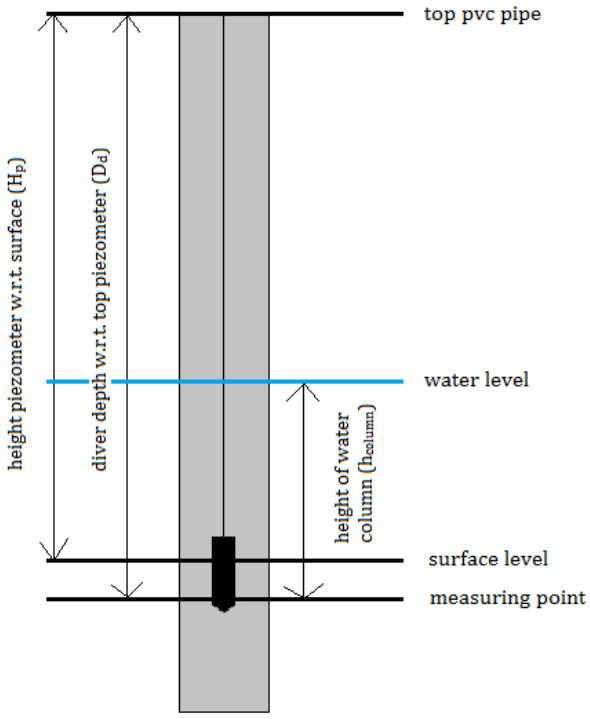

Figure 10 *Visualization piezometer with installed diver.*

To determine the discharge for each individual runoff event, a Q-h relationship (discharge-water level relation) is needed. During and after two rainfall events the water levels and the stream velocities in the gullies were measured manually with intervals between 5 and 20 minutes. In order to calculate the discharge the cross sectional area and therefore the gully profile is needed (formula 4). This profile is determined in the field. The following formula can be used to determine the discharge.

$$Q = v * A \quad (4)$$

With:

Q : discharge [m^3/s]

v : velocity [m/s]

A : area [m^2]

A Q-h relationship can be determined by plotting discharge against the water level.

3.3 Evapotranspiration

The reference evapotranspiration is estimated from meteorological data using the FAO Penman-Monteith method (Allen *et al.*, 1998). More details about the method can be found in Appendix I and in Rønde (2013).

To determine the potential evapotranspiration the following formula is used (Allen *et al.*, 1998):

$$ET_p = ET_0 * K_c * F_{veg} \quad (5)$$

With:

ET_p : potential evapotranspiration (mm/day)

ET_0 : reference evapotranspiration (mm/day)

K_c : crop factor (-)

F_{veg} : vegetation fraction (-)

A crop factor of 0.47 was used based on Consoli *et al.* (2010) who determined a crop factor for cactus pear.

To determine the evaporation for open water bodies the following formula is used:

$$ET = ET_0 * C_w \quad (6)$$

With:

ET_0 : potential evapotranspiration (mm/day)

C_w : evaporation coefficient of an open water body

A C_w value of 1.05 can be taken for water bodies less than 2 m (Allen *et al.,* 1998), which applies to the water bodies in the research area.

3.4 Water balance

In order to develop a water balance actual evapotranspiration is needed. Since both storage and actual evapotranspiration is unknown a simple linear reservoir model has been constructed. In this model it is assumed that storage in the root zone depends on the storage in the previous time step, precipitation, actual evapotranspiration (which depends on relative storage and potential evapotranspiration) and discharge:

$$W_i = W_{i-1} + P_i - \left(\frac{W_{i-1}}{W_x}\right) ET_{p,i} - Q_i \quad (7)$$

With:

W_i : storage (mm) at time i

W_{i-1} : storage (mm) at time i-1

W_x : maximum storage capacity

P_i : precipitation (mm) at time i

$ET_{p,i}$: potential evapotranspiration (mm) at time i

Q_i : runoff (mm) at time i

The maximum storage capacity is assumed to be 100 mm since a moderately coarse soil is assumed (Doneen and Westcot, 1984 (Appendix III)) and the storage would rather be underestimated than overestimated.

The actual evapotranspiration depends on the available water content and the potential evapotranspiration. The actual evapotranspiration will be equal to the available water amount, if this available water amount is lower than the potential evapotranspiration (formula 8). The

actual evapotranspiration will be equal to the potential evapotranspiration, when the available water amount is higher than the potential evapotranspiration (formula 9).

$$ET_a = P_i - Q_i + W_i \quad \text{if} \quad \frac{W_{i-1}}{W_x} * ET_p > P_i - Q_i + W_i \tag{8}$$

$$ET_a = \frac{W_{i-1}}{W_x} * ET_p \quad \text{if} \quad \frac{W_{i-1}}{W_x} * ET_p \leq P_i - Q_i + W_i \tag{9}$$

3.5 Sediment

Sediment load

To determine the suspended sediment load during the runoff events, water samples are taken at the same moments as the velocity was measured. To determine the sediment load 0.45 μm filters were used, since 20 μm filter were to coarse to separate the sediment particles from the water. Filters between the 0.45 μm en 20 μm were not available. First the filter was saturated and weighed. Subsequently subsamples of 20 or 60 mL were taken and filtered, after shaking the water sample to get a heterogeneous sediment distribution. To accelerate the process a vacuum pump is used (figure 11). After this process the filters were weighted again. The weight of the filters were measured by using a scale with an accuracy of 0.1 mg. Subtracting the weight of saturated filter from the filter with sediments gives the sediment weight :

$$Sediment\ weight\ [g] = Filter_{wet+sediment}[g] - Filter_{wet}[g] \tag{10}$$

The sediment load (g/L) can be calculated using the volume which is filtered:

$$Sediment\ load\ [g/L] = \frac{Sediment\ weight}{Sample\ volume} \cdot \frac{1000}{Sample\ volume} \tag{11}$$

Figure 11 *Experimental set-up to determine the sediment load.*

Sediment structure

Soil textures are determined by using a sediment sieve shaker (figure 12). The sieves had a pore size of 63, 125, 250, 500, 1000 and 2000 μm.

Figure 12 *Sediment sieve*

In order to determine the layering in certain areas, holes were drilled to a depth of 120 cm or until the limestone was reached. For each hole the different soil layers are determined. The layers are classified using an user guide (Appendix VI). The soil textures of the surface layers are also determined using a sediment sieve.

Saturated hydraulic conductivity

The hydraulic conductivity is determined by taking ring samples (100 cc). The soil in in the rings are saturated by putting them at least 24 hours in a container with water. The method by Dirksen (1999) is used to determine the saturated hydraulic conductivity (Appendix IV). Figure 13 shows the experimental set-up, where the inverted flask, with the tube reaching down to the taped rim (brown), serves as a Mariotte flask that maintains a constant water level above the sample (gray cylinder). The outflow is monitored by recording the flow rate in regular intervals until a steady flow is reached. The ordinary kriging interpolation technique is used to interpolate the point values and to generate a saturated hydraulic conductivity map.

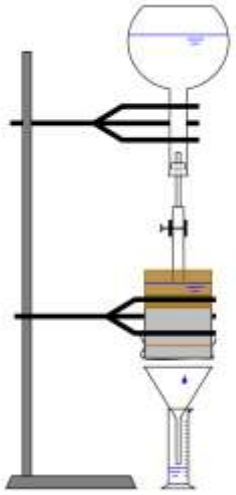

Figure 13 *Experimental set-up for measuring the saturated hydraulic conductivity with free outflow.*

3.6 Dams

Debrot *et al.* (2012) published a map with the locations of dams in the research area. This map was used to find all existing dams. Information about the height, orientation and length is collected for each dam.

4 Results

In this chapter the results will be shown and analysed, based on the research and sub question formulated in chapter 1.2.

4.1 Rainfall

To generate a fresh water flux (surface runoff or groundwater flow) towards the mangrove system rainfall is needed. Rainfall is the only fresh water input in the water balance on Bonaire and therefore an important component to analyse. In this paragraph the temporal distribution, the rainfall intensities over the research period and the spatial distributions of rainfall on Bonaire will be discussed.

The locations of the tipping bucket rain gauge and eight handmade rain gauges are shown in figure 14. Rainfall measurements are especially done at the north side of the bay, since overland flow towards the mangrove system through gullies (and therefore measurable) only occurred in this region.

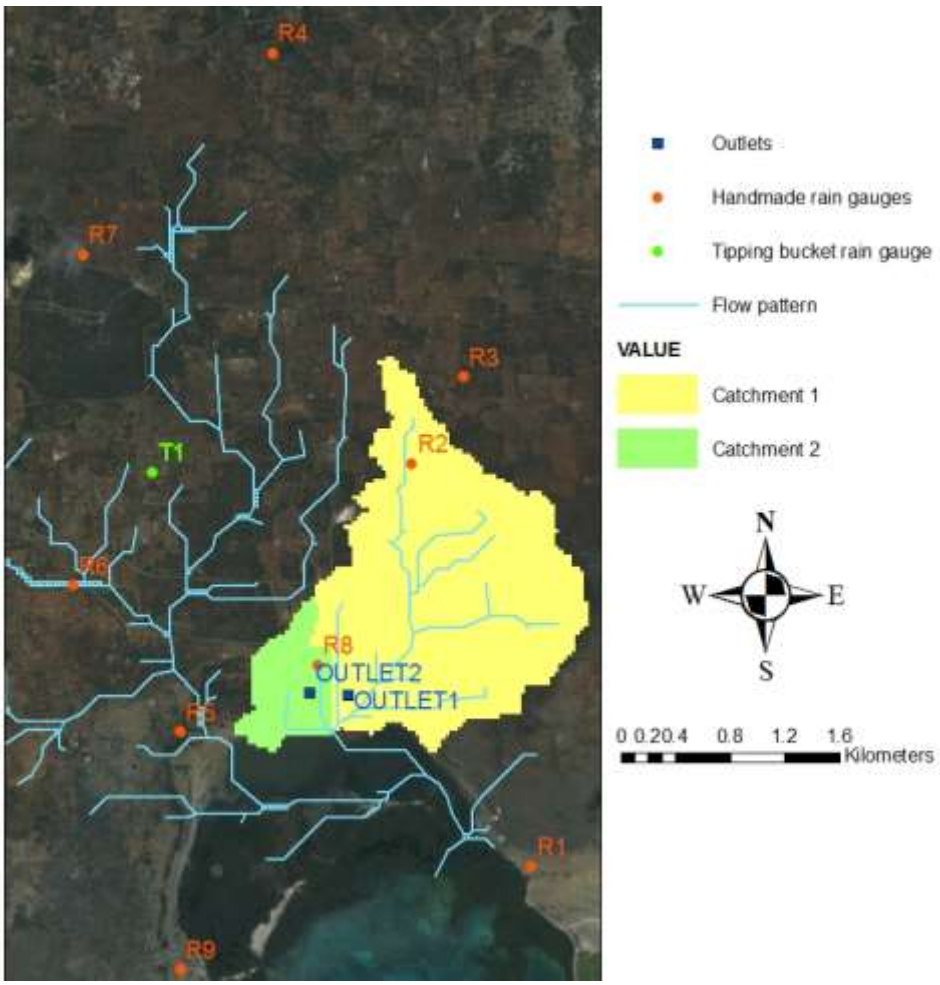

Figure 14 *Locations tipping bucket, handmade rain gauges and piezometers.*

Temporal distribution

The annual variation in rainfall for the period 1980-2009 from Flamingo Airport is shown in figure 15.

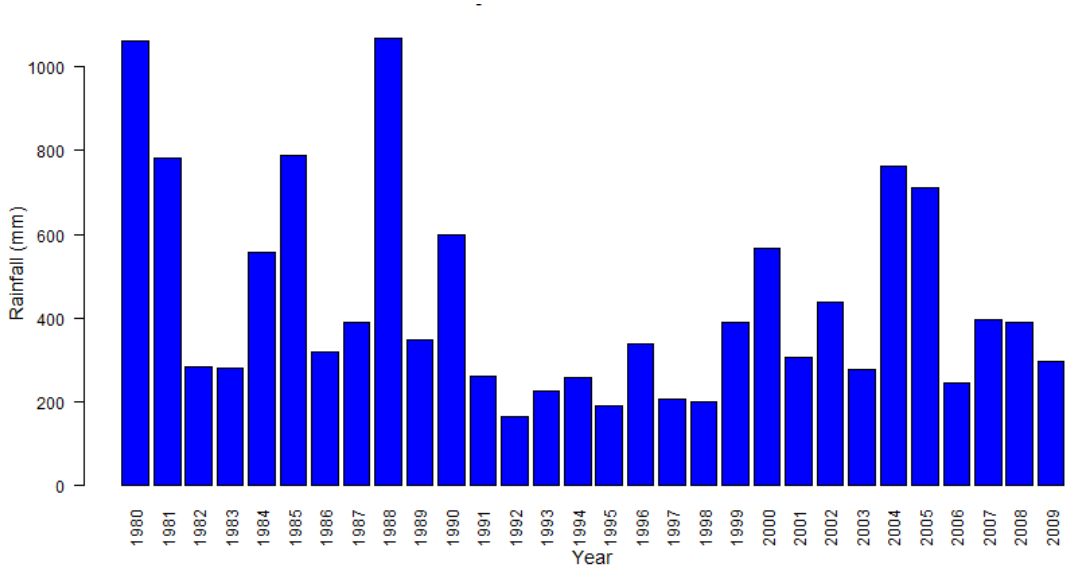

Figure 15 *Annual rainfall sums in mm from 1980 until 2009.*

Table 1 *Statistical values in mm of annual rainfall from 1980 until 2009.*

Max	Min	Mean	Median	Variance	St.dev
1069	164	436	342	62454	250

Table 1 shows a standard deviation of 250 mm for the annual rainfall sums. This, together with a difference between the highest and lowest annual rainfall sum of 905 mm, indicates a high temporal variation of rainfall on Bonaire over these 30 years. Noticeable are the rainfall sums in 1980, 1981, 1985, 1988, 2004, 2005 of at least two times the median and even three times in 1980 and 1988. In 1980 this high annual sum is mainly caused by 3 separate days with rainfall sums of 496 mm, 191 mm and 182 mm. No rainfall was detected on the day before and the next day, which indicates that the rain did not fall in long-lasting (over several days) but in relatively short (less than 1 day) intensive events. The high annual rainfall sums in 1988 is caused by 26 days with rainfall sums between 10 and 73 mm. In addition, rainfall was measured on 156 days in comparison with 45 days in 1980, which indicates that rain in 1988 fell in less intense but long lasting (several days) events. In 1981 a daily rainfall sum of 394 mm was measured. This year was characterised by short events (less than 1 day) instead of long lasting (several days) events, in comparison with 2005 where the high annual sum was especially caused by consecutive days of rain with a maximum daily rainfall sum of 122 mm. The high annual sums in 1985 and 2004 were especially caused by consecutive days of rain and less extreme daily rainfall

sums, with maximum daily sum of 96 mm and 63 mm respectively. A relatively dry period occurred from 1991 until 1998 with prolonged years of rainfall sums below the median.

Table 2 shows the statistical values for each month for the period 1980-2009. Especially the months May, October, November and December have a high variance. This indicates a high variation in rainfall sums for these months between different years. Also the highest rainfall sums and the highest average rainfall sums (except for May) are measured in these months. Logically, variation in rainfall is especially high in the wettest months (October, November, December).

Table 1 *Statistical values in mm for each month in the period of 1980 until 2009.*

	Max	**Min**	**Mean**	**Median**	**Variance**	**St.dev**
January	212	0.0	42	39	1504	39
February	105	0.0	20	17	445	21
March	206	0.0	17	7	1456	38
April	113	0.0	14	3	644	25
May	527	0.0	31	5	9428	97
June	46	0.0	10	8	123	11
July	76	4.1	27	26	340	18
August	122	0.3	23	19	686	26
September	71	0.0	29	24	446	21
October	306	0.0	67	36	5560	75
November	351	0.0	82	52	6996	84
December	409	0.0	73	39	8230	91

Table 2 *Comparison of monthly sums between research period and 30 year average.*

	Monthly sum tipping bucket (mm)	**Monthly sum tipping bucket (mm) with correction for time gap.**	**30 year average monthly sum (mm)**	**Percentage monthly sum tipping bucket (corrected) of 30 year average (%)**
October 2012	60.6	86	67	128
November 2012	37.3	37.3	82	45
December 2012	51.3	51.3	73	70
January 2013	66.7	66.7	42	159
October 2012 - January 2013	215.9	241	264	91

Table 2 shows a comparison between the monthly rainfall sums during the research period and the 30 year average monthly sums. However, the tipping bucket just started to measure on the 17th of October. To fill the gap a relation is determined between the 5 min rainfall sums of the tipping bucket (used in this research) and another tipping bucket nearby (used in the study of Koster (2013)). This relation is used to give a rough estimation of the rainfall sum from the 1st until the 16th of October 2012. This resulted in an monthly sum for October of 86 mm, which is 19 mm higher than the 30 year average. The monthly sum of January is 25 mm higher than the 30 year average. The monthly sums in November and December are respectively 45 and 22 mm lower than the 30 year average. The rainfall sum over the whole research period is 23 mm lower than the 30 year average.

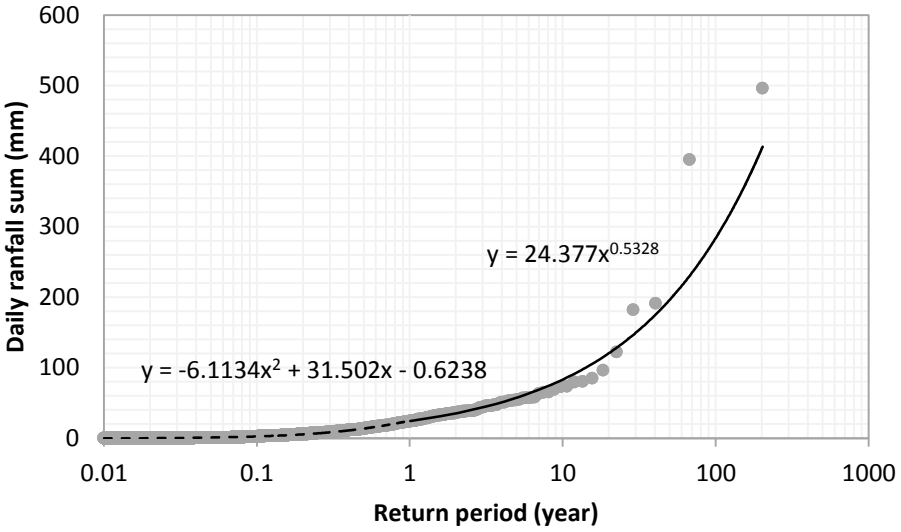

Figure 16 *Probability plot of daily rainfall sums. Dotted trend line corresponds to polynomial function and the solid line for the power function.*

In order to determine the likelihood of a rainfall event a probability plot is made (figure 16). The trend line is divided into two parts, because of the curve which made it impossible to fit one trend line through all the points. It is clearly visible that the return period increases with an increase in daily rainfall sum. The 1, 5, 10, 50, 100 and 200 year return period are shown in table 4.

Table 4 *Return periods.*

Return period [years]	Daily rainfall sum [mm]
1	24
5	57
10	83
50	196
100	284
200	410

Rainfall intensity

The highest daily rainfall sum occurred on the 21st of October 2012. On this day 30.3 mm was measured. This day was also associated with the highest rainfall intensity. In one hour 23.3 mm fell. Since the tipping bucket (TB1) started to measure on the 17th of October 2012, data of another tipping bucket (TB2), installed approximately 2.5 km away from the tipping bucket used in this research, is used to verify the findings. Table 5 shows that also TB2 measured the highest intensities on the 21st of October 2012, with a rainfall sum of 52.4 mm and rainfall intensity of 32.5 mm/h. The second highest daily rainfall sum measured by TB1 was 16.8 mm on the 22nd of December 2012, with a rainfall intensity of 8.8 mm/h. This differs from the second highest daily rainfall sum measured by TB2, which was 39.8 mm on the 17th of October 2012 with a rainfall intensity of 29.3 mm/h. For both tipping buckets count that the highest rainfall sum is measured at the same day as the highest hourly rainfall intensity. This also counts for the second highest rainfall sum and the second highest hourly rainfall intensity. Table 5 shows therefore together with figure 17 that in general high intensities are measured on days with high total rainfall sums.

Table 5 *Daily rainfall and associated rainfall intensities for TB1 and TB2.*

	Highest daily rainfall sum [mm]		**Highest rainfall intensity** [mm/hour]	
TB1	30.3	21 October 2012	23.3	21 October 2012
TB2	52.4	21 October 2012	32.5	21 October 2012

	Second highest daily rainfall sum [mm]		**Second highest rainfall intensity** [mm/hour]	
TB1	16.8	22 December 2012	8.8	22 December 2012
TB2	39.8	17 October 2012	29.3	17 October 2012

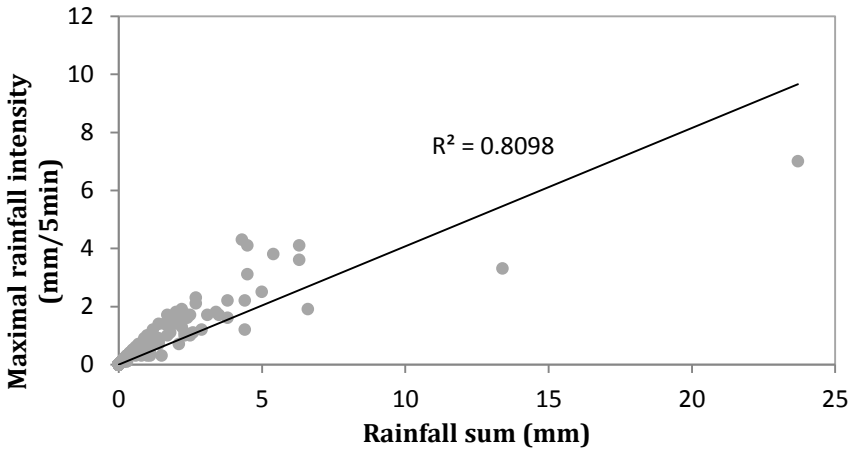

Figure 17 *Rainfall sum versus maximal rainfall intensity based on TB1 data.*

Figure 18 and 19 show that the variation in intensity is in general higher for short than for long lasting rain events. However, short events seems to have on average higher intensities than long lasting rain events. Figure 19 shows the relation between the duration of a rain event and the maximum rainfall intensity and figure 20 the relation between the duration of a rain event and the rainfall sum. Combining figure 19 and Figure 20 shows that there is hardly anything to say about the relation between the duration of an event, the intensity of an event and the rainfall sum, since there is hardly any relation between rainfall sum and the duration of a rainfall event. The expectation that the rain falls in short duration showers with high intensities during rain events with high rainfall amounts cannot be proven by this data set. The figures show that for the period October 2012 until February 2013 the rain seems to have fallen in multiple short to moderately long (20 min) showers.

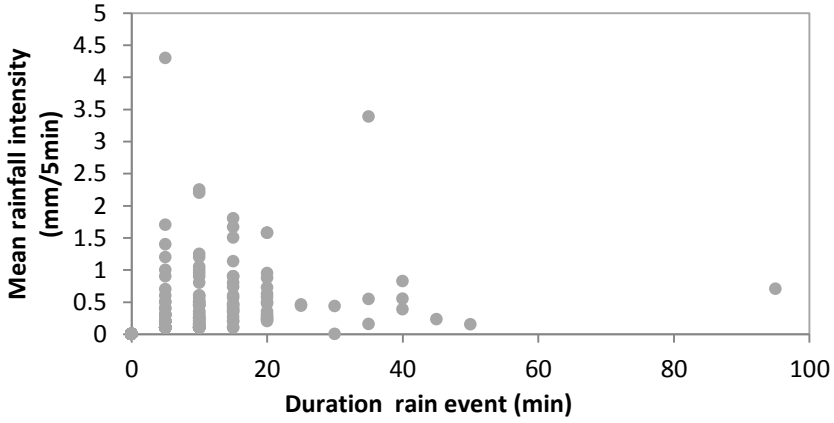

Figure 18 *Duration rain event versus mean rainfall intensity based on TB1 data.*

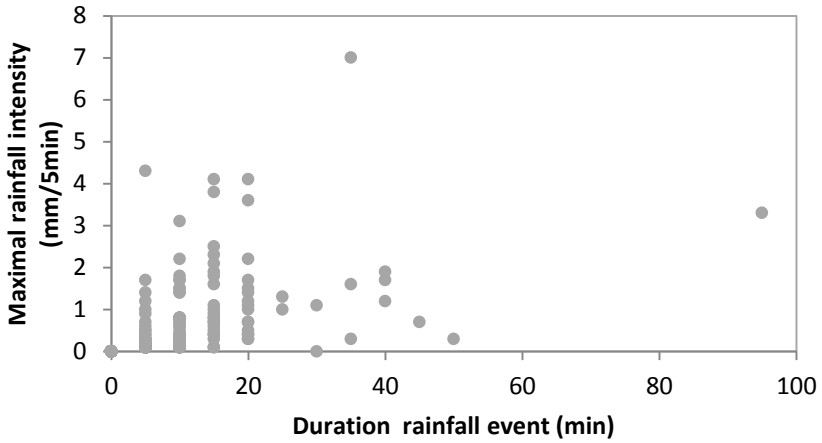

Figure 19 *Duration rain event versus maximal rainfall intensity based on TB1 data.*

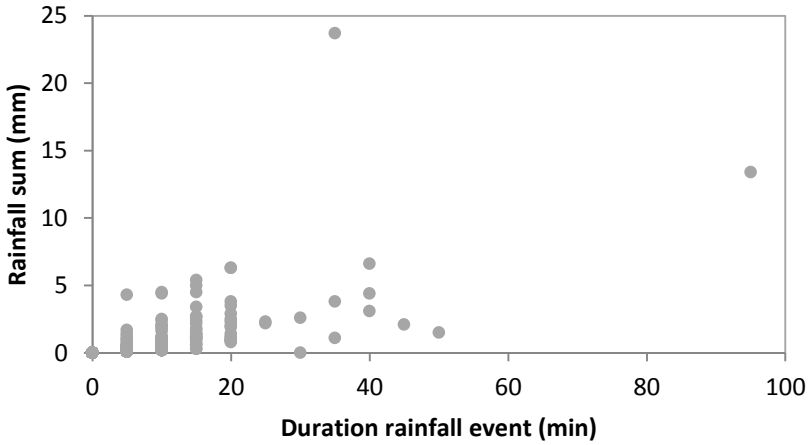

Figure 20 *Duration rain event versus rainfall sum based on TB1 data.*

Spatial distribution

In order to get insight in the spatial distribution of rainfall on Bonaire, 8 handmade rain gauges (figure 14) were installed in the catchment of Lac. Figure 21 shows the total rainfall sum over the entire research period measured by these rain gauges. Over a period of 3.5 months rain gauge 4 (R4) received twice as much rain than R8 which is located 4.5 km away and 82 mm more rain (1.3 times higher) than R7, the rain gauges located 2 km away with the second highest measured rainfall sum. This already indicates a high spatial distribution in rainfall. However, the difference is especially caused at the start of the research period when at location R4 a rainfall sum of 150 mm over 5 days was recorded. The relatively high rainfall sums in the north of the catchment (where R4 is located) is probably caused by the orographic effect, since the northern part of the catchment has relatively higher altitudes than the southern part.

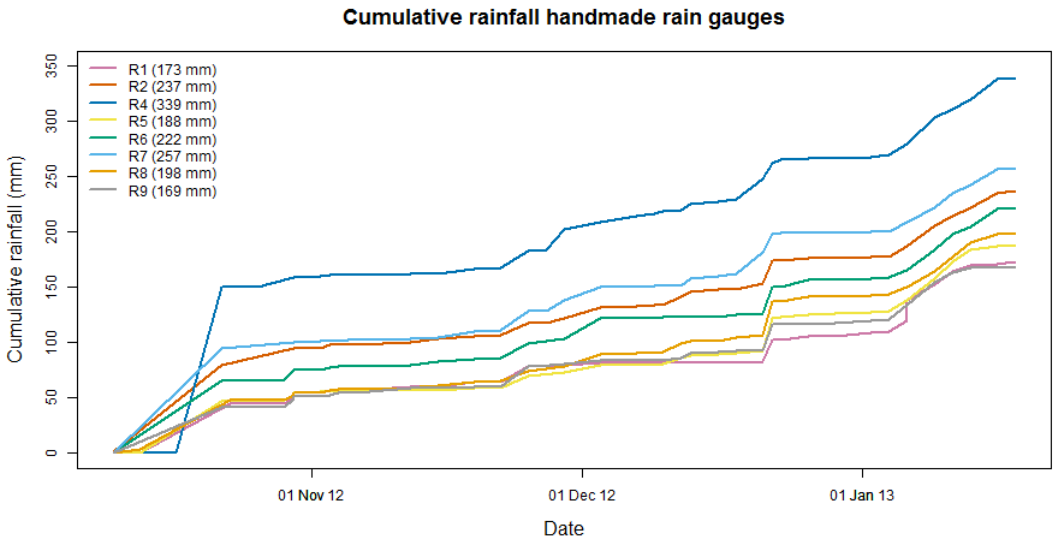

Figure 21 *Total rainfall sum measured by eight handmade rain gauges over the research period (October until mid-January).*

To get insight in the spatial distribution of rainfall in de study area, the rainfall sums measured by the handmade rain gauges are interpolated, using the inverse distance weighting interpolation method (table 6 and figure 22). With this interpolation values are determined for watershed 1 (figure 4). It should be taken into account that the rain gauges were mostly emptied only once in the 1 or 3 days and the time ranges are therefore not equal for all measurements. The values shown in table 6 and figure 22 are therefore not always 24h rainfall sums. A day has been selected when the measuring period was approximately 24h and/or there was a significant high total rainfall amount measured on that day. It was not possible to interpolate the rainfall sums to daily rainfall amounts using the tipping bucket, since the high temporal variations. Nevertheless, figure 22 shows a high spatial variation in rainfall sum in watershed 1, measured at the 25th of November, 3rd of December and the 22nd of December 2012. For example, at some location a rainfall sum of almost 18 mm is measured on the 3rd of December 2012, while at other locations a rainfall sum of only 2 mm is determined. The same counts for the 22nd of December 2012, where rainfall sums of 30 mm were measured and for some locations a rainfall sum of approximately 15 mm is determined.

The high spatial distribution in rainfall means that also the predicted values for the locations in between the rain gauges have a high uncertainty. In addition, the prediction map and as well the spatial distribution is highly dependent on the measurement locations.

Table 6 *Statistical values rainfall sums (number of * represents the number of days over which rain is measured)*

	Max	**Min**	**Mean**	**Median**	**Variance**	**St.dev**
25 November 2012**	17.	9	12	12	2	1
3 December 2012*	18	2	10	10	6	2
10 December 2012*	2	0	1	1	0	0
21 December 2012***	19	1	5	4	12	3
22 December 2012*	30	16	24	24	8	3
23 December 2012*	3	0	0	0	0	0
9 January 2013***	24	14	18	19	2	2
11 January 2013**	15	8	12	12	2	1

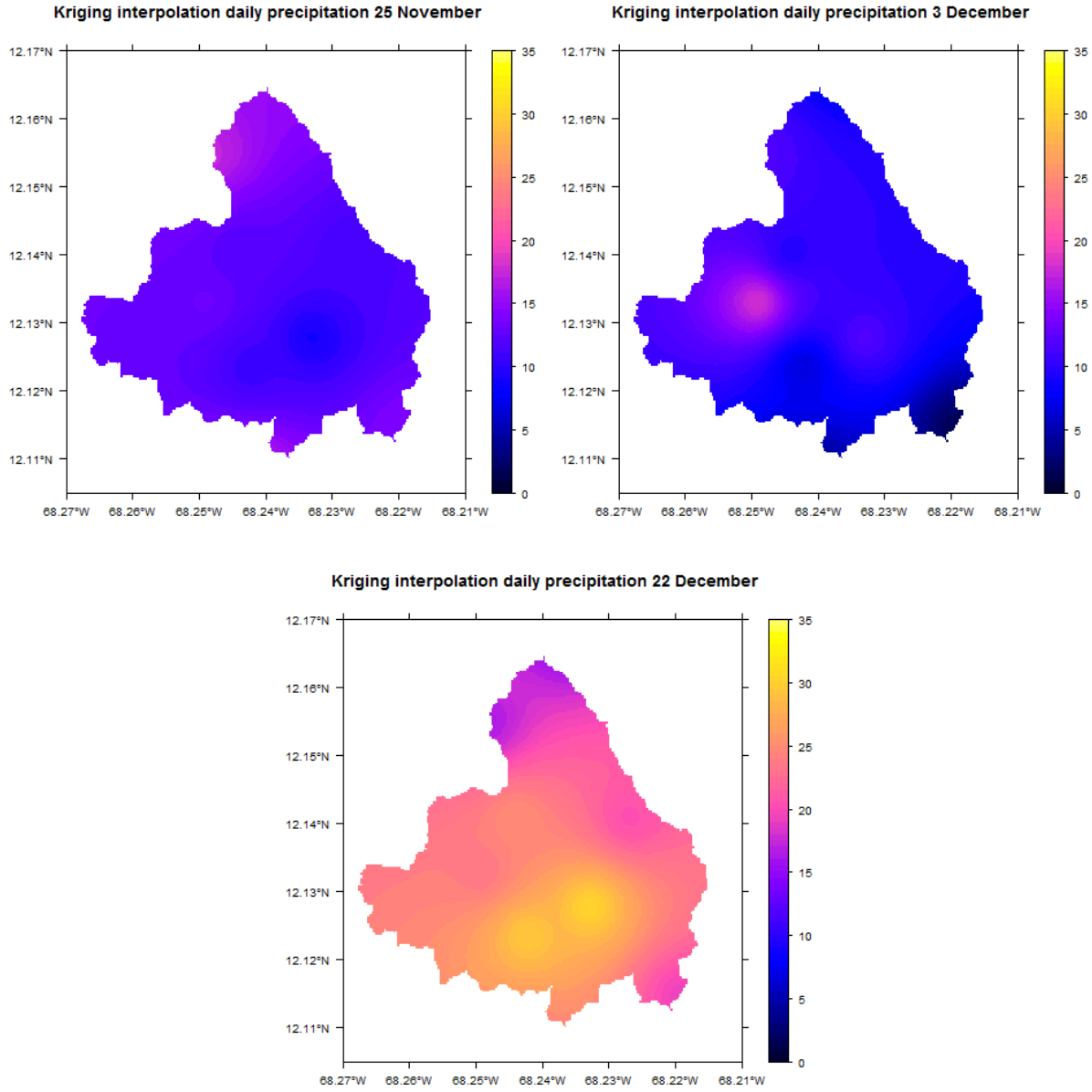

Figure 22 *Spatial distribution of rainfall (mm) on 25 November, 3 December and 22 December 2012.*

4.2 Surface runoff

Surface runoff and groundwater recharge are the two fresh water fluxes which can help to refresh and limit the salinization of the landside waters in Lac. The amount of fresh water that reaches the mangrove system by surface runoff, his distribution in time and the reaction of surface runoff on precipitation will be discussed in this paragraph.

Figure 23 shows the catchments of which runoff and sediment transport (paragraph 4.4: "*Sediment transport*") patterns are investigated. Both catchments (Catchment 1 and 2) are sub-catchments of watershed 1 shown in figure 4. Only in these sub-catchments overland flow towards the mangrove system through gullies occurred and therefore measurable. The catchment areas are 3.17 km^2 and 0.46 km^2 respectively for catchment 1 and 2. Due to some installation errors the diver at outlet 1 has measured from the 10th of October 2012 until the 29th of January 2013 and the diver at outlet 2 from the 25th of November 2012 until the 29th of January 2013.

The flow patterns generated by an elevation map suggest that also water transport occurs more to the west in watershed 1. Despite that a diver was installed in the field no water transport by surface runoff occurred towards the mangrove system in this area. Instead a pond developed during periods of rain just upstream of the culvert which actually was built to transport water towards the mangrove system. This problem was also been seen at other locations where culverts were built to discharge rainwater to the mangrove system. These culverts were therefore not functioning.

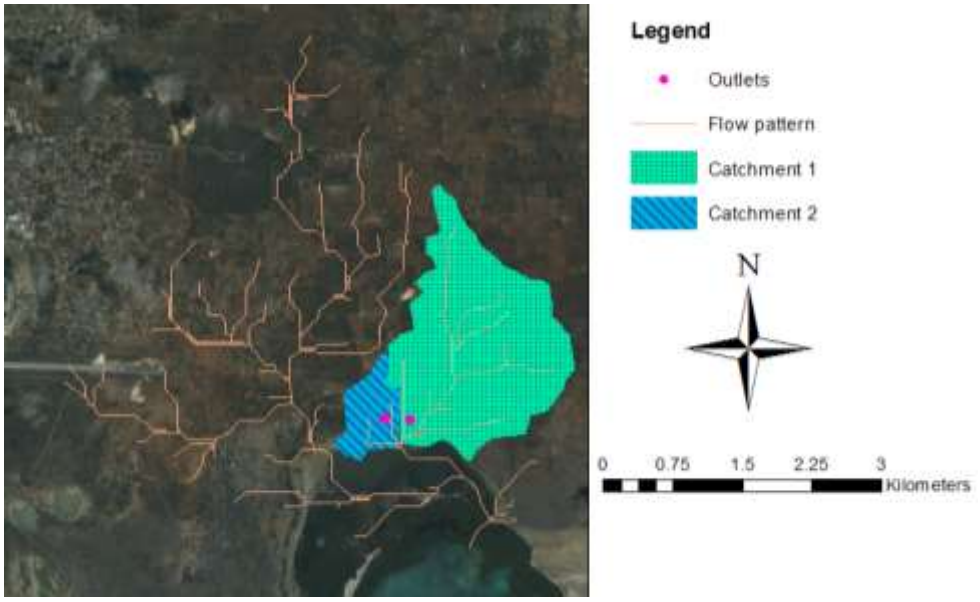

Figure 23 *Catchment 1 and 2, whose runoff and sediment transport patterns are investigated.*

Using the method to determine the water levels described in the method part (paragraph 3.2: "*Runoff*"), caused positive water levels at outlet 2 over the whole research period, which is not plausible based on the field observations. This gives the impression that there is a standard error between the air pressure measured by the baro divers and the air pressure measured by the divers at the outlets. Also a daily variations is been seen in the calculated water levels. For outlet 2 the water level are therefore determined in the following way:

- On the 22nd of December 2012 water samples are taken and it is therefore certain that water is detected by the diver. Based on the shape of this runoff profile and the runoff events at outlet 1 there is searched for multiple runoff events which occurred at outlet 2. This analysis showed that only at the 22nd of December and the 6th of December water is detected by the divers. At the moment that the diver is installed on the 25th of November (both divers, for outlet 1 and 2, were used for another study for a couple of days), the water level was already too low and is therefore not measured by the diver.
- Based on field observations it is known that the water level raised fast. The water level one time step before the water level raised (t_0) is assumed to be zero. The water level during the runoff event is determined by subtracting the water level based on diver calculations at t_0 from the water level based on diver calculation at t_i until t_n.

On the 25th of November 2012 and the 22nd of December 2012 rainfall events with runoff occurred. During and after these rain events the water levels in the gullies and the stream velocities were measured. On the 25th of November the water level and velocity measurements were done manually with an interval of 5 minutes. On the 22nd of December only the velocity measurement was done manually with intervals between 10 and 20 minutes. In order to calculate the discharge the cross sectional area and therefore the gully profile is needed. This profile is determined in the field, shown in figure 24 and figure 25. The profile measured in the field for outlet 1 seemed to be too small, since the highest water levels measured by the diver was higher than the profile depth. Therefore the profile is extrapolated to each side. Two trend lines are determined for the measurement points left and right from the lowest point. The extrapolation is based on these trend lines. It might be possible that the profile is less steep or steeper.

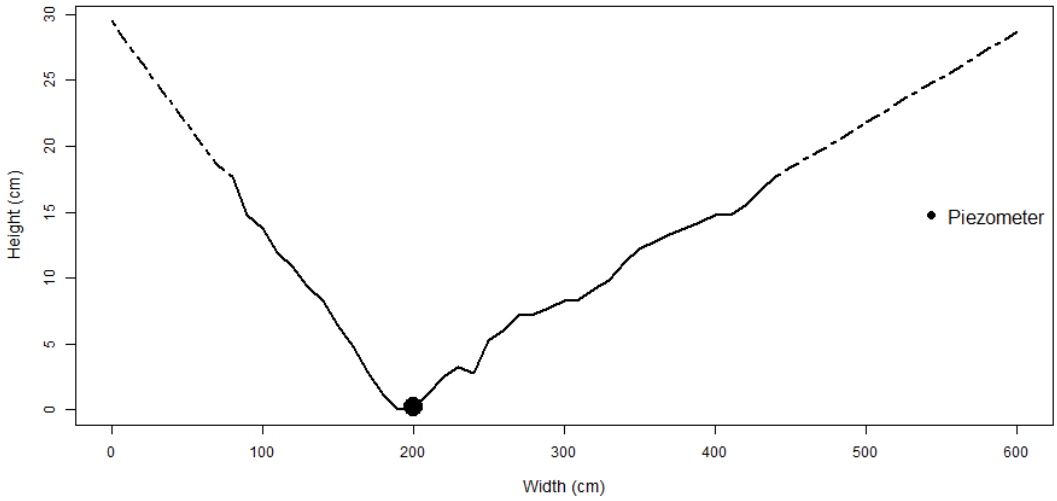

Figure 24 *Profile outlet 1. Dashed lines indicated the interpolated values. The solid dot indicates the location of the piezometer.*

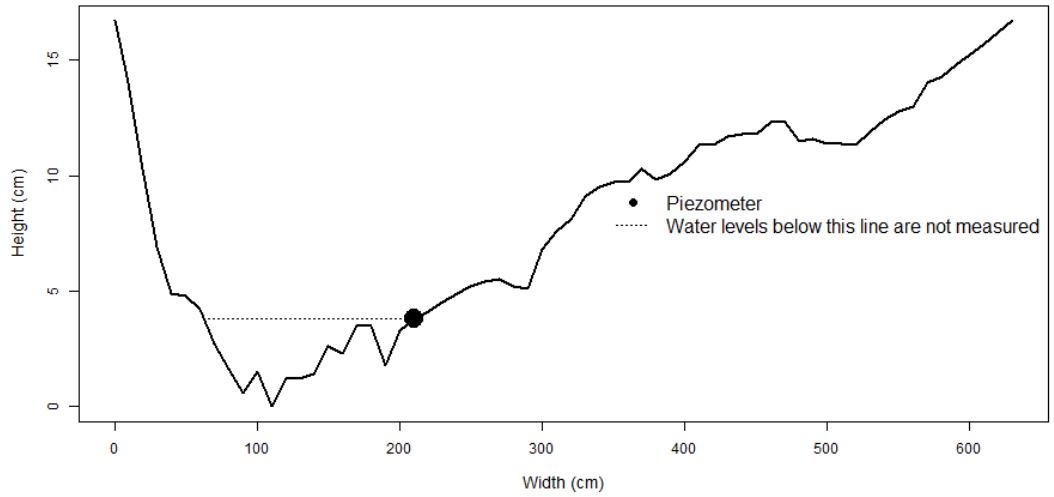

Figure 25 *Profile outlet 2. The solid dot indicates the location of the piezometer.*

Combining the water level and gully profile gives the cross sectional area. The discharge can be calculated by multiplying the cross sectional area with the stream velocity. This resulted in a Q-h relationship for both outlets (Figure 26 and figure 27). The following formulas are used to calculate the discharge for the whole research period:

Outlet 1	If h > 18.267	$Q = h^{9.2536}$	(4)
	If h < 18.267	$Q = 0.0018h - 0.0179$	(5)
Outlet 2	$Q = 0.0003h^3 - 0.0027h^2 + 0.0141h - 0.0181$		(6)

With:

Q : Discharge [m^3/sec]

h : Water level [cm]

The Q-h relationship is divided in two relations for outlet 1, since no accurate trend line could be drawn based on all data points. Therefore a linear relation (based on 2 points) is determined for water level lower than 18.3 cm and a power function for water levels higher than 18.3 cm. It should be kept in mind that especially the linear relation depends of the discharge at 18.3 cm. A small difference in the velocity measured at a water level of 18.3 cm would have led to another relationship.

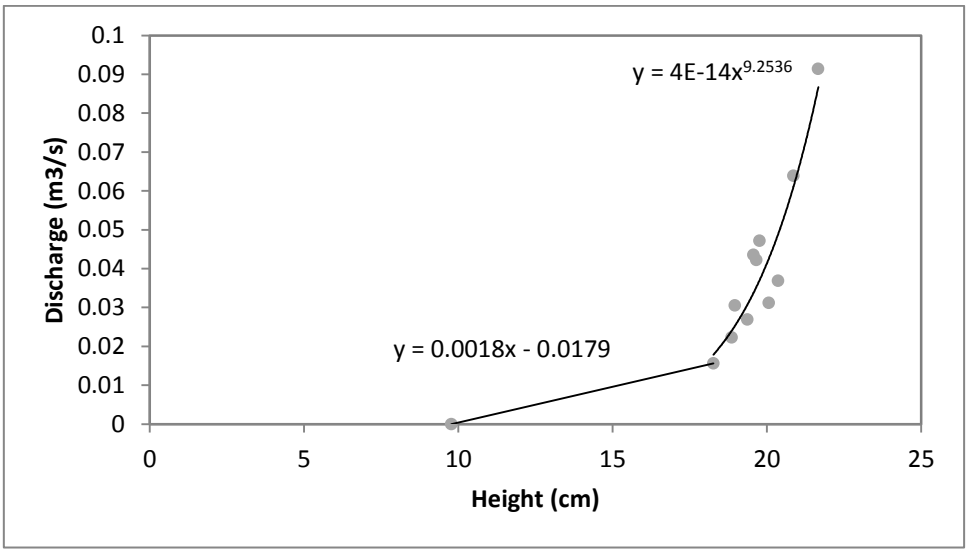

Figure 26 *Q-h relation 22 December 2012 outlet 1.*

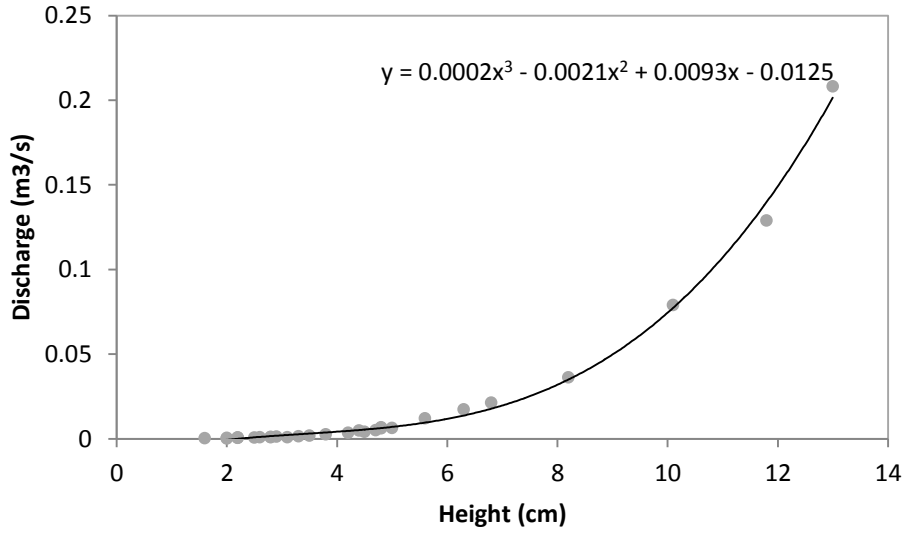

Figure 27 *Q-h relation 25 November 2012 and 22 December 2012 outlet 2.*

Outlet 1

Figure 28 shows the unit hydrograph of catchment 1. It should be mentioned that the rainfall plotted in the graph is the rainfall measured by the tipping bucket which is located outside the catchment and approximately 2 kilometres away from the outlet. Therefore, the rainfall intensities plotted in the graph is probably not the actual rainfall fallen on the catchment. And the analyses done based on these rainfall intensities probably do not have a high accuracy. However, since the lack of more data which is measured with a relative high temporal resolution, it is assumed that the data measured by the tipping bucket is representative for catchment 1.

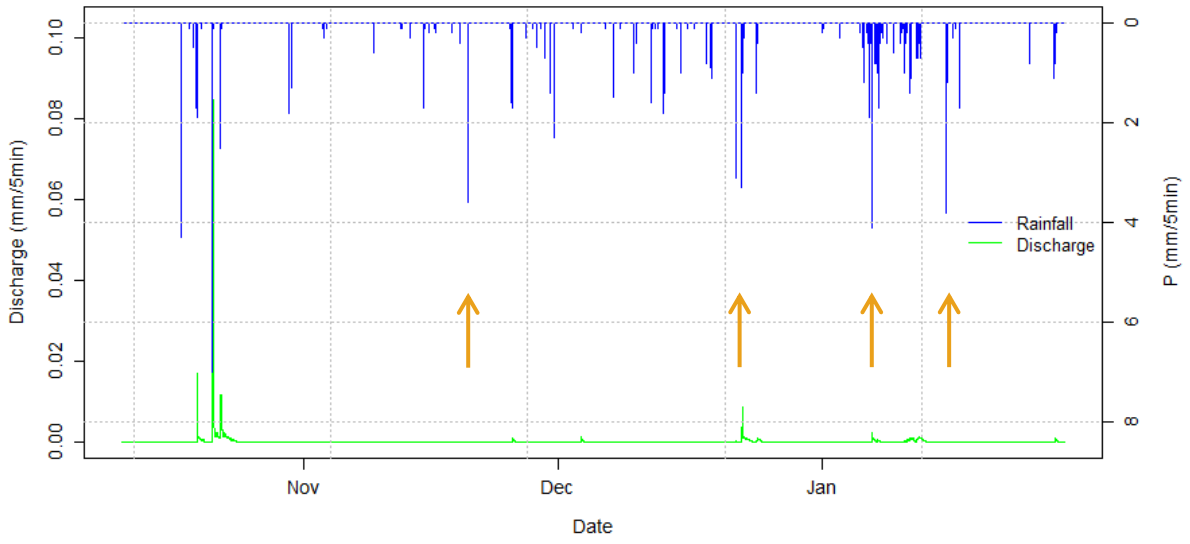

Figure 28 *Unit hydrograph of catchment 1. The orange arrows indicate points where discharge reacts in different ways on rainfall.*

In figure 28 can be seen that despite the relatively high amount of rainfall only a small part is discharged by surface runoff. The tipping bucket has measured a total rainfall amount of 216 mm over the whole research period. The total amount of rainfall measured by the rain gauges and interpolated for catchment 1 is 215 mm. Nevertheless, the total amount which is discharged by surface runoff is only 3.8 mm, which only approximately 2% of the total rainfall for both catchments.

Besides the difference in cumulative amounts of discharge and rainfall it can also be noticed that discharge does not react always in the same way on the approximately same rainfall intensity. The orange arrows in figure 28 indicate four points where discharge reacts in different ways on rainfall, which has to do with the initial soil moisture content. The following part goes deeper into the runoff response, looking to different surface runoff events.

Rainfall events

To get insight whether overland flow occurs due to infiltration excess (Hortonian overland flow) or saturation excess (Dunnean overland flow), a water balance is made. The components of the water balance are plotted in figure 29. This graph shows that the assumed maximum soil storage capacity of 100 mm is not been reached during the research period. The amount of storage still increases after a rainfall events. Based on the water balance it can be conclude that surface runoff in catchment 1 occurs due to events that exceed the infiltration capacity.

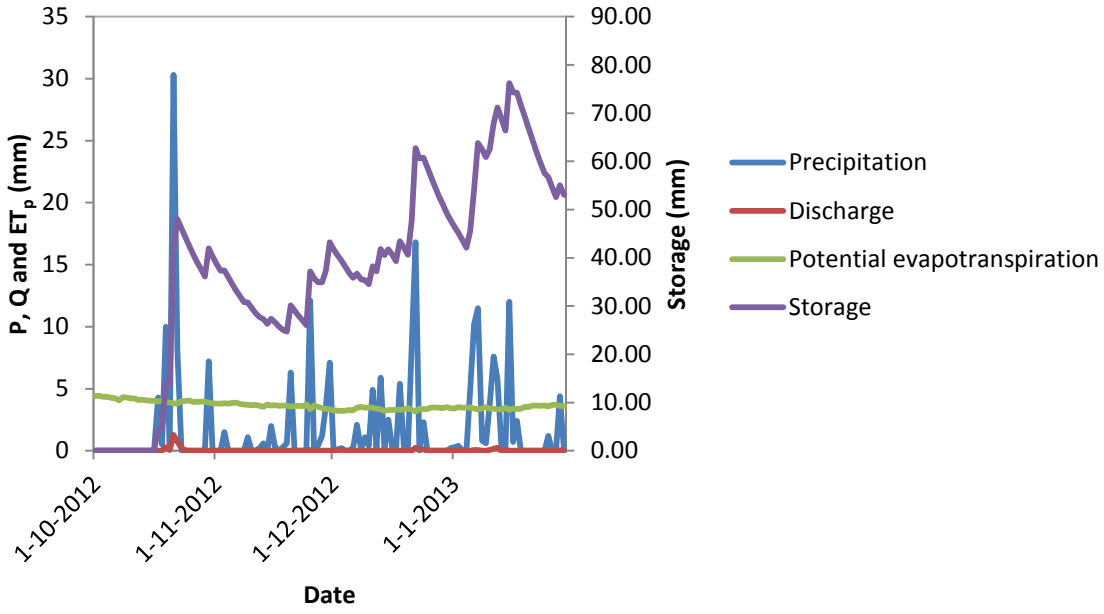

Figure 29 *Water balance catchment 1 with initial storage of 0 mm and a maximum storage of 100 mm.*

Figure 30 shows the distribution of the saturated hydraulic conductivty (K_{sat}). It should be noticed that K_{sat} gives an underestimation of the infiltration capacity in catchment 1, since the soil is never been saturated over the whole research period. The rainfall intensity have not exceeded the mean K_{sat} value of 21 mm/5min for catchment 1 during the research period. The minimum K_{sat} value of 2 mm/min is exceeded on the 21st and 22nd of October 2012, the 22nd of December 2012 and the 6th of January 2013 and caused surface runoff on these days. Nevertheless, surface runoff also occurred after rainfall events of lower intensities, but this only happened after it had rained continuously several days or a runoff event occured in the last three days. This can be explained since the moisture content affects the soil infiltration capacity. After a relative long dry period (no rainfall events) the infiltration capacity will be high, but after some rain events the soil moisture content will increase which causes a lower infiltration capacity. Based on this knowledge it can be assumed that the actual saturaded hydraulic conductivity in catchment 1 is lower than the K_{sat} measured in the laboratory using field

samples. However, on the 25th of November and the 28th of January runoff occured without a runoff event in the past three days, continuously rainfall, or a high rainfall intensity. It might be possible that the rainfall which caused these runoff events is not measured at the location of the tipping bucket (high spatial distribution).

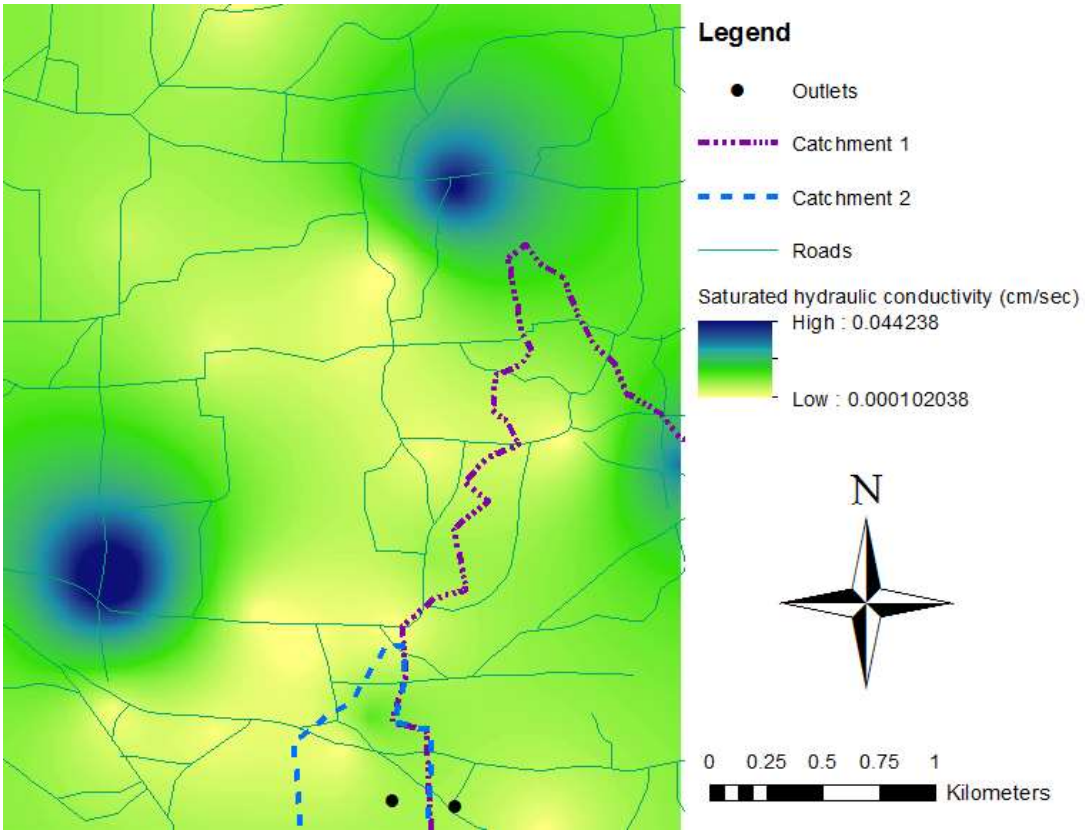

Figure 30 *Map of saturated hydraulic conductivity in cm/sec, based on ordinary kriging interpolation of laboratory measurements.*

Table 7 *Minimum and mean saturated hydraulic conductivity for catchment 1 and 2.*

	Minimum (mm/5min)	**Mean (mm/5min)**
Catchment 1	2	21
Catchment 2	4	13

Rainfall runoff relationship

In order to gain insight in what will happen after an extreme rainfall events regarding to surface runoff, rainfall runoff relationships are determined. The relationships are determined in three different ways. The handmade rain gauges are emptied only every 1 to 3 days. The rainfall sums measured by these rain gauges are therefore not comparable with the daily rainfall sum measured by the tipping bucket. The rainfall sums for both the handmade rain gauges and the tipping bucket are therefore determined over a longer time period. The results are shown in table 8, figure 31 and figure 32.

Table 8 *Total rainfall and runoff amounts over a certain time period for catchment 1.*

Time series	Q [mm]	P (Tipping bucket) [mm]	P (Handmade rain gauges) [mm]
10-30 October 2012	2.5	86	92.2
25-26 November 2012	0.1	12.1	11.1
3-4 December 2012	0.1	11.0	9.6
21 December 2012	0.001 ~ 0	8.4	NA
21-25 December 2012	0.4	27.5	27.4
6-8 January 2013	0.1	28.1	26.6
10-13 January 2013	0.5	17.2	19.9
28 January 2013	0.036 ~ 0	4.4	NA

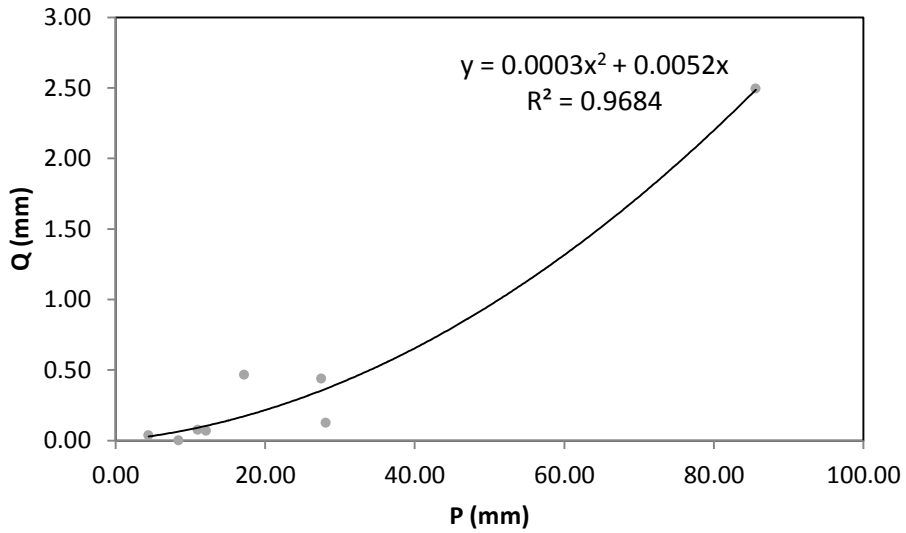

Figure 31 *Rainfall runoff relationship for catchment 1 based on handmade rain gauge data over a certain time period described in table 8.*

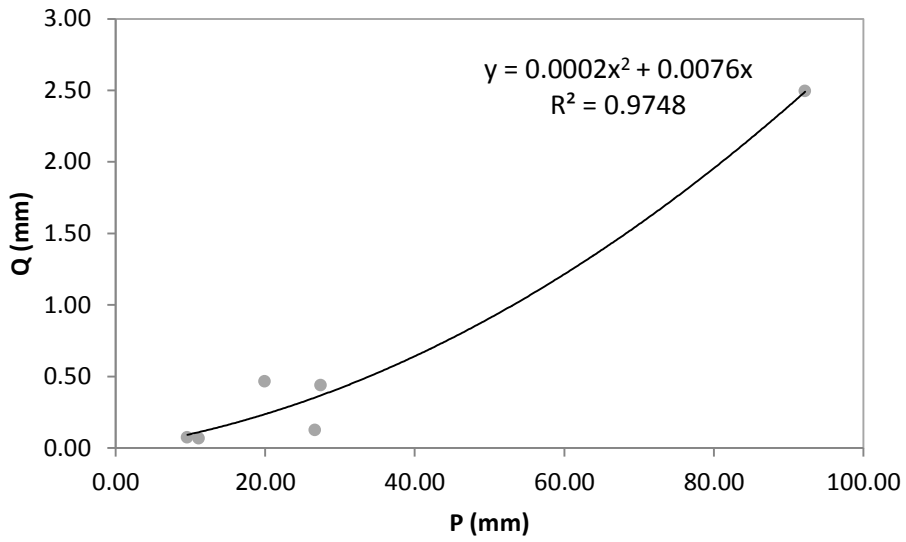

Figure 32 *Rainfall runoff relationship for catchment 1 based on tipping bucket data over a certain time period described in table 8.*

Return periods for daily rainfall are determined in paragraph 4.1. The amount of water that will be discharge towards the mangroves can be estimated for these rainfall return periods based on the rainfall-runoff relationship using handmade rain gauges and tipping bucket data. The return periods with the associated runoff amounts are shown in table 9.

Table 9 *Rainfall return periods with associated runoff amounts for catchment 1. The rainfall runoff relationship is based on tipping bucket and rain gauge data over a certain time period.*

Return period [years]	**Daily rainfall sum** [mm]	**Discharge (Tipping bucket)** [mm]	**Discharge (Handmade Rain gauges)** [mm]
1	24	0.3	0.3
5	57	1	1
10	83	2	2
50	196	13	9
100	284	26	18
200	410	53	37

However, there is also a rainfall runoff relationship determined based on only tipping bucket data, since a rainfall runoff relationship over these relatively long time series is not quite accurate. Nevertheless, also here the assumptions has to be made that the tipping bucket data is representative for catchment 1. In this case only rainfall that caused surface runoff directly is used to determine the rainfall runoff relation, since infiltration excess is expected. In table 10, per event is shown how much rainfall is needed to generate a certain amount of runoff. Figure 33 shows the relationship between rainfall and runoff. Table 11 shows the return periods with the associated runoff amounts based on the rainfall runoff relationship with only tipping bucket

data. These runoff amounts are higher than the runoff amounts estimated by the rainfall runoff relationship based on tipping bucket and handmade rain gauge data over a certain time period (table 9). In this relationship more precipitations is required to generate the same runoff amount in comparison with the relation based on only tipping bucket data. It is assumed that the relationship based on tipping bucket data (figure 33) (where only rainfall is used that caused surface runoff directly) is more accurate and will therefore be used in the rest of the report.

Table 10 *Amount of rainfall which caused a certain amount of runoff in catchment 1 (where only rainfall is used that caused surface runoff directly).*

Event	Q [mm]	P (Tipping Bucket) [mm]
19 October 2012	0.3	6.8
21 October 2012	1.3	24
22 October 2012	0.9	8.1
25 November 2012	0.1	9.3
3 December 2012	0.1	0.2
22 December 2012	0.3	14.9
24 December 2012	0.1	2.3
6 January 2013	0.1	6.4
7 January 2013	0.03 ~ 0	8.9
10 January 20 13	0.5	16

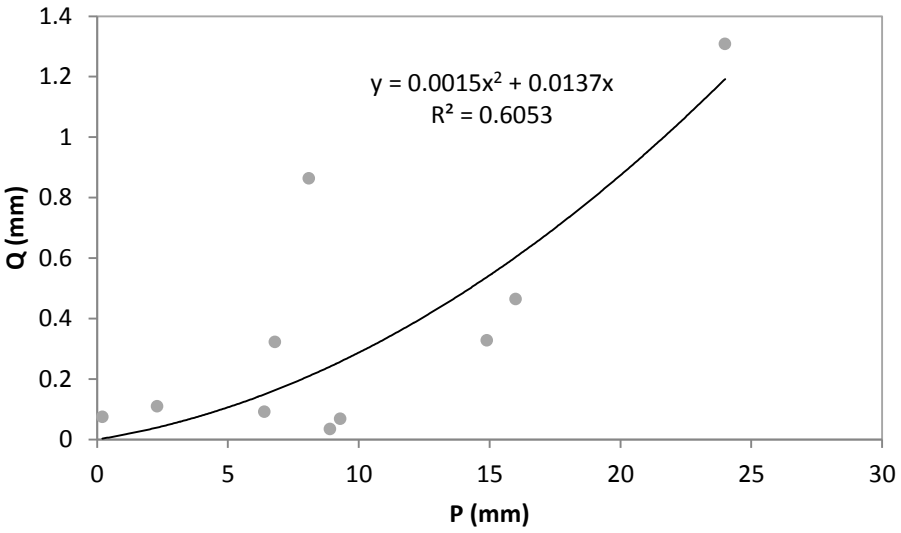

Figure 33 *Rainfall runoff relationship for catchment 1 based on tipping bucket data (where only rainfall is used that caused surface runoff directly).*

Table 11 *Return periods for rainfall with associated runoff amounts for catchment 1. Rainfall runoff relationship is based on tipping bucket data (where only rainfall is used that caused surface runoff directly).*

Return period [years]	Daily rainfall sum [mm]	Discharge (Tipping bucket) [mm]
1	24	1
5	57	6
10	83	11
50	196	60
100	284	125
200	410	258

Outlet 2

Figure 34 shows the unit hydrograph of catchment 2. It is assumed that the data measured by the tipping bucket is representative for catchment 2. The total rainfall amount measured by the tipping bucket and measured by the handmade rain gauges and interpolated for catchment 2 over the whole research period is in both cases 132 mm. The total runoff amount is 2.3 mm, which is therefore approximately 2% of the total rainfall.

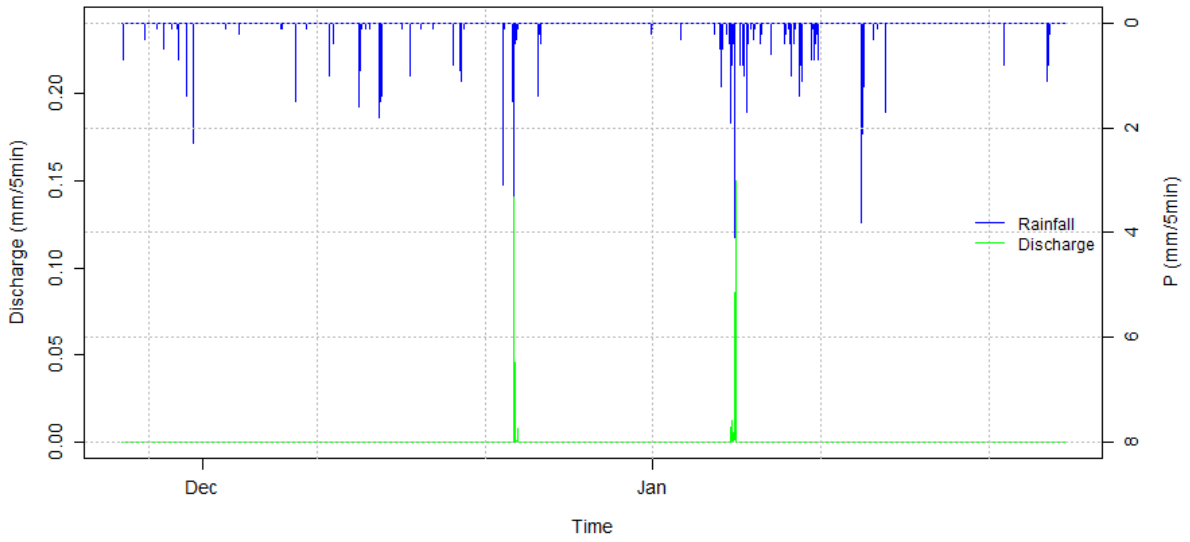

Figure 34 *Unit hydrograph outlet 2*

Rainfall events

Based on the water balance (figure 35) of catchment 2 it is assumed that the maximum storage capacity of 100 mm is not been reached during the research period. The amount storage thereby still increases after rainfall events. Based on the water balance it can be concluded that surface runoff in catchment 2 occurs due to events that exceed the infiltration capacity (Hortonian overland flow).

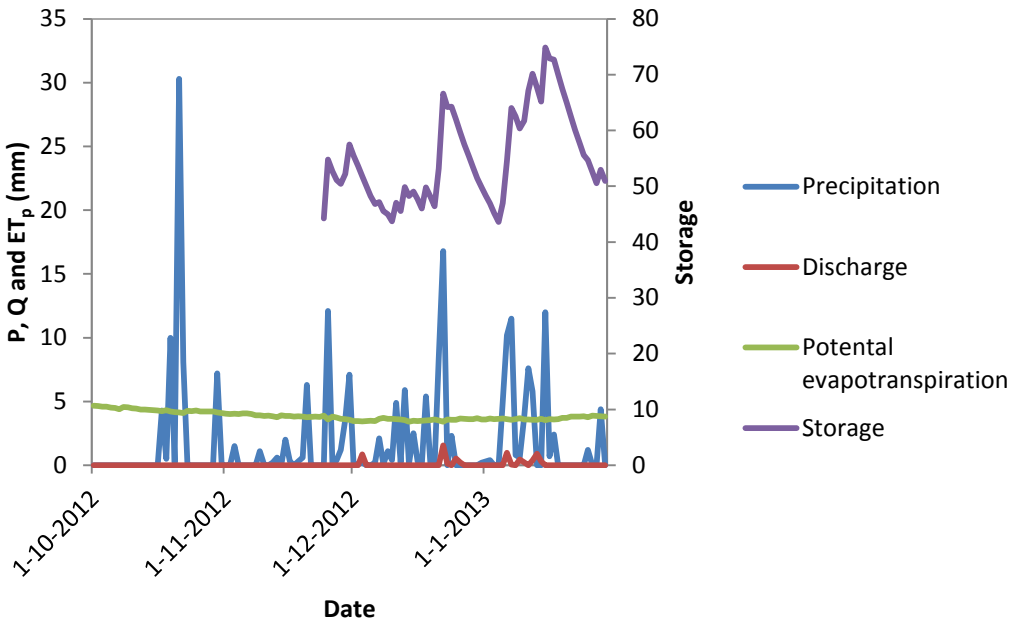

Figure 35 *Water balance of catchment 2 with initial storage of 0 mm and a maximum storage of 100 mm.*

The mean saturated hydraulic conductivity for catchment 2 is 13.4 mm/5min. The minimum K_{sat} value is 3.6 mm/5min. This minimum infiltration rate is exceeded two times during the research period at the 6th of January 2013 (4.1 mm/5min) and the 15th of January 2013 (3.8 mm/5min). However, the rain at the 15th of January did not generate runoff (either for catchment 1) which suggests that this rain event is not fallen on catchment 2. Runoff did occur after a rain event of 6.2 mm in 10 minutes (2.9+3.3 mm/5min) on the 22nd of December 2012. This might have been occurred due to a rainfall event of 3.1 mm/min on the 21th of December 2012, whereby the initial soil moisture content increased. Based on this analysis it is assumed that runoff occur in catchment 2 when the rainfall intensity exceeds a infiltration rate between the 3.1 mm/5min and 4.1 mm/5min. However, taken the soil moisture content into account the infiltration rate is probably higher in the beginning of the rainy season.

Rainfall runoff relationship

The assumptions is made that the tipping bucket data is representative for catchment 1 to determine the rainfall-runoff relation. In this case only rainfall that caused surface runoff directly is used to determine the rainfall runoff relation. In table 12 is per event shown how many rainfall is needed to generate a certain amount of runoff. Figure 36 shows the relationship between rainfall and runoff. Based on this relationship the runoff amounts are determined for the precipitation return periods (table 13). However, using the rainfall runoff relationship caused higher runoff amounts than precipitation amounts for the precipitation return periods of 50, 100 and 200 years. This indicates a low accuracy of the relationship and the transgression

line would probably be less steep when more data point are used. In the rest of the report it is assumed that the runoff amount is equal to the precipitation for the 50, 100 and 200 years return period, since it is assumed that the evaporation amounts are negligible in comparison with these rainfall amounts.

Table 12 *Per event the amount of rainfall which caused a certain amount of runoff in catchment 2.*

Data series	Q [mm]	P (Tipping bucket) [mm]
25 December 2012	0.11	9.3
22 December 2012	1.55	14.9
6 January 2013	0.64	4.5

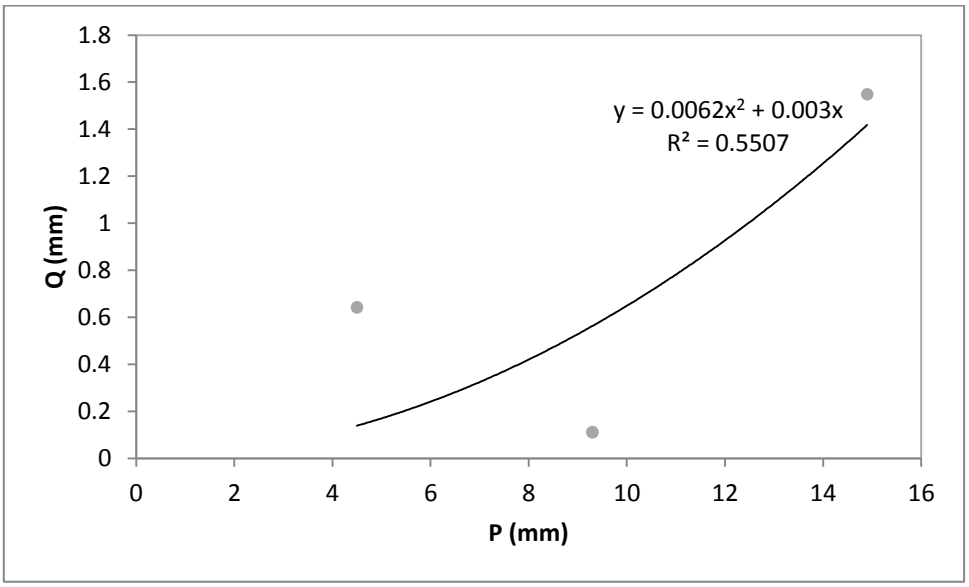

Figure 36 *Rainfall runoff relationship for catchment 2 based on tipping bucket data.*

Table 13 *Return periods for rainfall with associated runoff amounts for catchment 2.*

Return period [years]	Daily rainfall sum [mm]	Discharge [mm]	Corrected discharge [mm]
1	24	4	4
5	57	20	20
10	83	43	43
50	196	239	196
100	284	501	284
200	410	1043	410

4.3 Evapotranspiration

To determine the storage change over time also evapotranspiration has to be known. The potential evapotranspiration (ET_p) for the research period is determined based on the FAO Penman-Monteith method (Allen *et al.*, 1998) using meteorological data from Flamingo Airport. The vegetation cover was based on 100 random points in catchment 1 and 69 random points in catchment 2 (figure 23) which resulted in a vegetation fraction of 0.39 and 0.30 respectively. This resulted in different ET_p values for both catchments. For both catchment the same trend is been seen (figure 37). From the beginning of October until the beginning of December ET_p is decreasing and from then on it slightly increases again. This trend is probably caused by a decrease and increase in the net incoming solar energy, probably due to variations in cloud cover. The mean difference between the ET_p between catchment 1 and 2 is 0.2 mm, which is caused by a higher vegetation fraction in catchment 1. This higher vegetation fraction causes lower ET_p values due to a higher fraction with stomata and canopy resistance.

Based on a simple model the actual evapotranspiration (ET_a) is determined. In figure 37 can be seen that over the whole period ET_a is lower than ET_p. This shows that the catchments are water limited. This is logical, since the average annual precipitation of 470 mm and an average annual potential evapotranspiration of 2600 mm (Borst and de Haas, 2005). Also in this research the highest measured total rainfall amount was 339 mm was less than the total ET_p, which was 441 mm and 467 mm for catchment 1 and 2 respectively. ET_a can therefore never be equal to ET_p. After the rainfall event on the 19th of October 2012, ET_a decreased and increased from time to time due to an increase in the amount of precipitation and storage.

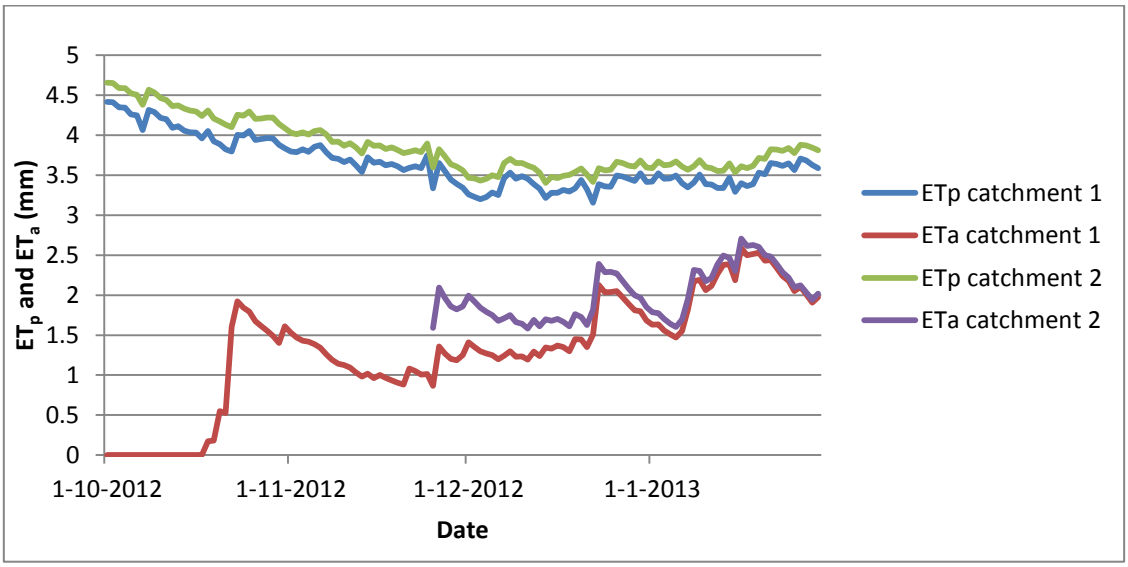

Figure 37 *Potential and actual evapotranspiration of catchment 1 and 2.*

4.4 Sediment transport

In order to get insight in the sediment transport towards Lac, water samples are taken during runoff events. In addition, also soil samples are taken in the catchment area to determine the sediment size fractions. An user guide is used to classify the soil texture in the delta area, the area downstream the outlets and upland from the mangrove forest. In this paragraph the results will be given.

Sediment load transport

Sediment load was measured during two events at both outlets. Nevertheless, the sediment loads for November the 25th at outlet 1 were not plausible and therefore not taken into account for further analysis. The discharge and measured sediment load is plotted against time for each runoff event (figure 38 until Figure 40). Based on these events sediment discharge relationship are determined for both catchments (figure 41 and figure 42). The relationships do not have a high accuracy, since these relationships are based on only one event for catchment 1 and two events for catchment 2. In addition, it is assumed that the trend line crosses the y axes at zero in both plots since positive values of sediment loads are not acceptable when no water is transported. The points in the graph for catchment 1 deviates from the trend line above a discharge of 0.003 mm/5min. In the beginning of the measurements high sediment loads were measured around a discharge of 0.004 mm/5min. After a fast increase in discharge, the sediment load only increased slightly. This fast increase in discharge was followed by a gradual decrease in discharge and sediment load. These steps can also be seen in the hysteresis graph (figure 43), which will be discussed in the next paragraph.

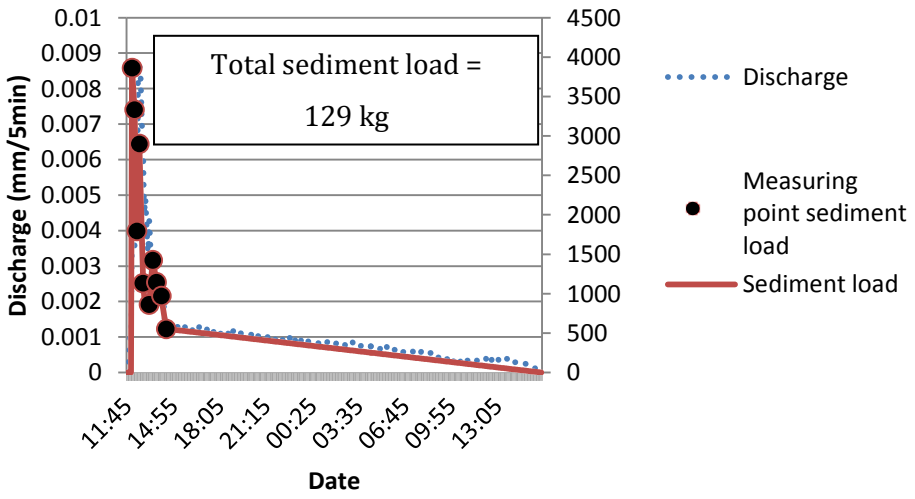

Figure 38 *Sediment load and discharge on the 22nd of December 2012 at outlet 1.*

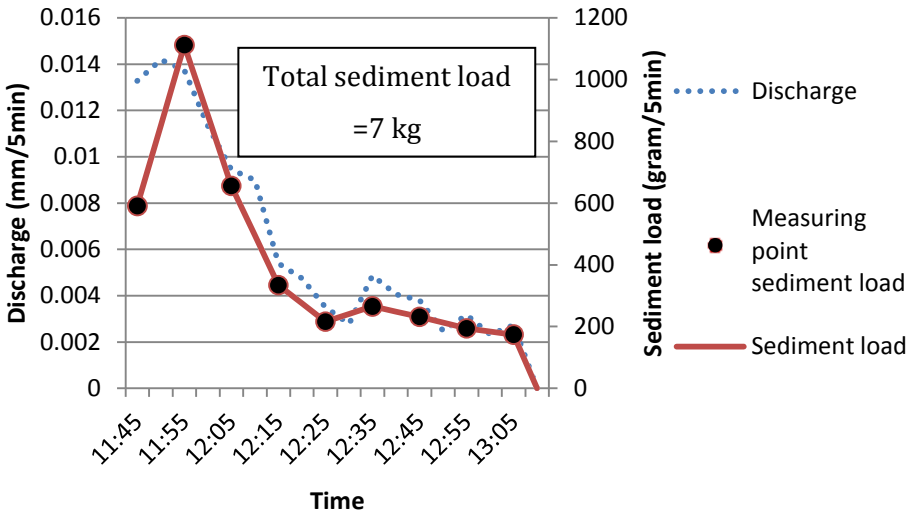

Figure 39 *Sediment load and discharge on the 25th of November 2012 at outlet 1.*

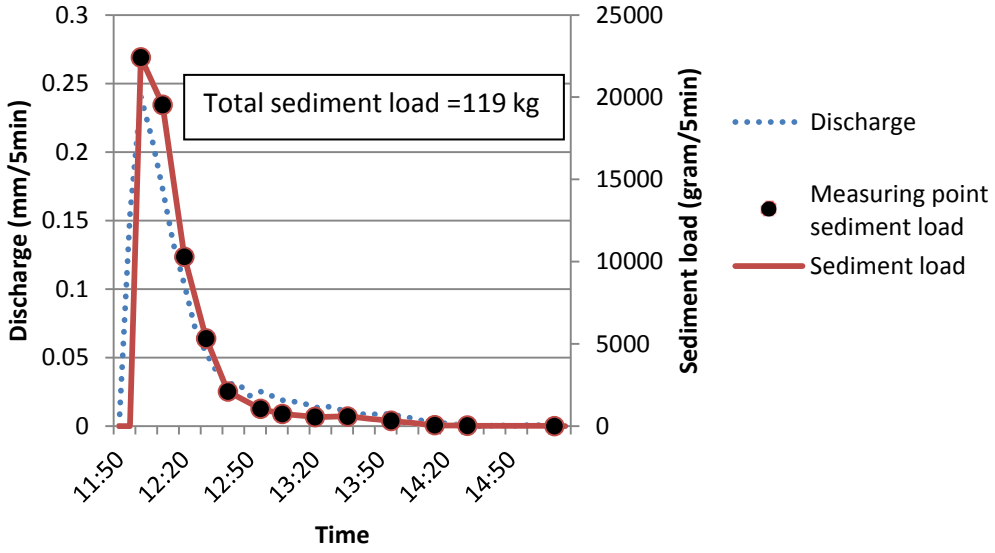

Figure 40 *Sediment load and discharge on the 22nd of December 2012 at outlet 2.*

The total sediment loads per event are shown in table 14 and table 16 for both catchment 1 and 2 respectively. The temporal pattern in sediment transport is the same as for runoff, because of the linear relation between runoff and sediment load transport. The total sediment load measured at outlet 1 over the whole research period is 1.35 ton. Since the transported sediment has a particle size between 0.45 and 20 µm, it is assumed that silt and clay particles are transported during the runoff events. A particle density of 2.8 g/cm^3 is used to calculate the volume of sediments that is transported. A sediment load of 1.35 ton will therefore correspond approximately to a sediment volume of 480 L. Table 15 shows the sediment load corresponding to the rainfall return periods for catchment 1.

The total amount of sediment measured at outlet 2 over the whole research period is 0.23 ton, which corresponds to a volume of 80 L of sediments. The sediment load corresponding to the rainfall return periods for catchment 2 are shown in table 17.

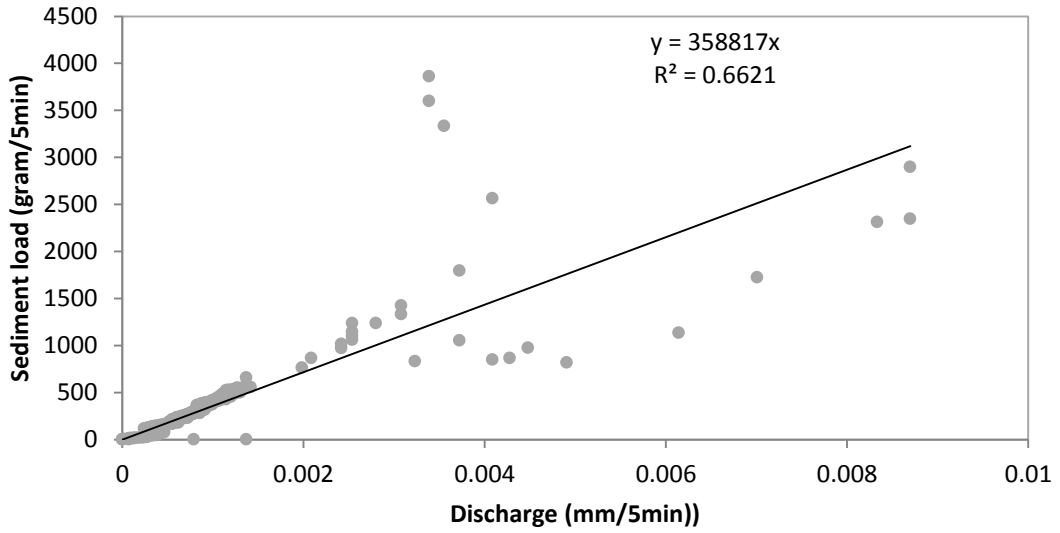

Figure 41 *Discharge sediment load relationship for catchment 1. Line crosses the y axes at zero, otherwise the calculated sediment loads are not plausible.*

Table 14 *Total sediment load transported during runoff events at outlet 1.*

Day event	Total sediment load [kg]	Total sediment load [dm³]	Runoff [mm]
19 October 2012	118	42	0.3
21 October 2012	483	173	1.3
22 October 2012	320	114	0.9
25 November 2012	24	9	0.1
3 December 2012	27	9	0.1
22 December 2012	123	44	0.3
24 December 2012	39	14	0.1
6 January 2013	33	12	0.1
7 January 2013	12	1	0.03 ~ 0
10 January 2013	167	60	0.05
Over whole research period	1346	481	3.8

Table 15 *Rainfall return period with associated discharge and sediment load for catchment 1.*

Return period [years]	Daily rainfall sum [mm]	Discharge [mm]	Sediment load [ton]	Sediment load [m³]
1	24	1	0.4	0.1
5	57	6	2	0.6
10	83	11	4	1
50	196	60	22	6
100	284	125	45	12
200	410	258	93	24

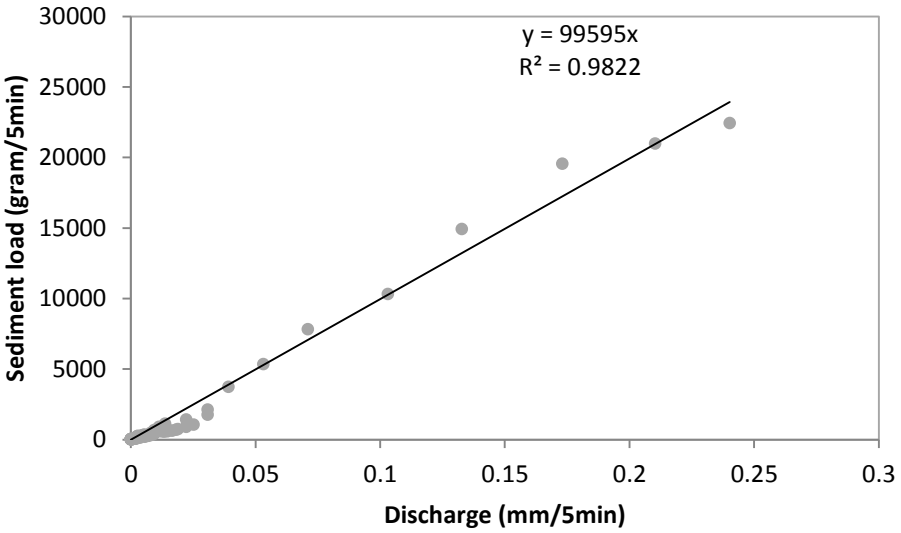

Figure 42 *Discharge sediment load relationship for catchment 2. Line crosses the y axes at zero, otherwise the calculated sediment load are not plausible.*

Table 16 Total sediment load transported during runoff events at outlet 2.

Day event	**Total sediment load [kg]**	**Total sediment load [dm³]**	**Runoff [mm]**
25 November 2012	7	3	0.11
22 December 2012	154	55	1.55
6 January 2013	64	23	0.64
Over whole research period	225	80	2.30

Table 17 *Rainfall return period with associated discharge and sediment load for catchment 2.*

Return period [years]	**Daily rainfall sum [mm]**	**Discharge [mm]**	**Sediment load [ton]**	**Sediment load [m³]**
1	24	4	0.4	0.1
5	57	20	2	0.7
10	83	43	4	2
50	196	196	20	6
100	284	284	28	10
200	410	410	41	15

Sediment sources

"Analysis of the flow sediment hysteresis shape may assist in determining the sediment source area in a small basin". (Klein, 1984) Therefore hysteresis curves are generated based on discharge and sediment load measurements on the 25th of November 2012 and the 22nd of December 2012 (figure 43 until figure 45). "A clockwise hysteresis occurs when sediment is derived from the bed and banks of the channel or areas adjacent to the channel, whereas an anti-clockwise hysteresis occurs when the upper part of the slopes is the sediment source area (Klein,

1984)." The hysteresis curve of the 25th of November 2012 runoff event at outlet 1 is let aside, since the sediment load measurements were not plausible. Figure 43 shows a clockwise hysteresis for catchment 1, which let assume that the transported sediments are from the beds or banks or areas near the gullies. Figure 44 and figure 45 show that the sediment comes from the areas further away from the channel in catchment 2, because of the anti-clockwise hysteresis.

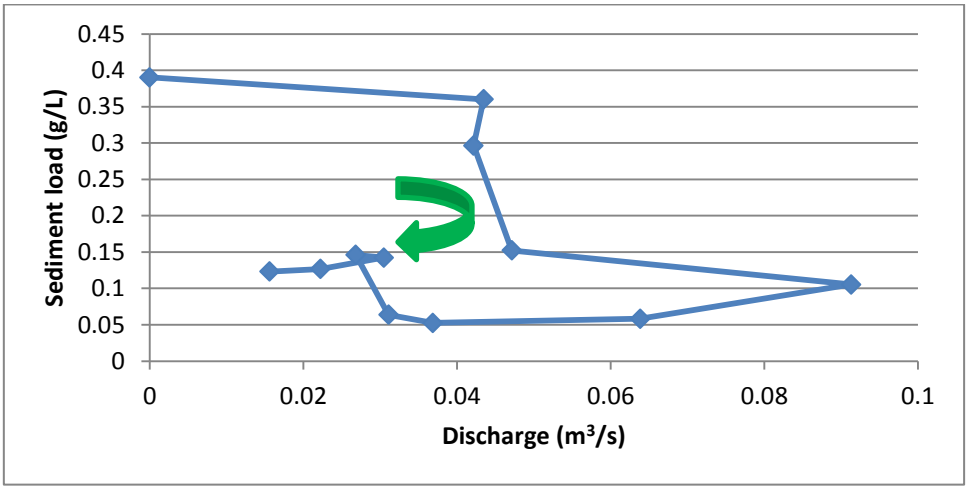

Figure 43 *Hysteresis curve Outlet 1 December 22 2012*

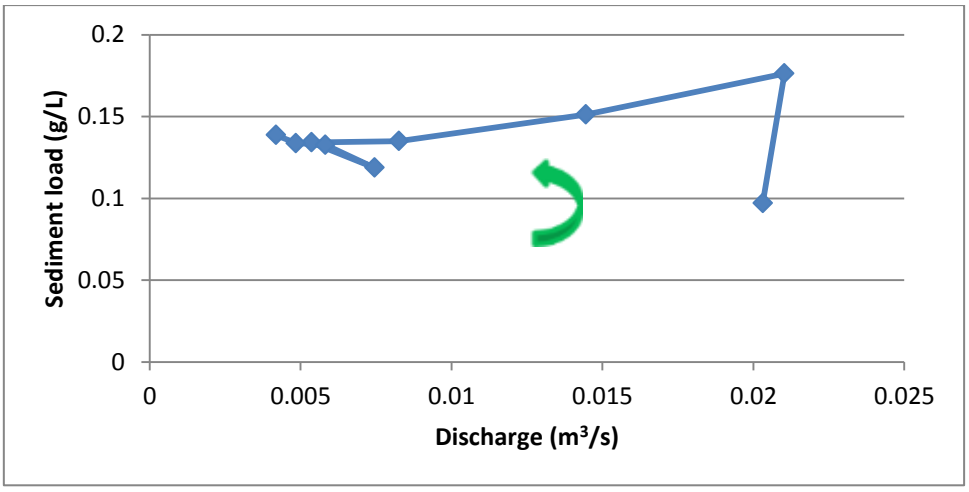

Figure 44 *Hysteresis curve Outlet 2 November 25 2012*

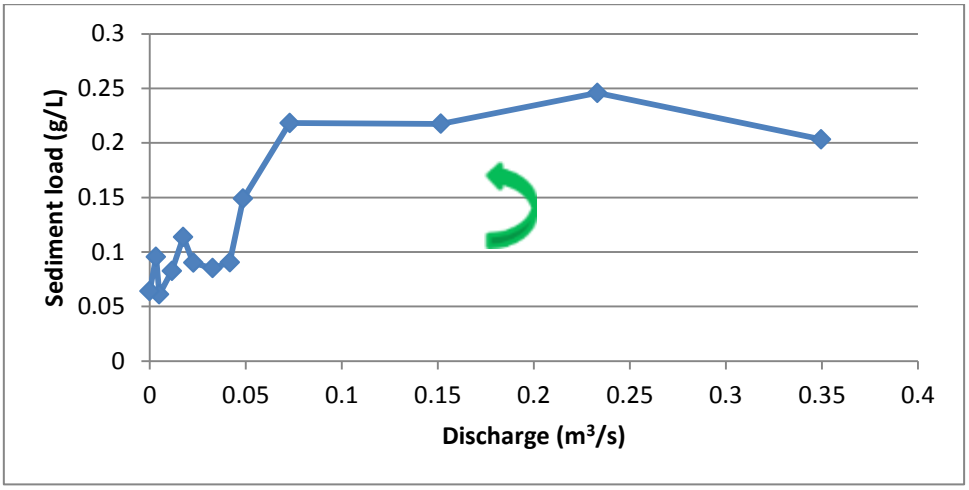

Figure 45 *Hysteresis curve Outlet 2 December 22 2012*

Figure 46 shows the locations where soil samples are taken. The sediment fractions are determined for all samples and a map is created using the Kriging interpolation technique. In appendix VII these maps can be found showing the sediment fractions distributed over the catchment areas. The maps include the flow patterns. Combining the flow patterns and the sediment fractions, no clear relation can been seen between the flow paths and the particle size fractions. However, assuming that the sediment which are transported by surface runoff have a particle size less than 63 μm, it seems that the areas further away from the flow paths and outlets are more sensitive to erosion than the areas nearby (figure 47). This does not corresponds to the hysteresis curves for outlet 1, but does for catchment 2. One has to be aware that the hysteresis curves are based on a small data set and the maps are created by the kriging interpolation technique. The accuracy of the patterns created by the kriging interpolation technique are questionable.

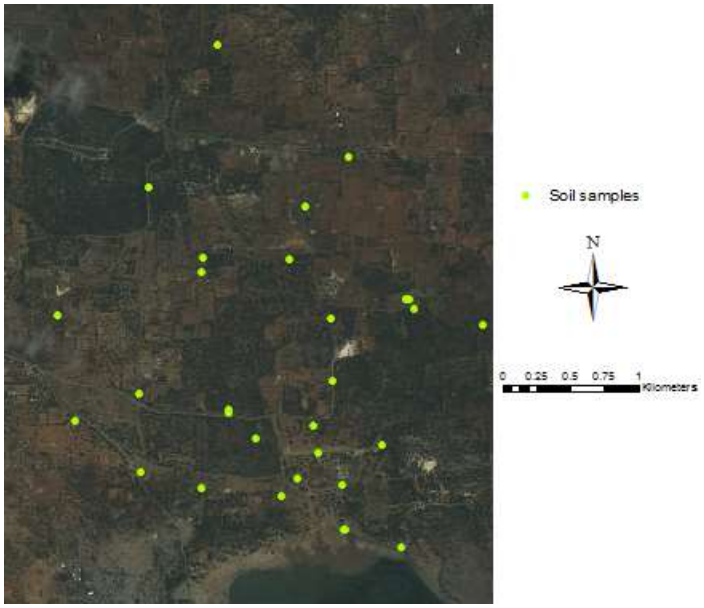

Figure 46 *Locations of soil samples.*

To say something about the sediment source in the sense if especially road or catchment material is transported towards the mangrove system, the suspended sediments are filtered by filters with different pore sizes. This resulted in a sediment size between 0.45 and 20 µm. Although the particle sizes are determined in the laboratory, the smallest sieve had a pore size of 63 µm. This means that no distinction can be made between areas which might contain the sediments that are transported and which not. However, based on a short interview with Pedro de Jong (appendix X), who told that each year approximately 2000 m^3 new diabase (volcanic rock) is deposited on the road it is expected that a high amount of road material is transported to the mangrove system. Although this is not proven by this study. Besides that is shown in figure 48 that road material (BSW1 and BSW2) mainly consist of soil particles bigger than 2 mm. It could be possible that the small particle were already eroded when the sample was taken.

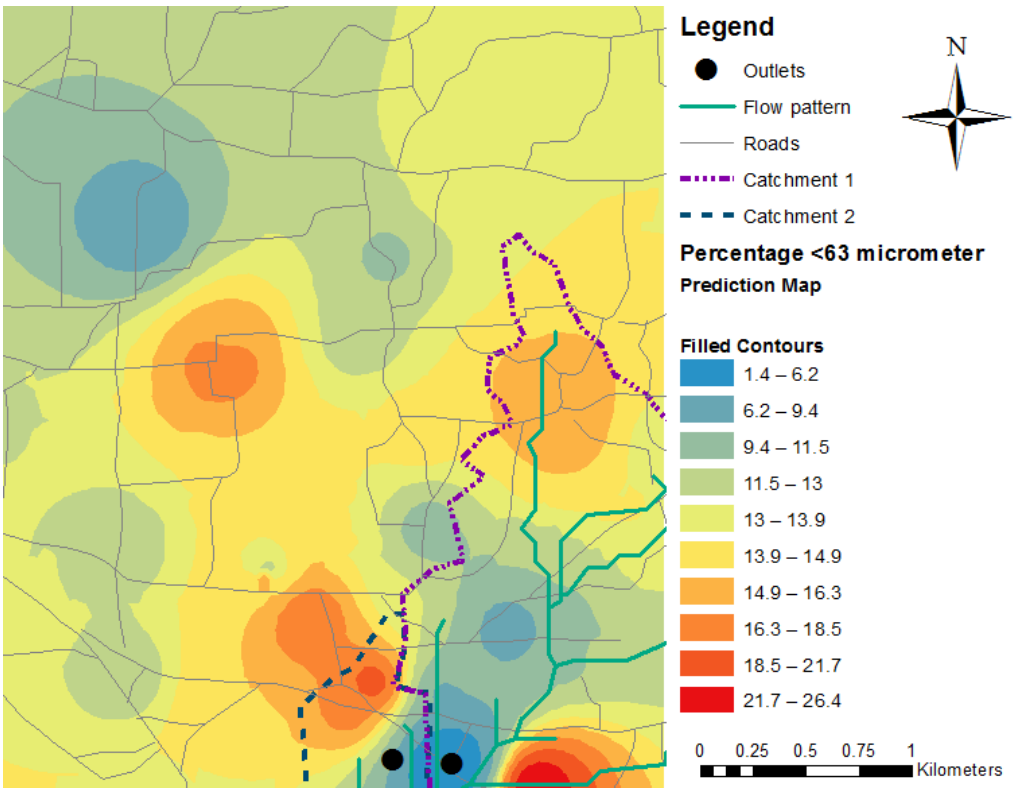

Figure 47 Soil fraction <63 *µm*.

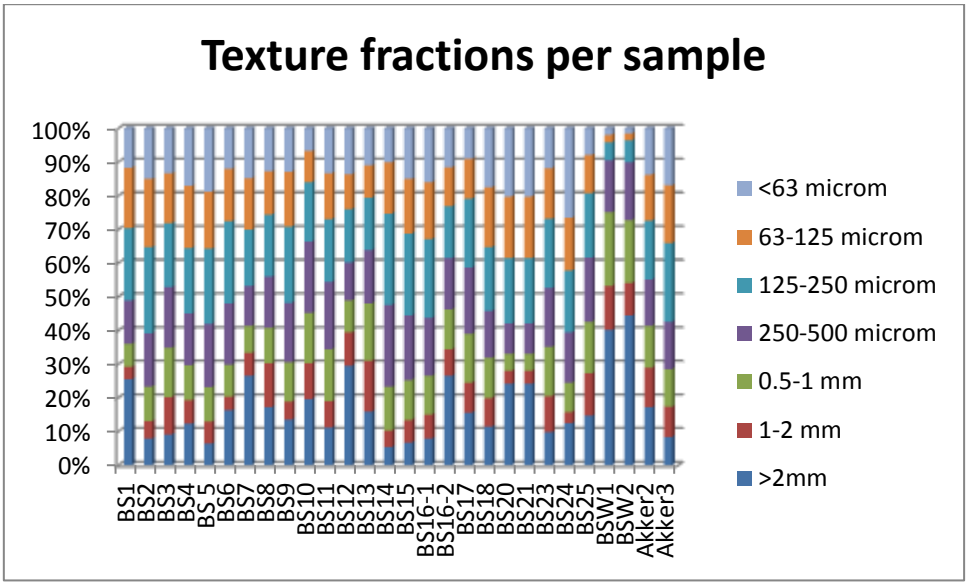

Figure 48 *Soil particle distribution per sample.*

4.5 Dam structures

Figure 49 shows all dams and excavations found within the watershed. It might be possible that there are more dams in the catchment area but these are not found because the major part of the area is inaccessible due to the dense vegetation of cacti und bushes. Nowadays, the dams serve primarily as water source for the livestock, especially goats and donkeys. Some farmers also have their own small dams. They use the collected water to irrigate their farmland, as drinking water for their livestock and sometimes for toilets and showers. Nevertheless, some dams are abandoned and their water storage is not optimal.

Figure 49 *Dams in research area.*

Most of the dams are found outside catchment 1 and 2. However, the biggest dam, the Mona Passage, overlaps both catchment 1 and 2 as also the remaining part of the upper catchment (figure 49). At eight points the dam height and the profile behind the dams is more precise determined (figure 51 and table 18), to get a more accurate insight in the storage capacity. There are two storage capacities determined as it is assume that during the rainy season at least the major part of the basin is filled with water. The basin is a tub just behind the wall of the dam (figure 51). In this case the dam stores approximately 8 dam^3 of water and when the whole area behind the dam is filled with water approximately 167 dam^3 of water is stored. It is assumed that there is no water flow through the dam. The mean storage during the research period was 3 dam^3, which is less than the maximum storage capacity. The rapid increase in water level after a rain event on the 22nd of December caused for an increase in storage behind the dam of approximately 180 m^3. Since the dam overlaps both catchment 1 and 2 as also the remaining

part of the upper catchment, it was not possible to estimate the runoff amount for catchment 1 and 2 when no dam would be present.

In order to determine whether the decrease in water level behind the dam is dominated by evaporation or infiltration a simple water balance has been made over the period from the 23th of December until the 5th of January. The evaporation equation (formula 6) for open water bodies is used for this purpose. In figure 50 can be seen that at some days rain events occurred. The cumulative amount of precipitation which is fallen until then is subtracted from the water level for each day. The water levels are corrected for the evaporation to determine the infiltration. The mean infiltration rate in this period was 1.1 cm/day and the mean evaporation was 0.5 cm/day, which show that infiltration behind the dams dominates. Rønde (2013) showed that the groundwater flows from the north towards Lac. It is therefore be assumed that water that infiltrates behind the dam will flow towards the mangrove system.

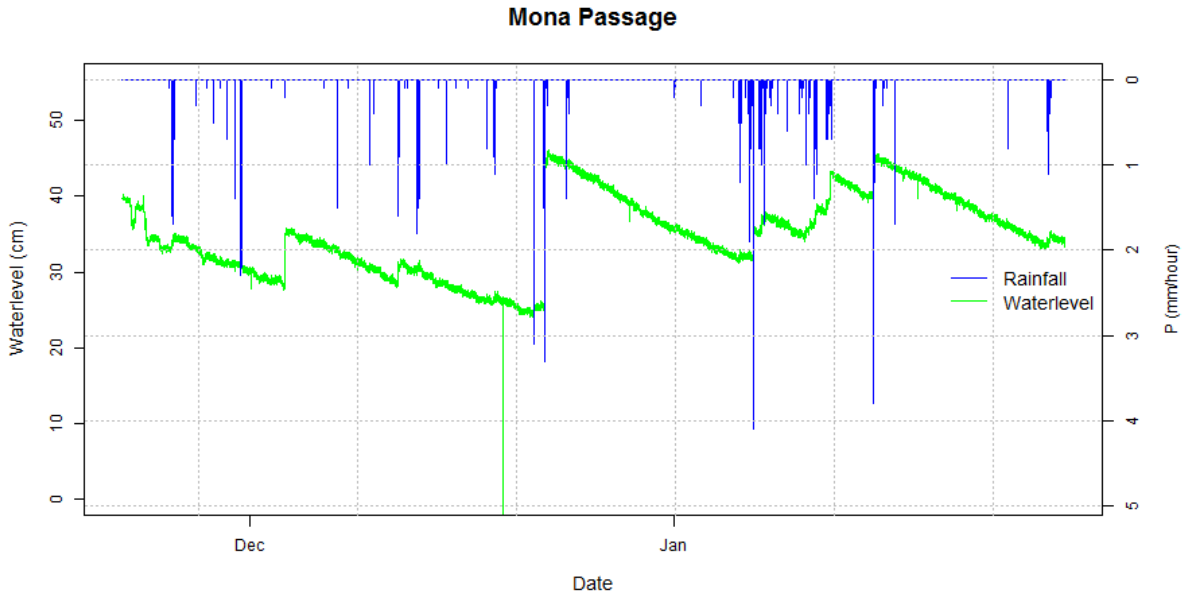

Figure 50 *Water level fluctuations behind the Mona Passage in relation to rainfall from 21 November 2012 until 29 January 2013.*

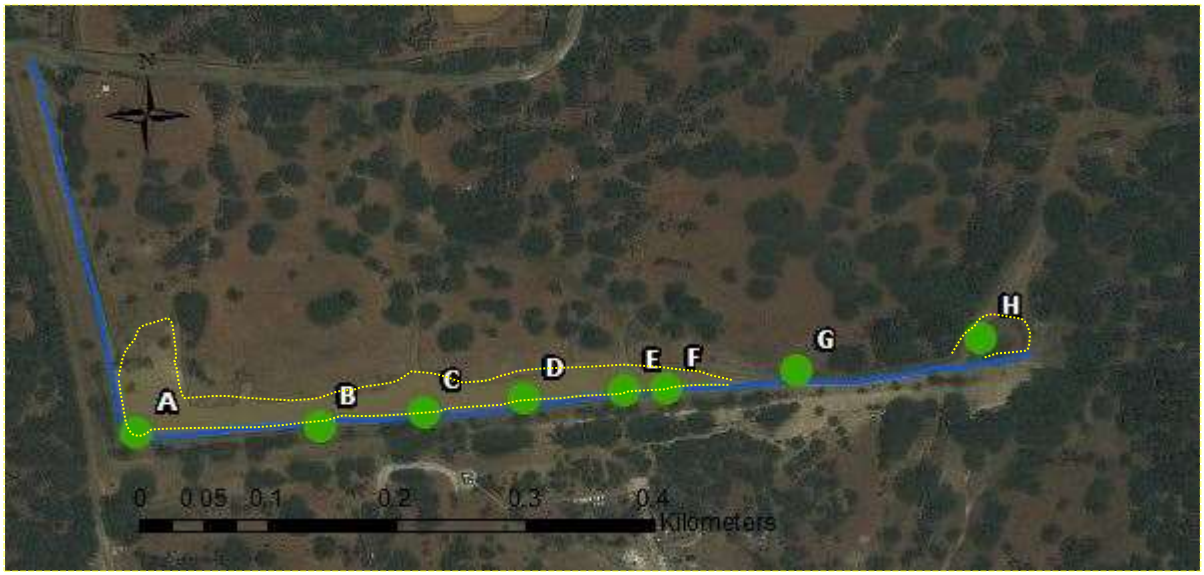

Figure 51 *Mona Passage, the biggest dam in the research area. The green dots are corresponding to Fout! Verwijzingsbron niet gevonden. which illustrates the basin profile (yellow dotted line).*

Table 18 *Dam height w.r.t. lowest point basin, field height w.r.t. lowest point basin, and basin width. The basin is a tub just behind the wall of the dam.*

	Dam height [m]	**Field height [m]**	**Basin width [m]**
A	4	1	48
B	3	1	16
C	Water inflow, gully.		
D	3.8	1.2	14
E	Water inflow, gully.		
F	4	1.6	14
G	3	1	4
H	3	-	-

5 Discussion

The accumulated rainfall over the research period (October 2012 until January 2013) was low in comparison with the 30 year average and median. This low rainfall amount resulted in low runoff amounts with return periods of less than 5 years and transported sediment loads with a return period of less than 1 year. However, this low accumulated rainfall sum is not exceptional, since for example a long lasting relatively dry period occurred from 1991 until 1999. On the other hand also extreme annual rainfall sums are measured in the past (1980, 1981, 1985, 1988, 2004 and 2005). This shows that the temporal variation in precipitation on Bonaire is high. The variation in runoff and sediment transport is linked to this variation in rainfall, but is less pronounced because of the power function that describes the relation between precipitation and runoff. Nevertheless, when a sufficient amount of precipitation is reached, evaporation can be neglected. In this situation it can be assumed that runoff is equal to precipitation.

Based on the water balance it is assumed that the runoff events and therefore sediment transport in the research period only occurred due to rain events that exceed the infiltration capacity. This occurred despite of a precipitation sum of less than the 30 year average. During relatively wet years, the soil profile can be relatively wet prior to rain events, causing saturation and runoff at relatively small rainfall events. This means that in relatively wet periods not only more fresh water will runoff due to the higher rainfall amounts, but it will also response faster to relatively low rainfall intensity events. It is therefore expected that soil saturation will influence the rainfall runoff relationship.

There are more causes that might influence the rainfall runoff relationship except the soil saturation. The rainfall runoff relationship determined in this research is therefore questionable due to various reasons. The southern part of Bonaire is rather flat which makes accurate runoff measurements difficult, since the water will not only flow through gullies, but will also flow towards the mangrove system as sheet flow. In addition, this small relief makes it difficult to determine the gully profiles. The measured gully profile of catchment 1 was for example too small, since the highest water levels measured by the diver were higher than the profile depth. Therefore the profiles are extended to each side. It is questionable if that represents the gully profile correctly. Besides that, rainfall measured by the tipping bucket is used to determine the rainfall runoff relationship for both catchments. Since the tipping bucket is located outside the catchment areas an uncertainty can be expected in the rainfall runoff relationships.

Since sediment transport is directly linked to water transport also uncertainties are expected in the runoff sediment load relations. In addition, the sediment loads are determined by taking water samples in the field and taking subsamples from those water samples in the laboratory. Lang (1992) showed that the use of bottle samplers and soil pipettes to sample soil water mixtures is inadequate and gives an underestimation of the actual sediment concentration. This poor sampling ability is attributed to rapid settlement of larger particles and to lacks in the sediment trapping ability of the samplers. The estimated sediment loads in this research period and the sediment loads for the different return periods are therefore probably underestimated due to various uncertainties. In addition, the type of sediment transported will differ for larger runoff amounts with larger water velocities than for small runoff amounts. So not only a higher total amount of sediments but also larger sediment particles will be transported during extreme events.

Figure 52 *Plumes of sediment loaded water flowing in the sea near Kralendijk (Antoin, 2004).*

Odum *et al.* reported in 1982 that mangroves grow best in depositional environments were accumulation of fine sediments occurs. This is the case on Bonaire where clay and silt particles dominate the sediments reaching the mangrove system. However, Ellison (1998) mentioned that excess input of sediments can cause dead of mangrove trees due to root smothering. Wagenaar Hummelink and Roos (1969) reported already in 1969 that the channels of Lac were overgrown in the last years probably due to increased sediment transport. The feeder tidal channels are favourable for net export of mud towards the major channels and the bay (Anthony, 2004; Wolanski et al., 1980, 1992; Boto and Bunt, 1981). Besides the negative effect on refreshment of the landside waters, overgrowing of creeks have therefore also an adverse effect on the net export of sediment. In 2004 flooding occurred on Bonaire with peak flows and high sediment fluxes near Kralendijk (figure 52) (Borst and de Haas, 2005). This flooding was caused by consecutive days of rainfall, with daily rainfall sums with a return period of less than 10 years.

However, the annual rainfall sums in the extreme years (1980, 1981, 1985, 1988 and 2005) were in comparison with 2004 more extreme and/or the high annual sums were caused by more extreme daily rainfall sums (return period larger than 10 years). Therefore it is expected that in these years also a significant amount of precipitation occurred, causing significant runoff and sediment deposition rates. The area is in addition very sensitive to erosion, since deterioration of the landscape occurs since the 17th century (Nolet and van der Veen, 2009), due to deforestation and overgrazing by goats and sheep's. Besides that, Peterson *et al.* (2002) showed that the maximum number of consecutive dry days is decreasing and the number of heavy rainfall events increases in the Caribbean region. This could be beneficial in term of fresh water influx to Lac, but has a negative effect because of the increased sediment transport. The high sediment transport rates towards the mangrove system in the past might have caused dead of mangrove trees due to root smothering (Ellison, 1998) which might continue when the number of extreme rainfall events increases. In addition, the long lasting relatively dry period from 1991 until 1998 caused less water movement towards the mangrove system which might have caused less refreshment of the landside waters in Lac.

Summarized, it is reasonable that smothering of the roots occurred due to an excess input of sediments in years of extreme annual sums. This caused mangrove die off due to the poor functioning of the feeder channels. Prolonged relative dry periods on the other hand (1991 until 1998) caused hyper saline waters due to hardly any fresh water fluxes towards the waters in the back of the mangrove system. Both situations have negative impacts on the mangrove growth and reinforce each other. In addition, despite that 2/3 of the water that is stored behind the dam leaches to the groundwater it is questionable if it reaches the mangrove system due to the highly karstified limestone (Sambeek *et al.*, 2000; Rønde, 2013). Removal of dams would cause an increase in surface runoff towards the mangrove system. However these dams also serve as sediment traps, which is favourable in regards to the sediment transport toward Lac.

7 Conclusions

This study focusses on fresh water and sediment dynamics towards the Lac mangrove system. In addition possible causes for the seaward shift of the mangrove forest are given. The most important conclusion drawn from this research are:

- The spatial and temporal variation of rainfall on Bonaire is high. It is been shown that high daily rainfall sums are associated with high rainfall intensities. However, the expectation that the rain falls in short duration showers with high intensities during rain events with high rainfall amounts cannot be proven.

- During the period of October 2012 until January 2013 less than 2% of the rainfall is transported by surface runoff towards the mangrove system in both catchments. This means that runoff have brought only relatively minor quantities of fresh water to Lac during the research period. The variation in runoff is linked to the variation in rainfall, but is less pronounced because of the power function that describes the relation between precipitation and runoff.

  For catchment 1 the rainfall runoff relation is:

  $$Q = 0.0015*P^2 + 0.0137*P$$

  For catchment 2 the rainfall runoff relation is:

  $$Q = 0.0062*P^2 + 0.003*P$$

  With:

  P : Rainfall [mm]

  Q : Runoff [mm]

Nevertheless, when a sufficient amount of precipitation is reached, evaporation can be neglected. In this situation it can be assumed that runoff is equal to precipitation.

- Low sediments amounts are transported to the mangrove system, associated with the low runoff amounts. During the period of October 2012 until January 2013 approximately 0.5 and 0.1 m^3 of sediments is transported toward the mangrove system respectively for catchment 1 and 2. The amount of sediment transported to the mangrove system depends on linear relationships.

For catchment 1 the runoff sediment load relation is:

*S = 358817*Q*

For catchment 2 the runoff sediment load relation is:

*S=99595*Q*

With:

Q : Runoff [mm]

S : Sediment load [gram]

- During the period of October 2012 until January 2013 surface runoff occurred due to events that exceed the infiltration capacity. This occurred despite of a precipitation sum of less than the 30 year average. During relatively wet years, the soil profile can be relatively wet prior to rain events, causing saturation and runoff at relatively small rainfall events. This means that in relatively wet periods not only more fresh water will runoff due to the higher rainfall amounts, but it will also response faster to relatively low rainfall intensity events.

- Extreme annual rainfall sums (1980, 1981, 1985, 1988, 2004, 2005) might have caused extreme sediment load transports toward the mangrove system. Along with the deterioration of the channels and the associated water circulation, this might have caused root smothering and mangrove die off. This mangrove die off is probably strengthened by a relatively dry period with less freshwater transport by surface runoff toward the mangrove system which enhances the hyper saline waters in the back of the system.

- A significant amount of water is stored behind the biggest dam in the catchment, the Mona Passage. Since the dam overlaps both catchment 1 and 2 as also the remaining part of the upper catchment, it was not possible to estimate the runoff amount in catchment 1 and 2 when no dam would be present. However, removal of dams would cause an increase in surface runoff towards the mangrove system. Approximately 2/3 of the water stored behind a dam will infiltrate. Depending of the direction of the groundwater flow and therefore the karstification, the water that infiltrates will flow towards the mangrove system.

8 Recommendation

- To gain more insight into the dynamics of the fresh water fluxes towards the Lac mangrove system in the Lac catchment and the associated sediment transport, precipitation, runoff and sediment measurements should be continued over a large number of years. This should result in better and more accurate rainfall runoff relationships and discharge sediment load relationships.

- Rainfall, surface runoff, and sediment transport monitoring over a large number of years together with monitoring the growth and the health of the mangrove forest could give more insight in how the mangrove systems reacts on hydrological changes over a number of years. Trends can be found by examining the changes over many years.

References

Alexander, C.S. (1961). The marine terraces of Aruba, Bonaire, and Curacao, Netherlands Antilles. *Annals of the Association of American Geographers*, *51*(1), 102-123.

Allen, R.G., Pereira, L.S., Raes, D., Smith, M. (1998). Crop evapotranspiration: Guidelines for computing crop water requirements. *Irrigation and drainage paper No. 56.* UN-FAO, Rome.

Anthony, E.J. (2004). Sediment dynamics and morphological stability of an estuarine mangrove complex: Sherbro Bay, West Africa*. Mar. Geol.* 208, 207–224.

Antoin, B., Antilliaans Dagblad, 2004.

Augustinus, P.G.E.F. (2005). *Een voorstudie van de te verwachten milieueffecten naar aanleiding vande bouw en exploitatie van een hotelschool, annex hotel, langs de westoever van het Lac, Bonaire.* Universiteit Twente, Enschede.

ArcGIS 9.2 Desktop Help. (2007). *How inverse distance weighted (IDW) interpolation works.* Environmental Systems Research Institute, Inc.

Borst, L., S.A. de Haas (2005). Hydrological Research Bonaire: A hydrogeological investigation of Bonaire's water system. Acacia Institute.

Boto, K.G., Bunt, J.S. (1981). Tidal export of particulate matter from a northern Australian mangrove system. *Estuar. Coast. Shelf Sci*. 13, 247–255.

Debrot, A., Meesters, E., Slijkerman, D. (2010). Assessment of Ramsar site Lac Bonaire – June 2010. IMARES (Institute for Marine Resources & Ecosystem Studies) Report C066/10, 31 pp.

Debrot, A., Wentink, C., Wulfsen, A. (2012). Baseline survey of anthropogenic pressures for the Lac Bay ecosystem, Bonaire. IMARES (Institute for Marine Resources & Ecosystem Studies) Report C092/12, 71 pp.

Dirksen, C. (1999). Soil physical measurements.

Doneen, L.D., Westcot, D.W. (1984). Irrigation practice and water management (Rev. 1)*. FAO Irrigation and Drainage Paper 1*. Rome, Italy.

Ellison, J.C. (1998). Impacts of sediment burial on mangroves. *Mar. Pollut. Bull*.37, 8–12.

Erdmann, W. and A. Sheffers. 2006. *Mangrove population of Lac (Bonaire) 1961 and 1996.* Universität Duisburg-Essen.

Ewel, K.C., Twilley, R.R., Ong, J.E. (1998). Different Kinds of Mangrove Foreststst Provide Different Goods and Services. *Global Ecol. And Biogeog. Lett.* 7, 83-94.

Van Kekem, A.J., Roest, C. W.J., van der Salm, C. (2006). *Critical review of the proposed irrigation and effluent standards for Bonaire*. Alterra.

Kirkman, H. (1978). Decline of seagrass in northern areas of Moreton Bay, Queensland. *Aquat. Bot*. 5, 63-76.

Kjerfve, B. (1990). Manual for investigation of hydrological processes in mangrove ecosystems. UNESCO/UNDP, New Delhi, 79 pp.

Klein, M. (1984). Anti-clockwise hysteresis in suspended sediment concentration during individual storms. *Catena*, 11: 251-257.

Koster, G. (2013). Mapping runoff and erosion to reduce urban flooding and sediment flow towards sea. A case study on the Playa catchment, Bonaire. MSc Thesis – Water and Resources Management Group Soil Physics and Land Management Group. Wageningen University.

Lang, R.D. (1992). Accuracy of two sampling methods used to estimate sediment concentrations in runoff from soil-loss plots. *Earth Surf Processes Landforms, 17*: 841-844.

van der Lelij, R., Spikings, R.A., Kerr, A. C., Kounov, A., Cosca, M., Chew, D., & Villagomez, D. (2010). Thermochronology and tectonics of the Leeward Antilles: Evolution of the southern Caribbean Plate boundary zone. *Tectonics*, *29*(6).

Van Loon, A.F. (2005). Water flow and tidal influence in a mangrove-delta system, Can Gio, Vietnam. M.Sc. Thesis. Department of Environmental Sciences, Sub-department Water Resources, Wageningen University, The Netherlands.

Lott, C.E. (2001). Lac Bay, Then and Now... a Historical Interpretation of Environmental Change During the 1900s: A Site Characterisation of Lac Bay for Resource Managers and Naturalists. Environics NV Bonaire.

Marshall, N. (1994). Mangrove conservation in relation to overall environmental consideration. *Hydrobiologia* 285: 303–309.

Moorsel, G.W.N.M. van, A.J.M. Meijer (1993). Base-line ecological study van het Lac op Bonaire. Bureau Waardenburg BV, adviseurs voor milieu en ecologie. 116 pp

Mumby, P.J., Edwards, A.J., Arias-Gonzalez, J.E., Lindeman, K.C., Blackwell, P.G., Gall, A. et al. (2004). Mangroves enhance the biomass of coral reef fish communities in the Caribbean. *Nature*, 427, 533–536.

Nagelkerken, I., van der Velde, G., Gorissen, M.W., Meijer, G.J., van't Hof, T., den Hartog, C. (2000). Importance of mangroves, seagrass beds and the shallow coral reef as a nursery for important coral reef fishes, using a visual census technique. *Estuar. Coastal Shelf Sci.* 51: 31-44.

Neverauskas, V. P. (1988). Response of a Posidonia community to prolonged reduction in light. *Aquat. Bot*. 31,361-366.

Nolet, C., van der Veen, M. (2009). Stofonderzoek Bonaire. Bachelor thesis Internationaal land- en Water Management. Commissioned by Stichting KibraHacha. Wageningen University.

Odum, W.E., McIvor, C.C., Smith III, T.J. (1982). *The ecology of the mangroves of south Florida: a community profile*. Virginia Univ Charlottesville Dept of Evnironmental Scienses.

Peterson, T.C., Taylor, M.A., Demeritte, R., Duncombe, D.L., Burton, S., Thompson, F., Porter, A., Mercedes, M., Villegas, E., Semexant Fils, R., Klein Tank, A., Martis, A., Warner, R., Joyette, A., Mills, W., Alexander, L., Gleason, B. (2002). Recent changes in climate extremes in the Caribbean region. *J. Geophys. Res.* 107 (D21), 4601, doi:10.1029/2002JD002251.

Pijpers, P.J. (1933). Geology and paleontology of Bonaire. *Dissert. Utrecht*.

Rivera-Monroy, V.H., Twilley, R.R. (1996). The relative role of denitrification and immobilization in the fate of inorganic nitrogen in mangrove sediments. *Limnology and Oceanography* 41: 284–296.

Saenger, P., Hegerl, E.J., Davie, J.D.S. (1983). Global status of mangrove ecosystems. *The Environmentalist 3* (supplement 3).

Rønde, V. (2013), Investigation of subsurface freshwater flow from southern Bonaire into Lac bay. MSc Thesis – Hydrology and Quantitative Water Management. Wageningen University.

Spalding, M.D., Blasco, F., Field C.D. (1997). World Mangrove Atlas. Okinawa(Japan): International Society for Mangrove Ecosystems.

Teas, H. (1977). Ecology and restoration of mangrove shorelines in Florida. *Environ. Conserv.,* 4, 51-7.

Valiela, I., Bowen, J. L. & York, J. K. (2001). Mangrove forests: One of the world's threatened major tropical environments. Bioscience 51, 807–815.

Wagenaar-Hummelink, P. and P. J. Roos. (1969). Een natuurwetenschappelijk onderzoek gericht op het behoud van het Lac op Bonaire. Nieuwe West-Indische Gids 47: 1-28, plus ill.

Wells, J. and Debrot, A.O. (2008). Bonaire. Pp. 95-102. In: D. C. Wege and V. Anadon-Irizarry. Important Bird Areas in the Caribbean: key sites for conservation. Cambridge, UK: BirdLife International (BirdLife Conservation Series 15).

Wolanski, E., Jones, M., Bunt, J.S. (1980). Hydrodynamics of a tidal creek-mangrove swamp system. *Aust. J. Mar. Freshw. Res.* 31, 431–450.

Tam, N.F.Y., Wong, Y.S. (1999). Mangrove soils in removing pollutants from municipal wastewater of different salinities. *Journal of Environmental Quality* 28: 556–564.

Thien, S.J. (1979). A flow diagram for teaching texture by feel analysis. *Journal of Agronomic Education.* 8:54-55.

Appendices

Appendix I Evapotranspiration

Reference evapotranspiration was estimated from the Penman-Monteith method (FAO56):

$$ET_0 = \frac{0.408\Delta(R_n - G) + \gamma \frac{900}{T+273} u_2 (e_s - e_a)}{\Delta + \gamma(1 + 0.34u_2)} \quad (1)$$

- ET_0 [mm d^{-1}]: reference evapotranspiration
- T [˚C]: mean daily air temperature
- u_2 [m s^{-1}]: wind speed at 2m height
- γ [kPa ˚C^{-1}]: psychrometric constant
- (e_s – e_a) [kPa]: vapor pressure deficit.
- Δ [kPa ˚C^{-1}]: slope of vapor pressure curve
- G [MJ $m^{-2}d^{-1}$]: soil heat flux density
- R_n [MJ $m^{-2}d^{-1}$]: net radiation at the crop surface

The parameters in equation 1 were estimated from the following input data:

- minimum daily temperature (T_{min}) [˚C]
- maximum daily temperature (T_{max}) [˚C]
- daily dew point temperature (T_{dew}) [˚C]
- wind speed (u) [m s^{-1}]
- altitude of measuring location (z) [m]
  (Flamingo airport is located at an altitude of 7m: z=7m)
- latitude [decimal degree]
  (a latitude of 12.13˚ is used)

Calculations are shown on the following pages.

- **Mean daily air temperature (T):**
  Mean daily air temperature was calculated as:
  $$T = \frac{T_{min} + T_{max}}{2}$$

- **Wind speed at 2m height (u_2):**
  Wind speed data was available from Flamingo airport. The airport is, however, located at an altitude of 7m+msl, so a correction for height was made:

  $$u_2 = \frac{u \cdot 4.87}{log(67.8 \cdot z - 5.42)}$$

- **The psychometric constant (γ)**
  First the pressure (P) at measuring location was calculated:
  $$P = 101.3 \cdot \left(\frac{293 - 0.0065 \cdot z}{293}^{5.26}\right) \text{kPa}$$

  Then γ was calculated as:
  $$\gamma = \frac{C_p \cdot P}{\varepsilon \cdot \lambda}$$

  - C_P [MJ kg-1 °C^{-1}]: specific heat (=1.013·10^{-3} MJ kg-1 °C^{-1})
  - λ [MJ kg^{-1}]: latent heat of vaporization (=2.45MJ kg^{-1})
  - ε [-]: ratio molecular weight of water vapor/dry air (= 0.622)

- **Vapor pressure deficit ($e_S - e_a$):**
  First minimum and maximum saturation vapor pressure was calculated:

  $$e_{s,min} = 0.6108^{\frac{17.27 \cdot T_{min}}{T_{min} + 237.3}}$$
  $$e_{s,max} = 0.6108^{\frac{17.27 \cdot T_{max}}{T_{max} + 237.3}}$$

  - $e_{s,min}$ [kPa]: daily minimum saturation vapor pressure
  - $e_{s,max}$ [kPa]: daily maximum saturation vapor pressure

  Then the saturation temperature was calculated as:
  $$e_S = \frac{e_{S,min} + e_{S,max}}{2}$$

  The daily actual vapor pressure was estimated from dew point temperature:
  $$e_a = 0.6108^{\frac{17.27 \cdot T_{dew}}{T_{dew} + 237.3}}$$

  Finally, the vapor pressure deficit could be computed:
  $$e_s - e_a$$

- **Slope of vapor pressure curve (Δ):**
  The slope of the vapor pressure curve was calculated by the following formula:

$$\Delta = \frac{4098 \cdot 0.6108^{\frac{17.27 \cdot T}{T+237.3}}}{(T+237.3)^2}$$

- **Soil heat flux density (G):**
  The soil heat flux density was neglected:
  G=0

- **Net radiation at the crop surface (R_n):**
  First, extra-terrestrial radiation was estimated as:

$$R_a = \frac{24 \cdot 60}{\pi} \cdot 0.082 \cdot d_r \cdot (\omega \cdot \sin(\varphi) \cdot \sin(\delta) + \cos(\varphi) \cdot \cos(\delta) \cdot \sin(\omega))$$

  - R_a [MJ m^{-2}d^{-1}]: extra-terrestrial radiation
  - d_r [-] inverse relative distance Earth-sun
  - ω [rad]: solar time angle
  - φ [rad]: latitude
  - δ [rad]: solar declination

  d_r and δ can be calculated from day of the year (J):

$$d_r = 1 + 0.033 \cdot \cos\left(\frac{2\pi}{365} \cdot J\right) \quad \text{and} \quad \delta = 0.409 \cdot \sin\left(\frac{2\pi}{365} \cdot J - 1.39\right),$$

  ω can be calculated from φ and δ:

$$\omega = Arccos(-\tan(\varphi) \cdot \tan(\delta))$$

  φ can be calculated from latitude in decimal degrees:

$$\varphi = latitude \cdot \frac{\pi}{180}$$

  Rather than estimating shortwave radiation from minimum and maximum temperature, an empirical formula for island conditions was used:

$$R_S = 0.7 \cdot R_a - b$$

  - R_S [MJ m^{-2}d^{-1}]: shortwave radiation
  - b [MJ m^{-2} d^{-1}]: empirical constant (=4MJ m^{-2}d^{-1})

  The net shortwave radiation was calculated as:

$$R_{nS} = (1 - \alpha) \cdot R_S$$

  - R_{nS} [MJ m^{-2}d^{-1}]: net shortwave radiation
  - α [-]: albedo (assumed to be 0.23)

  The clear-sky shortwave radiation is calculated from:

$$R_{SO} = (0.75 + 2 \cdot 10^{-5} \cdot z) \cdot R_a$$

- R_{S0} [MJ m^{-2}d^{-1}]: clear-sky shortwave radiation

The net longwave radiation can then be calculated via the following equation:

$$R_{nL} = 4.90310 \cdot^{-9} \frac{(T_{max}+273.15)^4+(T_{min}+273.15)^4}{2}\left(0.34 - 0.14\sqrt{e_a}\right)\left(1.35 \cdot \frac{R_S}{R_{SO}} - 0.35\right)$$

- R_{nL} [MJ m^{-2}d^{-1}]: net longwave radiation

Finally, the net radiation was calculated by:

$$R_n = R_{nS} - R_{nL}$$

Source: Rønde (2013)

Appendix II Air pressure

Because data from a baro diver in Bonaire due to technical reasons couldn't be downloaded, an air pressure data set was constructed from four different divers present in Bonaire. Diver locations and measuring periods can be seen in the table below:

Period	Start	End	Diver name	Location	Adjustment (mm)	St. dev. (mm)
A	2012-10-10 18:00	2012-10-19 10:55	1	12.125725, -68.230915	39	2
B	2012-10-19 11:00	2012-10-20 17:55	No data	-	-	-
C	2012-10-20 18:00	2012-11-23 10:55	2	12.125878, -68.233466	58	4
D	2012-11-23 11:00	2012-11-30 16:25	3	NA	15	2
E	2012-11-30 16:30	2013-01-29 12:50	4	12.160229, -68.280921	-20	9

A time series plot of the air pressure data set constructed as described above shows jumps in between the various divers, suggesting that absolute values are inaccurate. Therefore, air pressure measured by the divers is corrected with daily average values measured at the meteorological station at the airport on Bonaire in the following way:

The differences between daily averages measured at the airport and daily averages computed from the diver data set were calculated. Then for each of the periods A, C, D and E, the mean of this difference was calculated, respectively, and used as adjustment value in the corresponding periods of the high temporal resolution air pressure dataset. The first and last day and days overlapping two periods are not used in the calibration. Adjustment values and standard deviations are shown in the table above.

The period in which no air pressure measurements toke place, interpolation has been done by taking the average of last (calibrated) measurements at corresponding time step measured by baro diver 1 and first (calibrated) measurement at corresponding time step measured by baro diver 2.

Still, after the calibration, jumps in the transition from diver 2 to 3 and 3 to 4 were present (18 and 24mm, respectively). Because diver 3 operated for the shortest period, diver data from this diver is shifted 21mm (mean value of the jumps) to minimize the jumps. The final air pressure used for calibration is shown in the figure next page.

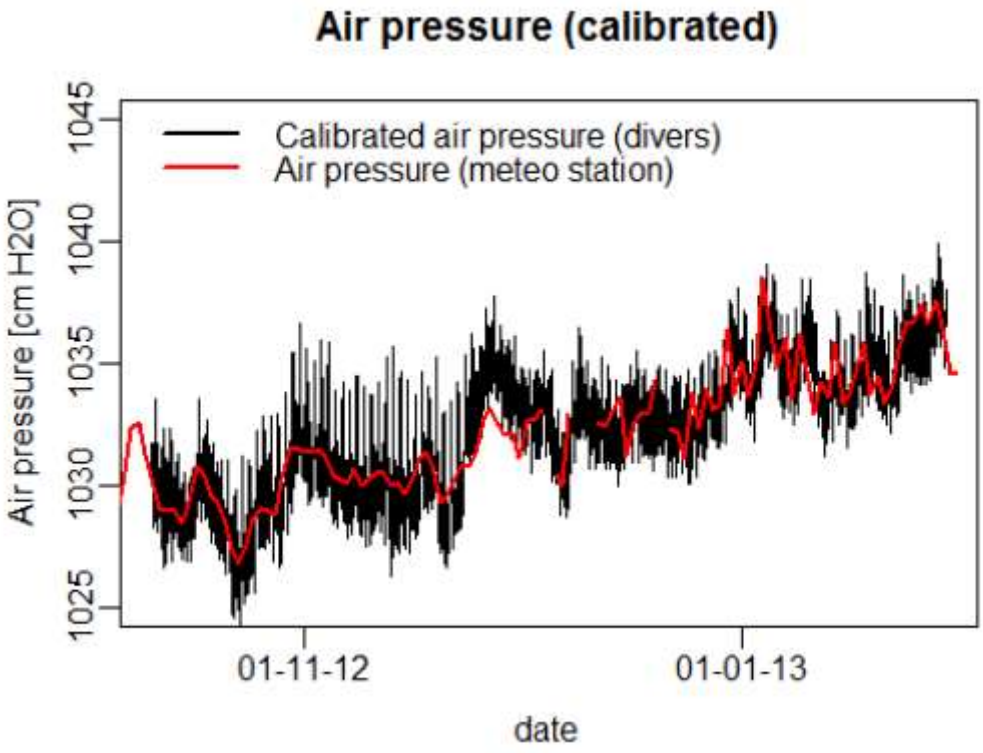

Source: Rønde (2013)

Appendix III Guide to soil moisture content.

	Texture			
	Coarse (sand, loamy sand)	**Moderately coarse (sandy or silt loam)**	**Medium (loam, clay loam, silty clay loam, silt, sandy clay)**	**Fine (clay, silty clay or light clay)**
At field capacity, contains:	60-100	100-150	150-200	200-250
	(mm available moisture per meter of soil)			
Soil moisture content				
Above field capacity	Water appears when soil is bounced in hand	Water released when soil is kneaded	Can sqeeze out water	Puddles and water form on surface
Field capacity	Upon squeezing, no free water appears on soil but wet outline of ball is left on hand			
75-100% available moisture	Tends to stick together slightly. Sometimes forms a weak ball under pressure.	Forms weak ball, breaks easily, will not slick.	Forms a ball and is very pliable, slicks readily if relatively high in clay.	Easily forms a ribbon between fingers, has a slicky feeling.
50-75% available moisture	Appears to be dry, will not form a ball under pressure.	Tends to ball under pressure, but seldom holds together.	Forms a ball, somewhat plastic, sometimes slicks slightly with pressure.	Forms a ball, ribbons out between thumb and forefinger.
25-50% available moisture	Appears to be dry, will not form a ball under pressure.	Appears to be dry, will not form a ball under pressure.	Somewhat crumbly, but forms a ball.	Somewhat pliable. Will form a ball under pressure.
0-15% available moisture	Dry, loose single-grained. Flows through fingers.	Dry, loose. Flows through fingers.	Powdery, dry, sometimes slightly crusted, but easily broken down into powder.	Looks moist but will not quite form a ball.

Source: Doneen, L.D. and Westcot, D.W. (1984)

Appendix IV Saturated hydraulic conductivity

Use the saturated sample(s) you did not weigh, and that remains on the K_{sat} sandbox. Build the set-up as depicted in figure X-1 (according Dirksen (1999) page 76-79). Note that the taped rim around the top of the sample should extend at least 2 cm above the top of the sample, and needs to be water tight. When sample rings are damaged, the edge is sometimes honed, which shortens the sample. Measure the sample height z (cm) in order to accurately calculate K_{sat}.

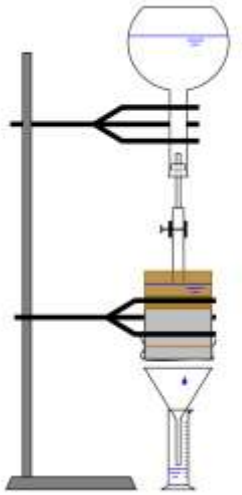

Figure IV-1 *Experimental set-up for measuring the saturated hydraulic conductivity with free outflow. The inverted flask with the tube reaching down to within the taped rim (brown) serves as a Mariotte flask that maintains a constant water level above the sample (gray cylinder).*

After completing the set-up, slowly open up the valve to release water gently from the inverted flask until the water level reaches the bottom of the outflow tube. Then, completely open the valve. When the water level is constant, record the depth d (in cm) of the water layer.

Monitor the outflow by recording the flow rate in regular intervals and wait until the flow is steady (you may need a separate work form for this). At that time, make at least five readings of time intervals and cumulative percolation (this amounts to six readings of the time t_i (s) and the percolated volume V_i (cm3)).

Calculate the flux densities q_i (cm d^{-1}) for each of the five intervals from the sample radius r (cm), and the percolation data, and pay particular attention to the first one or two, and discard them if they deviate too much from the later readings. Treat the remaining intervals as a single large interval and work out the value of Ksat (in cm d^{-1}) from the aggregated flux density by proper application of Darcy's Law (eq 2).

Darcy's law: $$q = -k[\theta] * \frac{\partial H}{\partial s} = -k[\theta] * (\frac{\partial z}{\partial s} + \frac{\partial h}{\partial s})$$

Source: Manual SEG-21306 Subsurface Solute Transport 2010

Appendix V Cumulative rainfall handmade rain gauges.

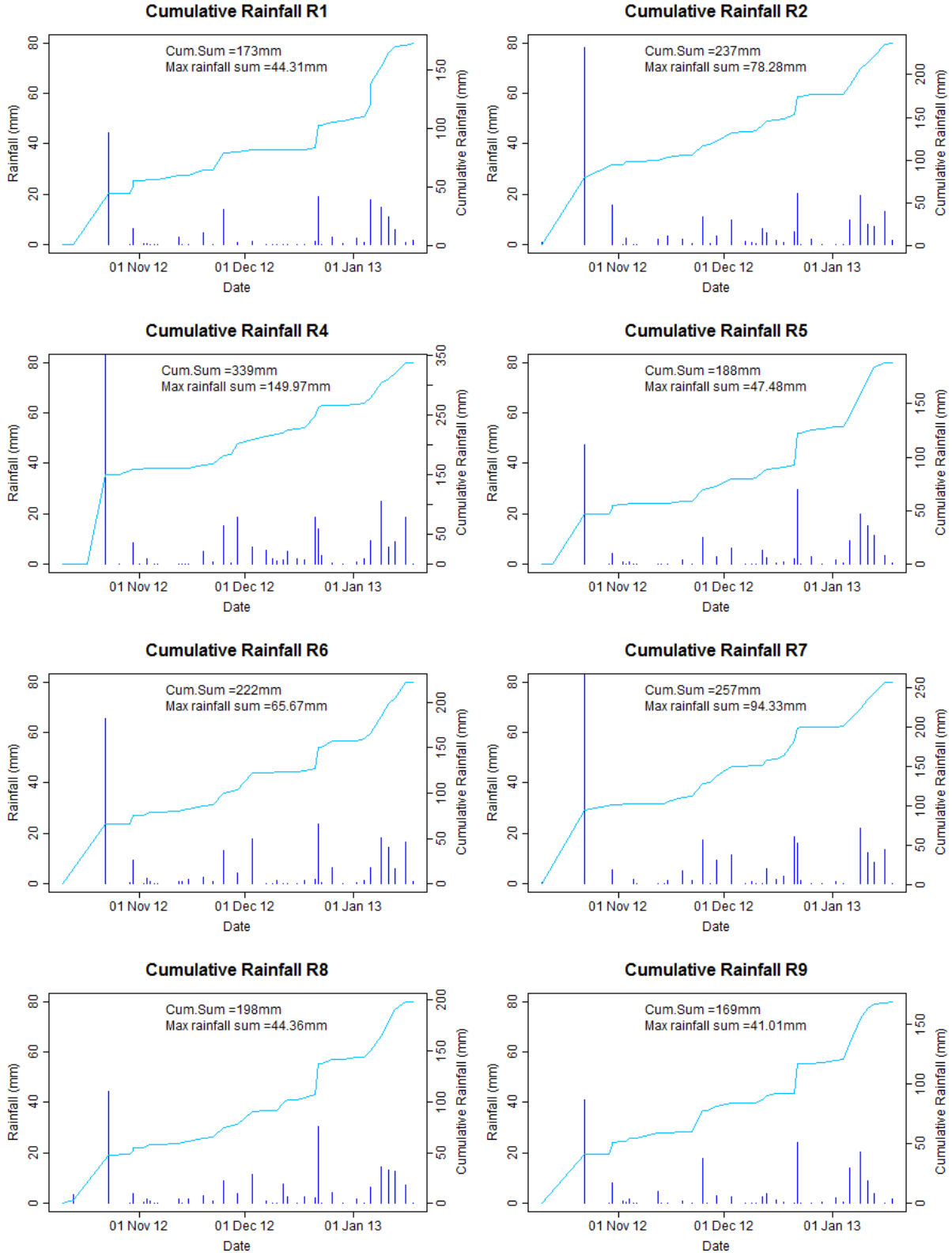

Appendix VI Instruction manual soil texture.

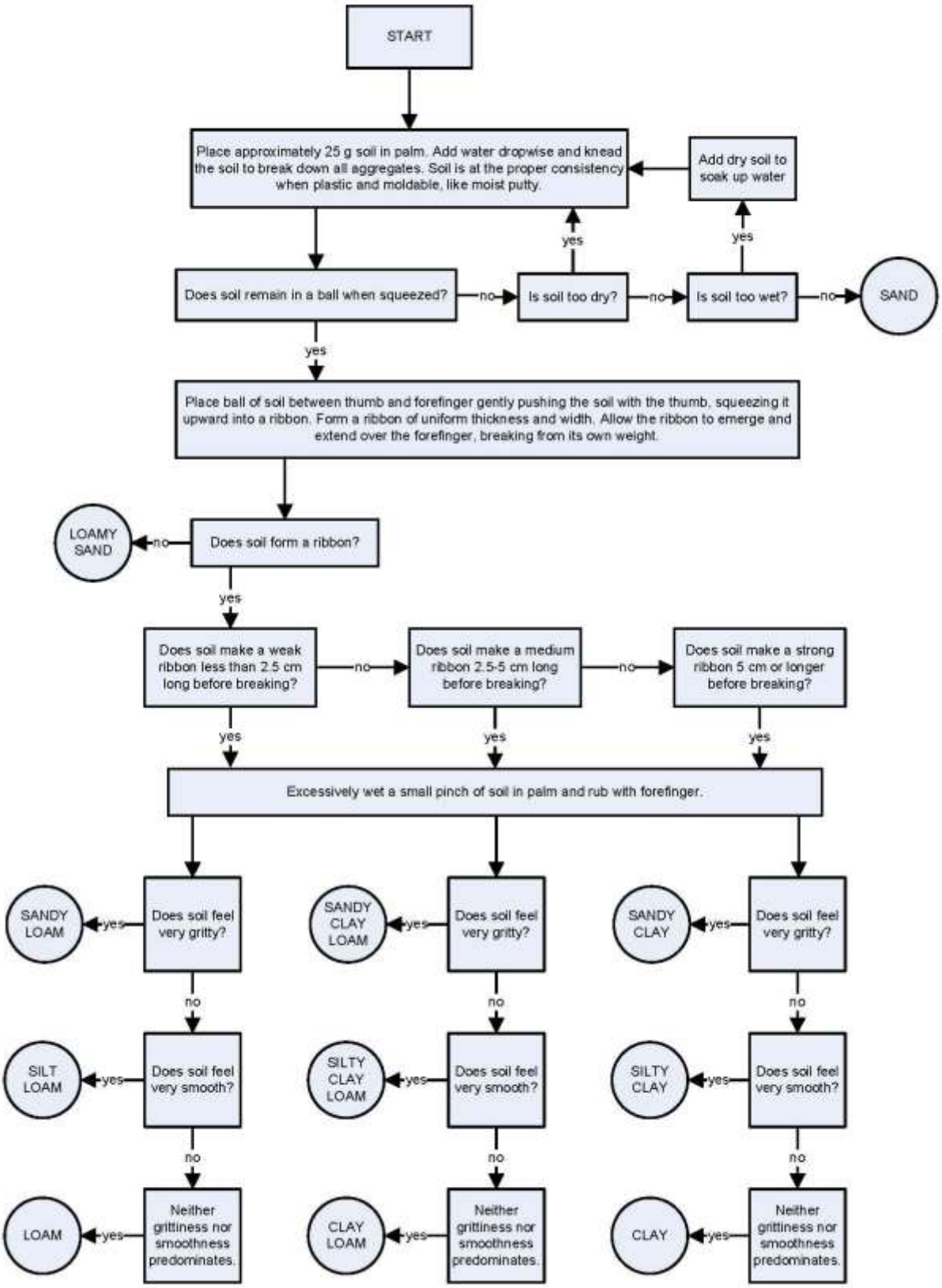

Source: Thien (1979)

Appendix VII Soil fraction prediction maps

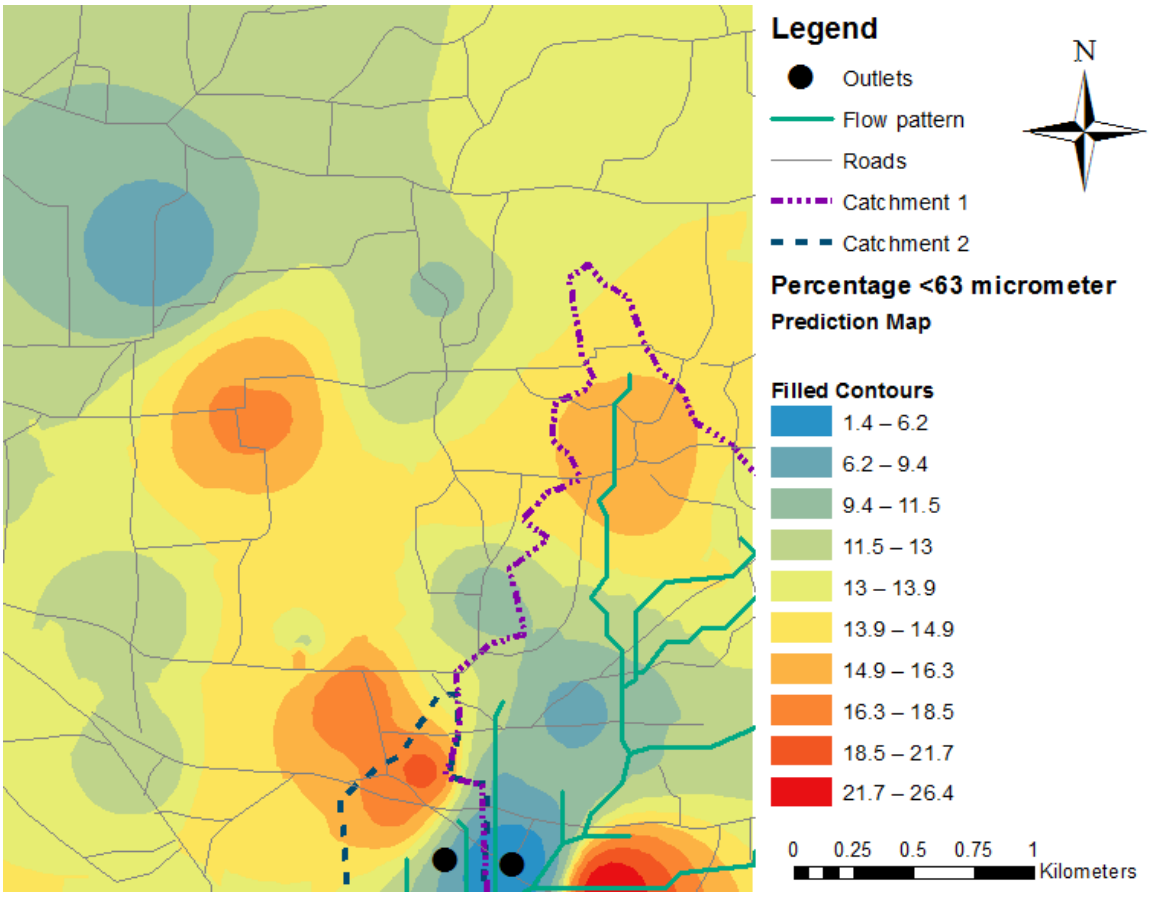

Figure VII-1 *Soil fraction <63 µm.*

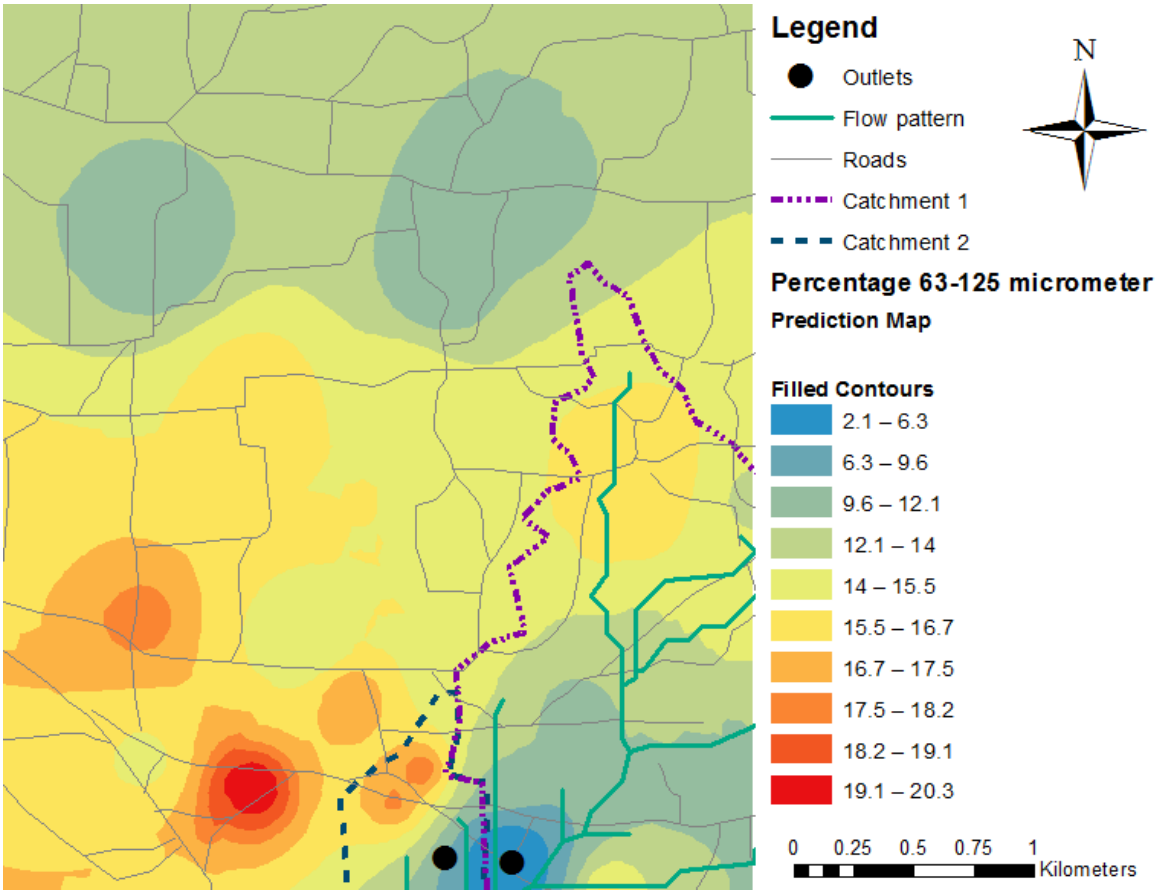

Figure VII-2 *Soil fraction 63-125 μm.*

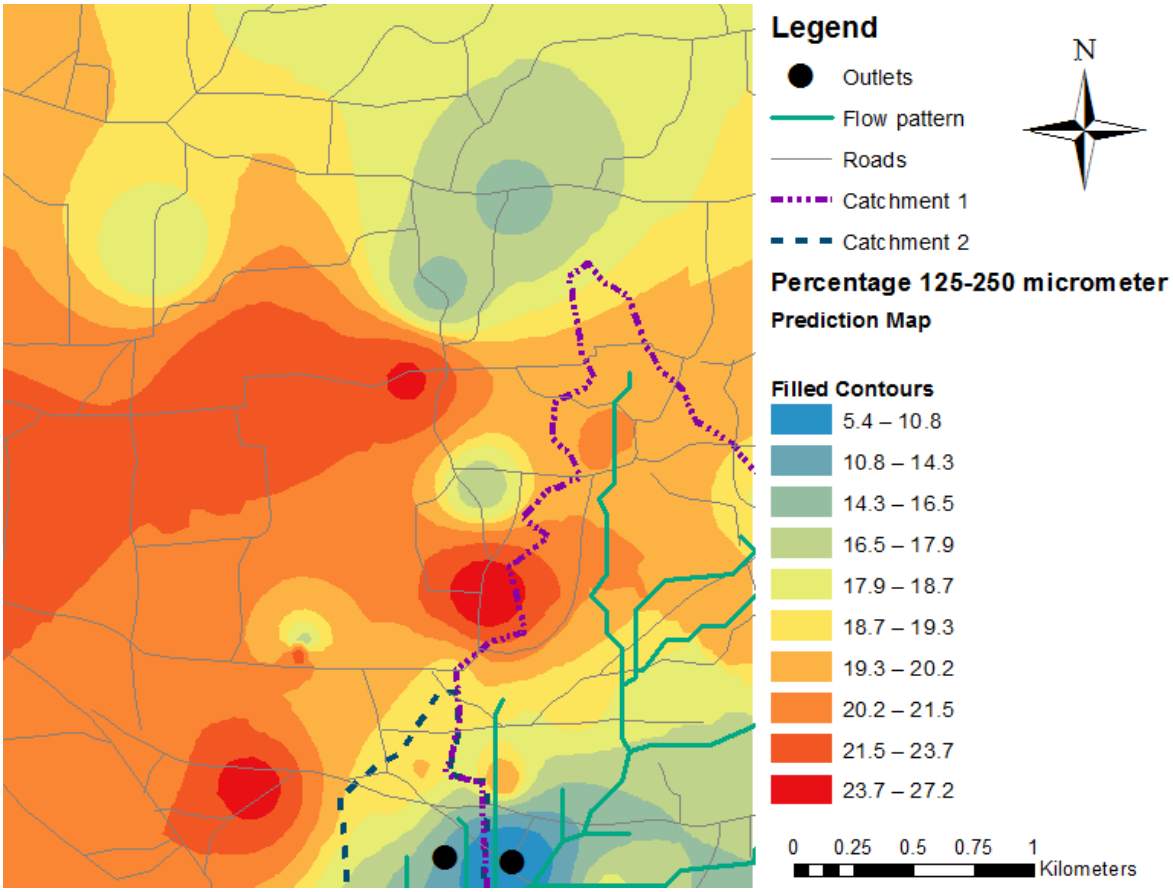

Figure VII-3 *Soil fraction 125-250 μm.*

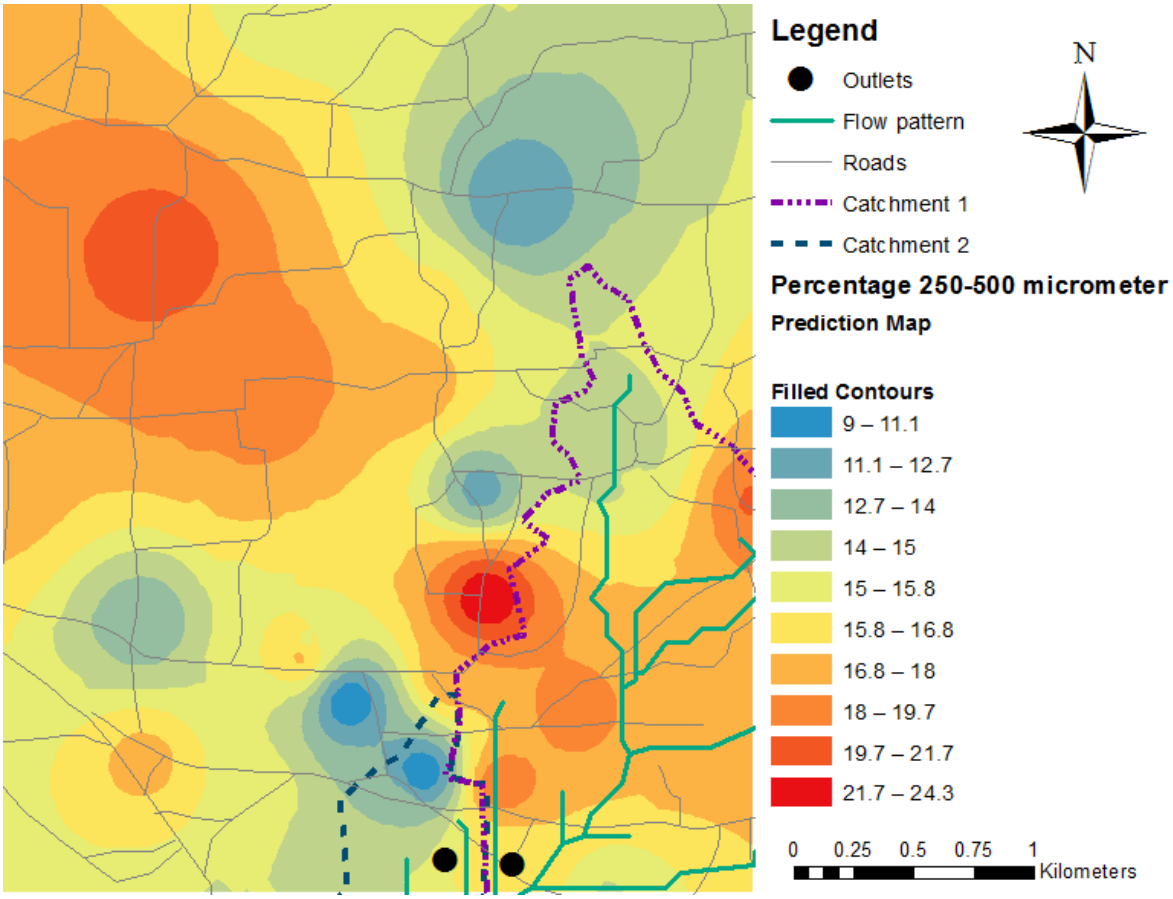

Figure VII-4 *Soil fraction 250-500 μm.*

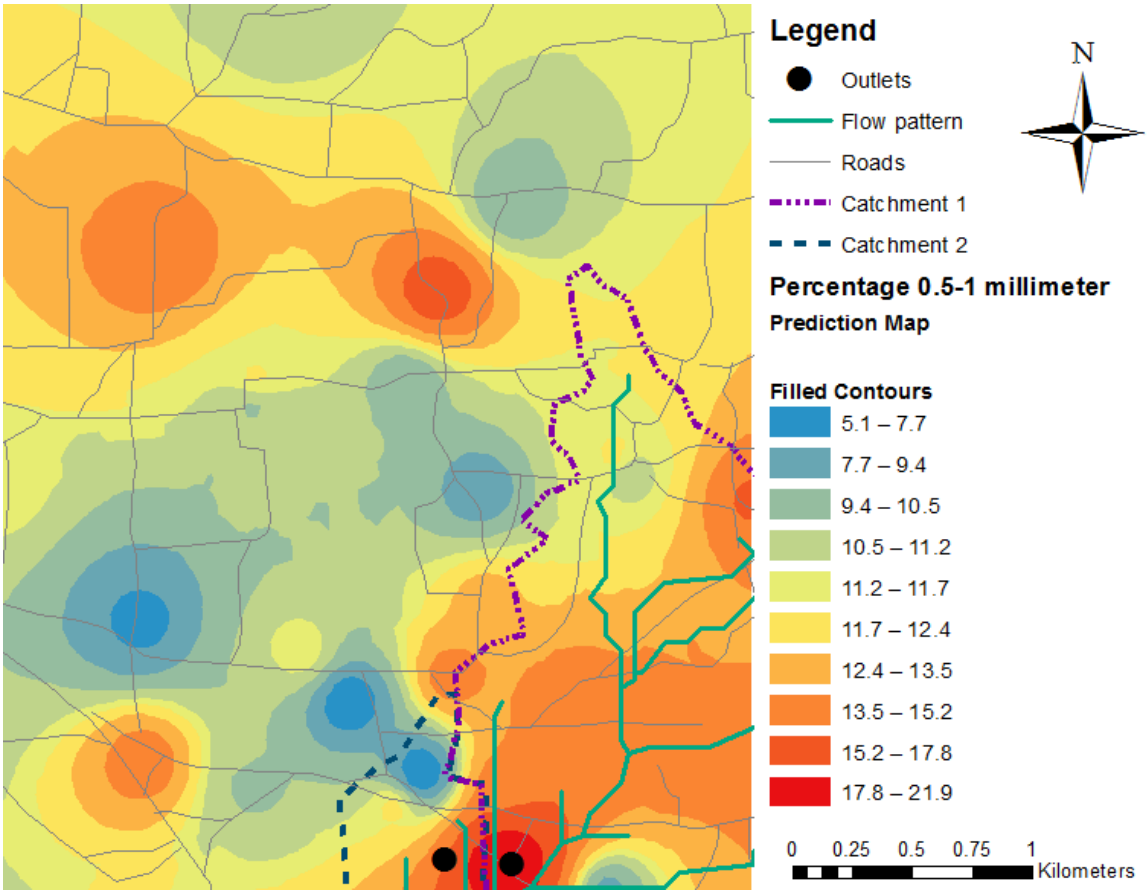

Figure VII-5 *Soil fraction 0.5-1 μm.*

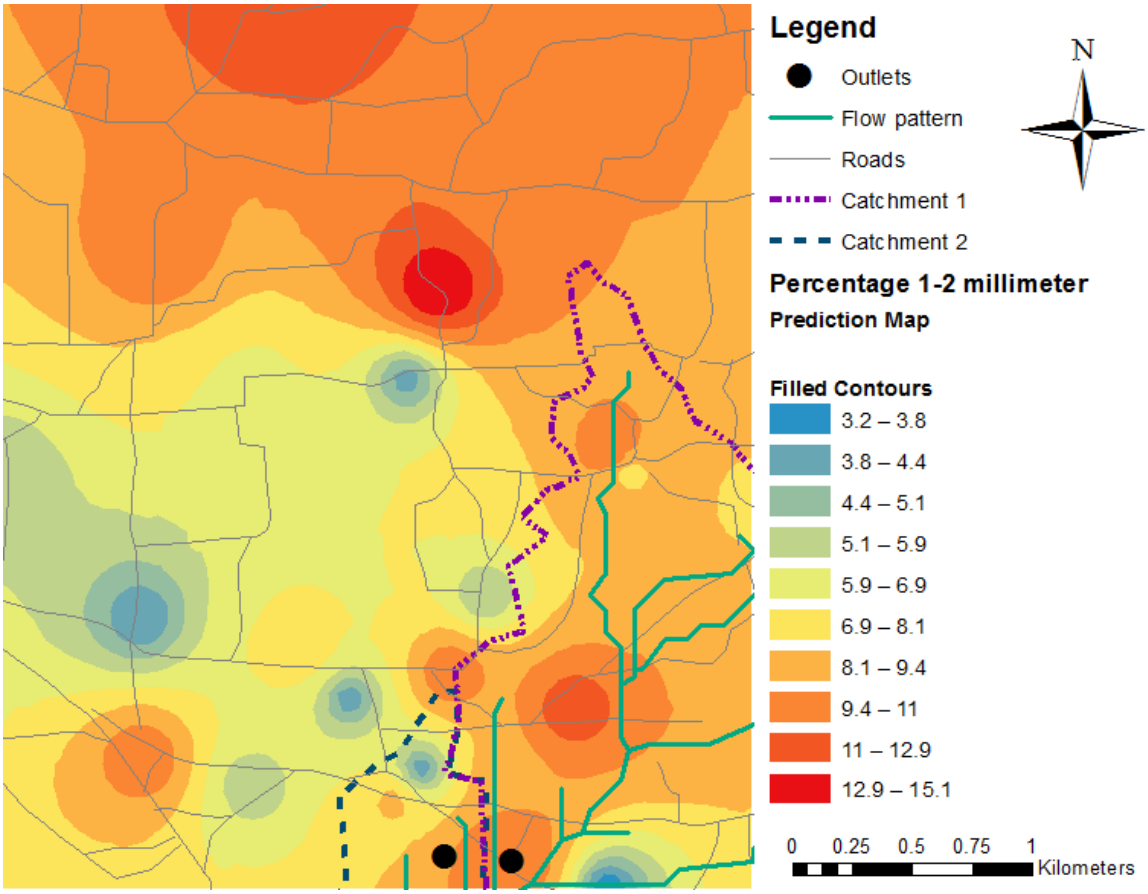

Figure VII-6 *Soil fraction 1-2 μm.*

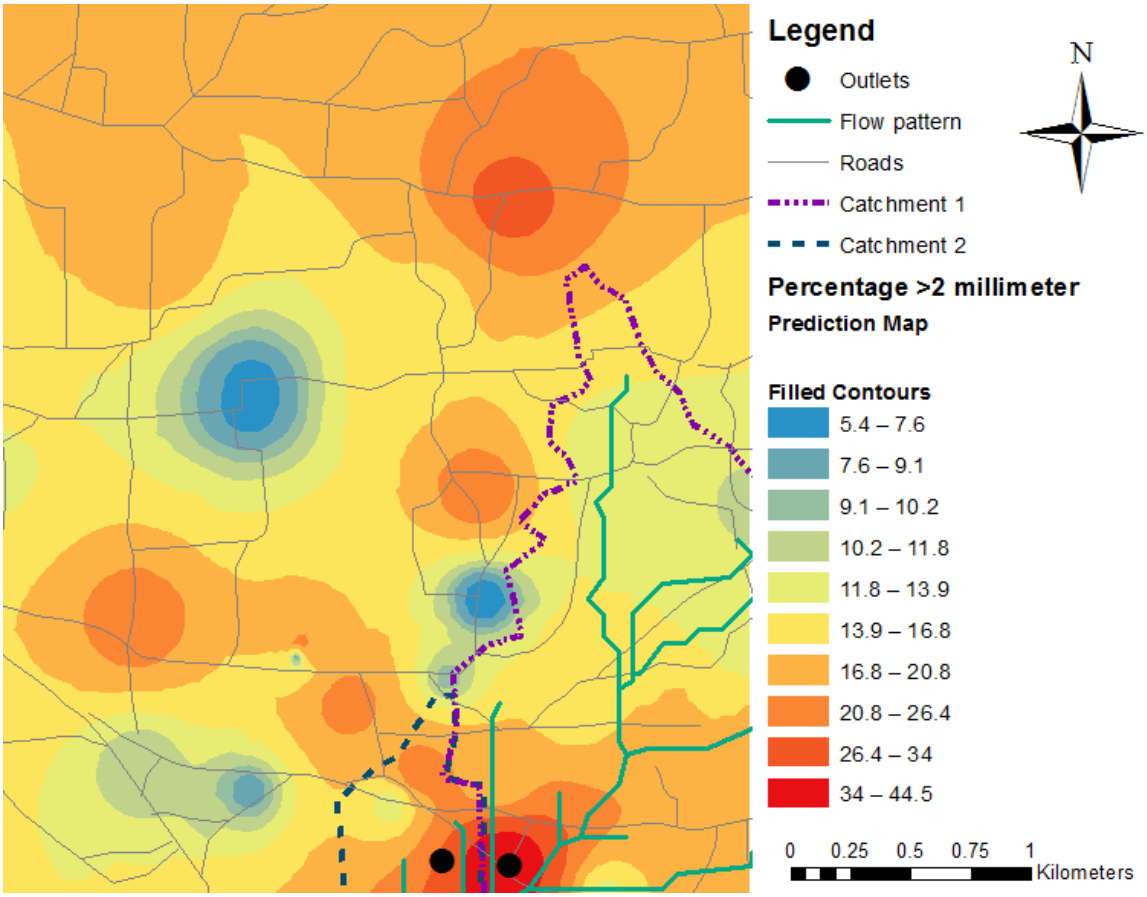

Figure VII-7 *Soil fraction >1 μm.*

Appendix VIII Unit hydrographs

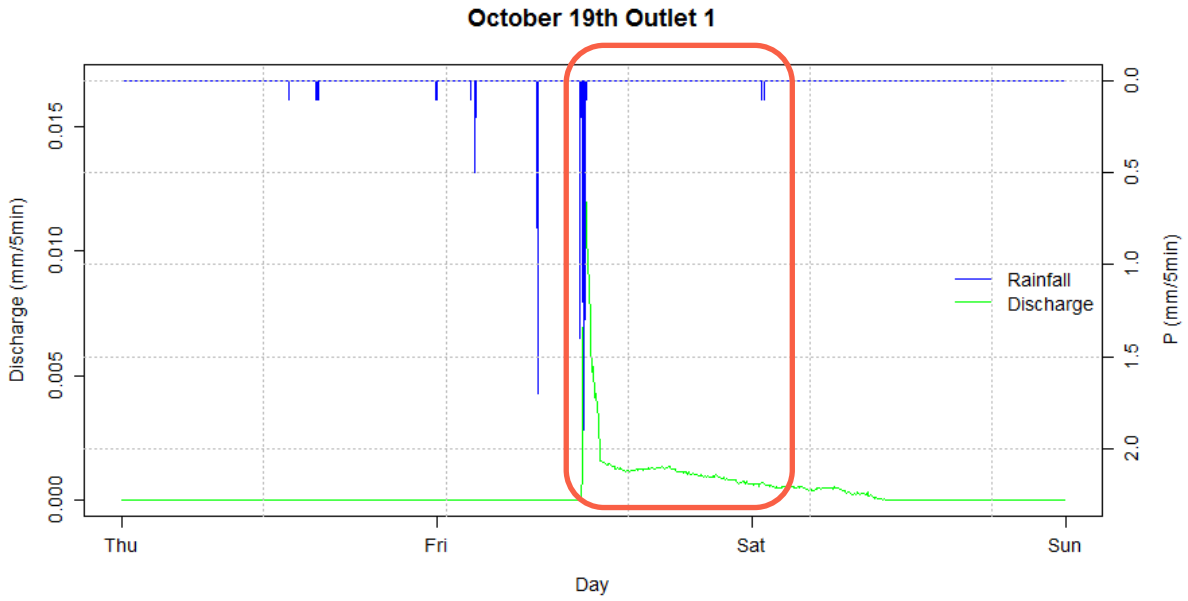

Figure VIII-1 *Unit hydrograph October 19th at outlet 1. Total rainfall sum TB1 is 6.8 mm and total runoff is 0.3 mm.*

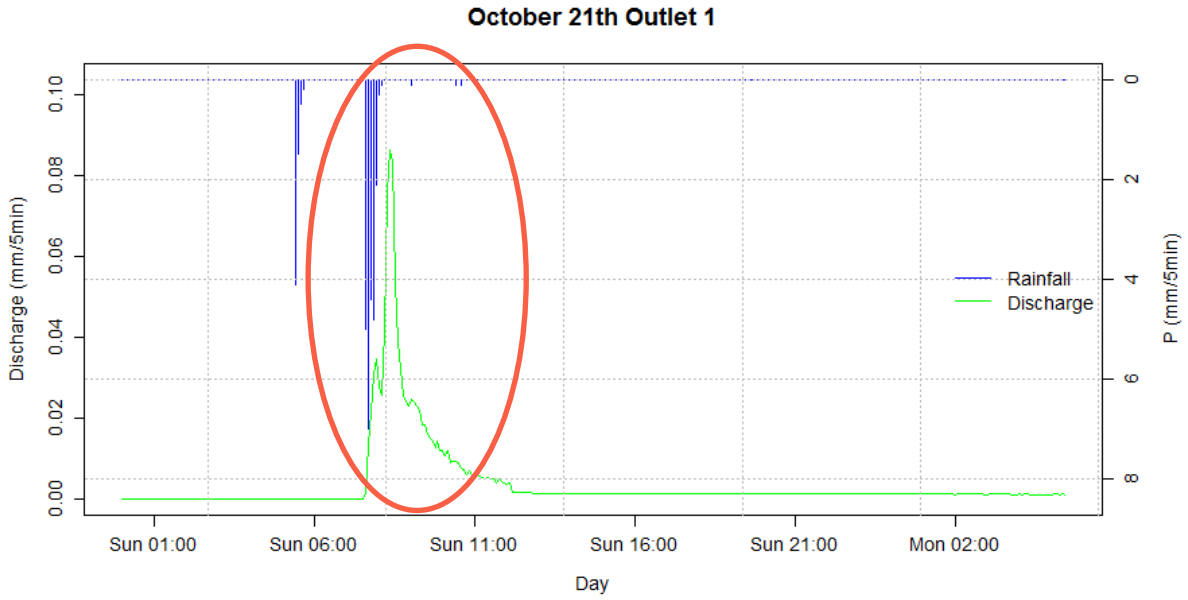

Figure VIII-2 *Unit hydrograph October 21th at outlet 1. Total rainfall sum TB1 is 24 mm and total runoff is 1.3 mm.*

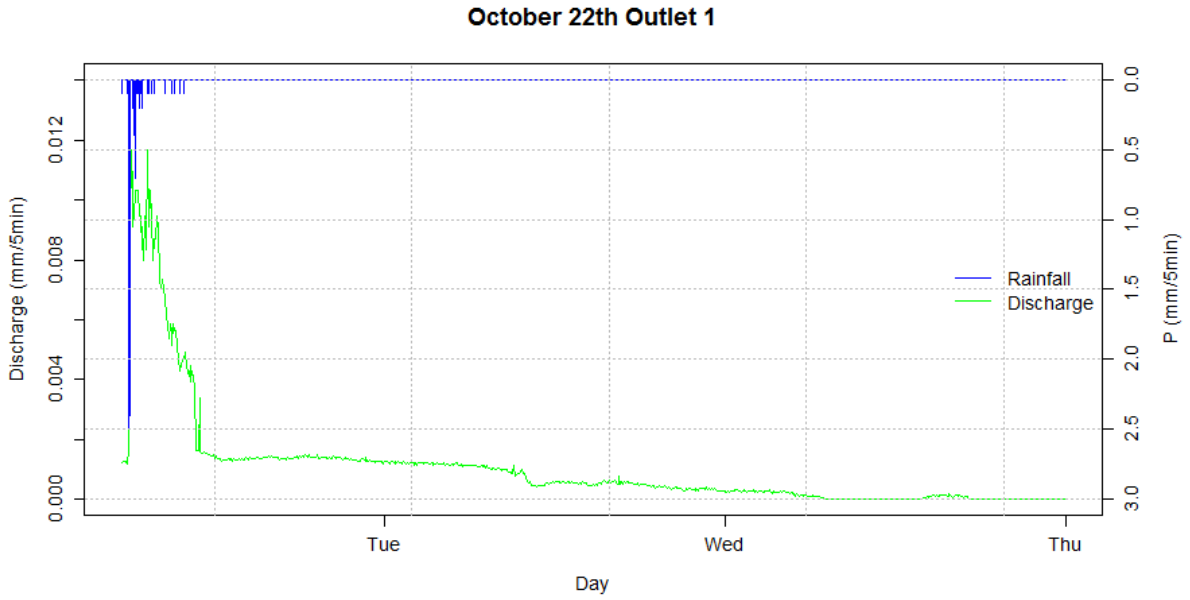

Figure VIII-3 *Unit hydrograph October 22nd at outlet 1. Total rainfall sum TB1 is 8.1 mm and total runoff is 0.9 mm.*

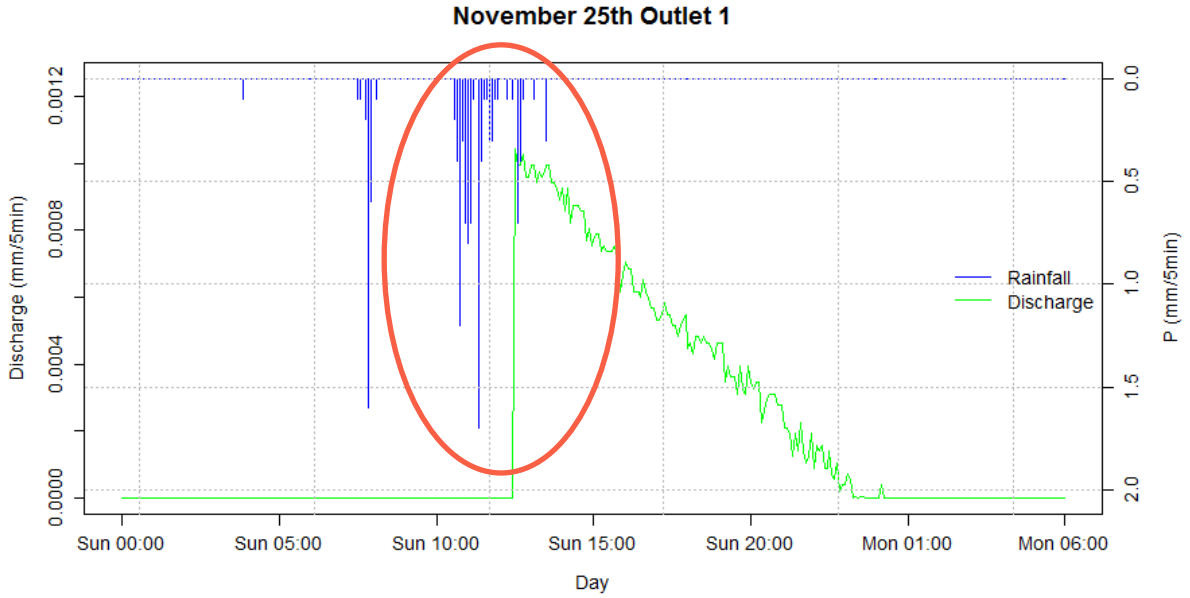

Figure VIII-4 *Unit hydrograph November 25th at outlet 1. Total rainfall sum TB1 is 9.3 mm and total runoff is 0.07 mm.*

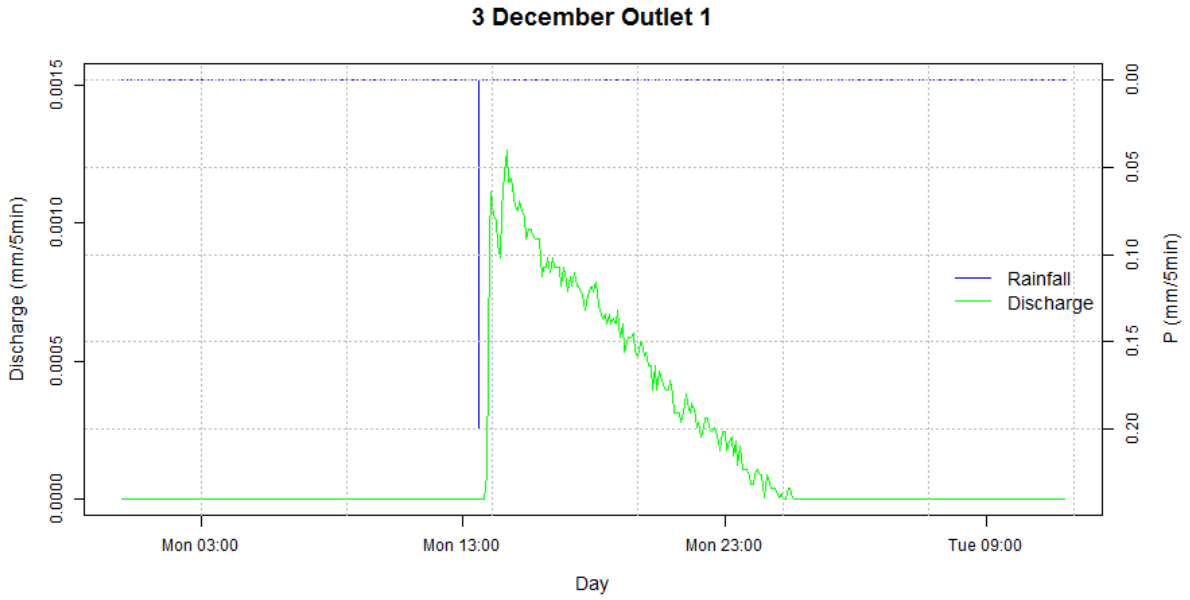

Figure VIII-5 *Unit hydrograph December 3th at outlet 1. Total rainfall sum TB1 is 0.2 mm and total runoff is 0.07 mm.*

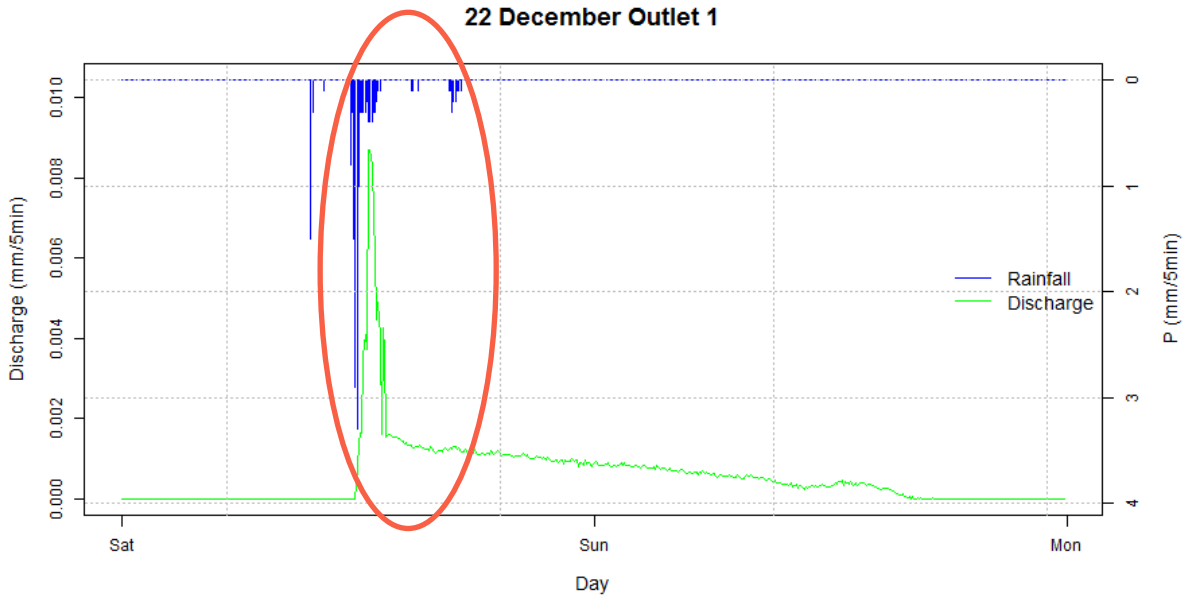

Figure VIII-6 *Unit hydrograph December 22nd at outlet 1. Total rainfall sum TB1 is 14.9 mm and total runoff is 0.3 mm.*

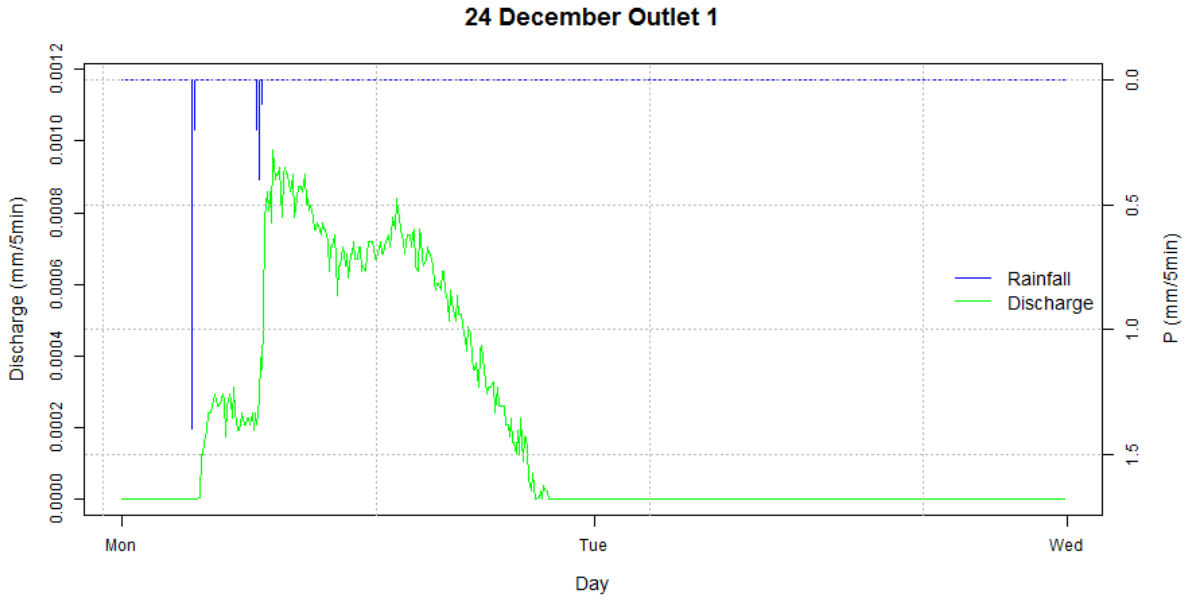

Figure VIII-7 *Unit hydrograph December 24th at outlet 1. Total rainfall sum TB1 is 2.3 mm and total runoff is 0.1 mm.*

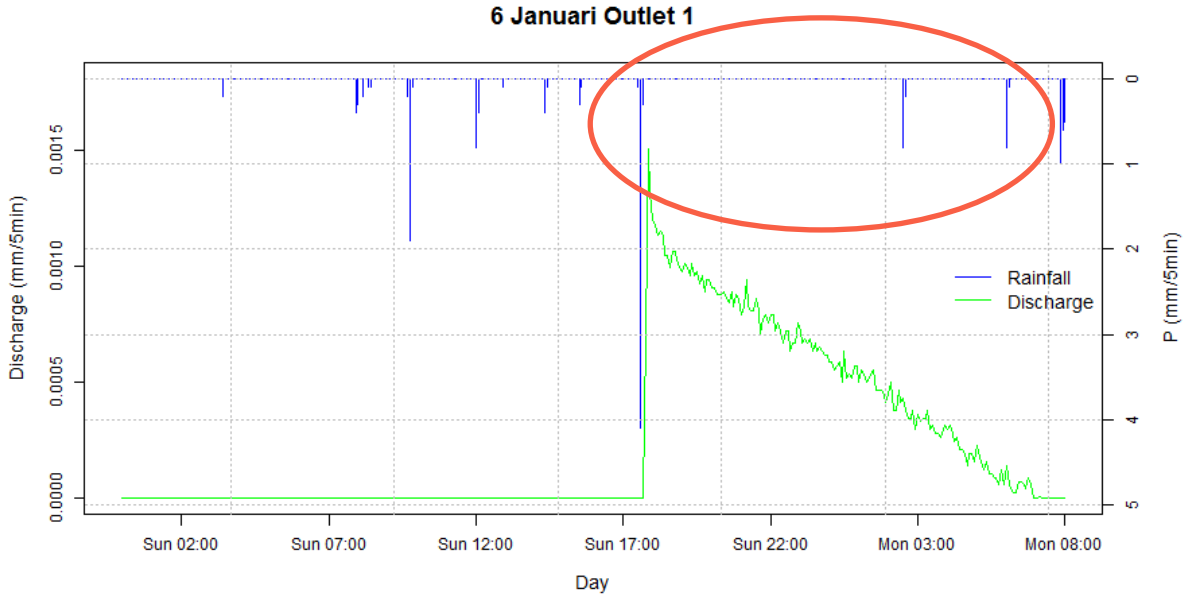

Figure VIII-8 *Unit hydrograph January 6th at outlet 1. Total rainfall sum TB1 is 6.4 mm and total runoff is 0.09 mm.*

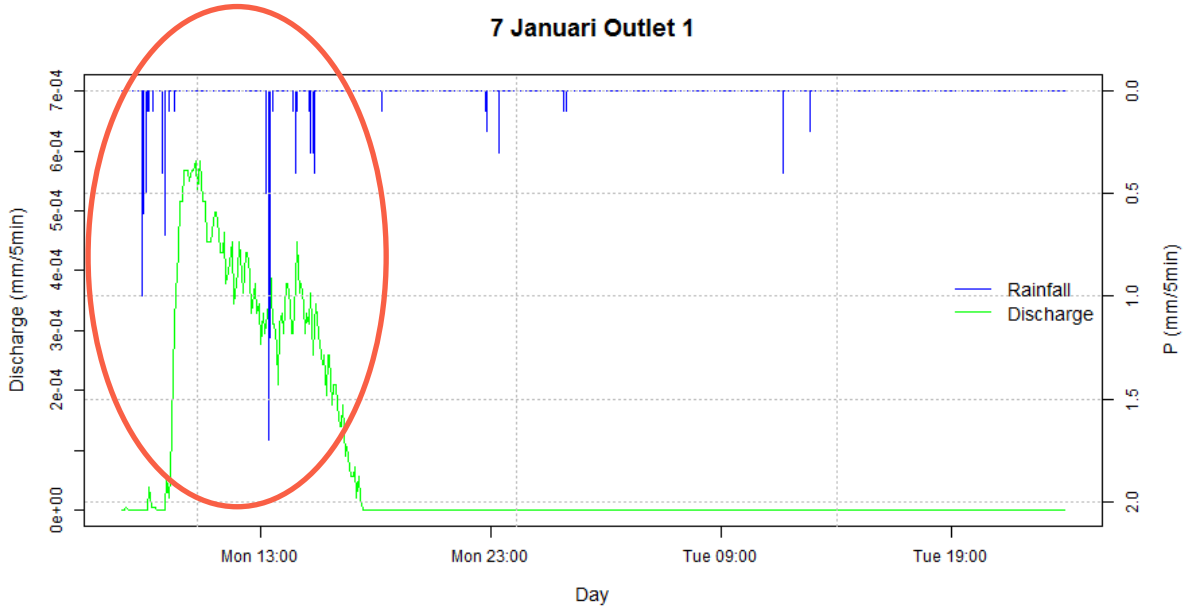

Figure VIII-9 *Unit hydrograph January 7th at outlet 1. Total rainfall sum TB1 is 8.9 mm and total runoff is 0.03 mm.*

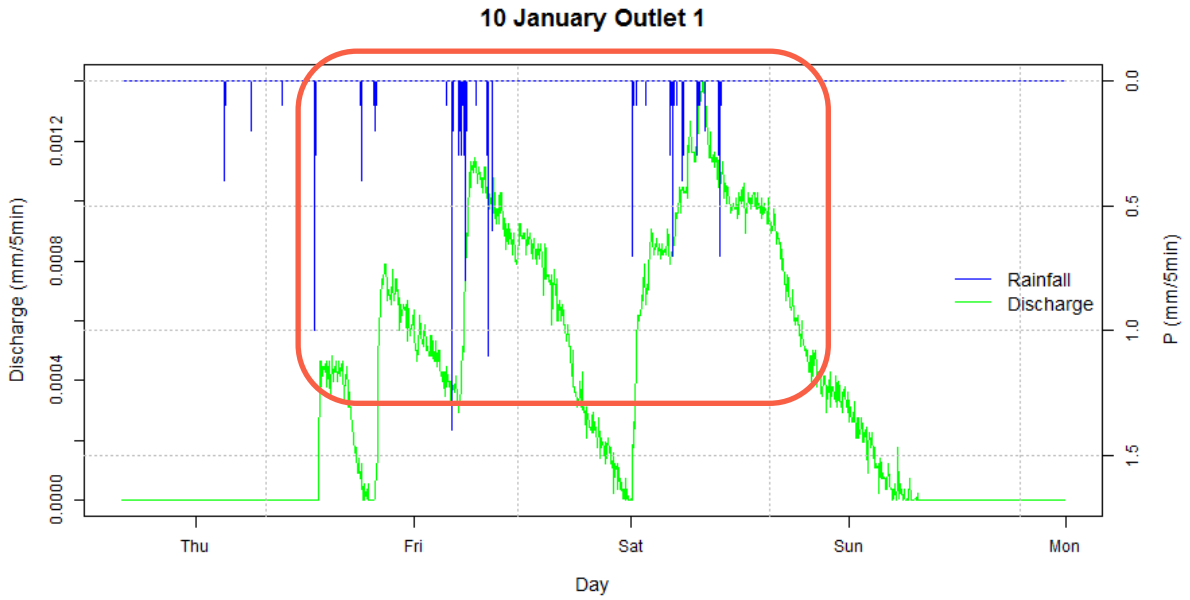

Figure VIII-10 *Unit hydrograph January 10th at outlet 1. Total rainfall sum TB1 is 16 mm and total runoff is 0.5 mm.*

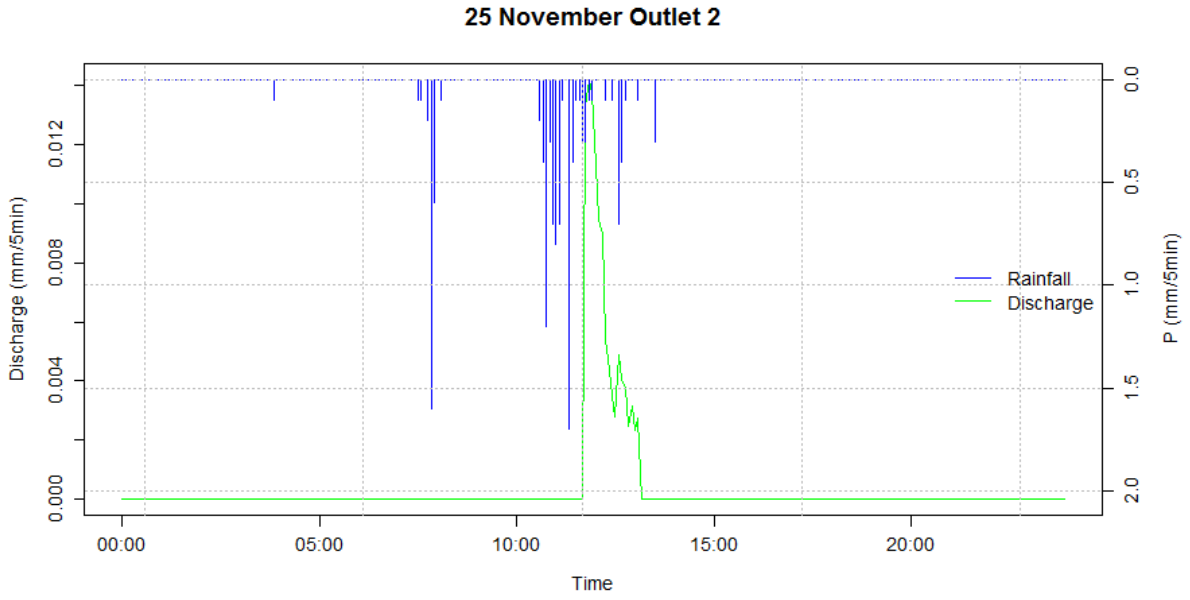

Figure VIII-11 *Unit hydrograph November 25th at outlet 2. Total rainfall sum TB1 is 9.3 mm and total runoff is 0.1 mm.*

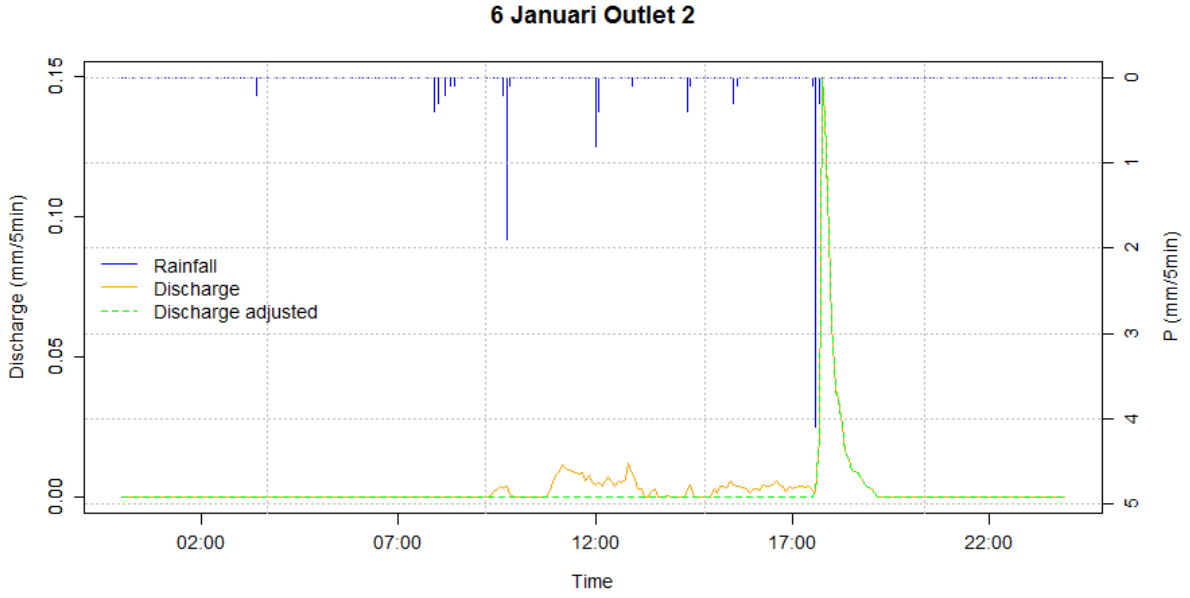

Figure VIII-12 *Unit hydrograph January 6th at outlet 2. Total rainfall sum TB1 is 4.5 mm and total runoff is 0.6 mm.*

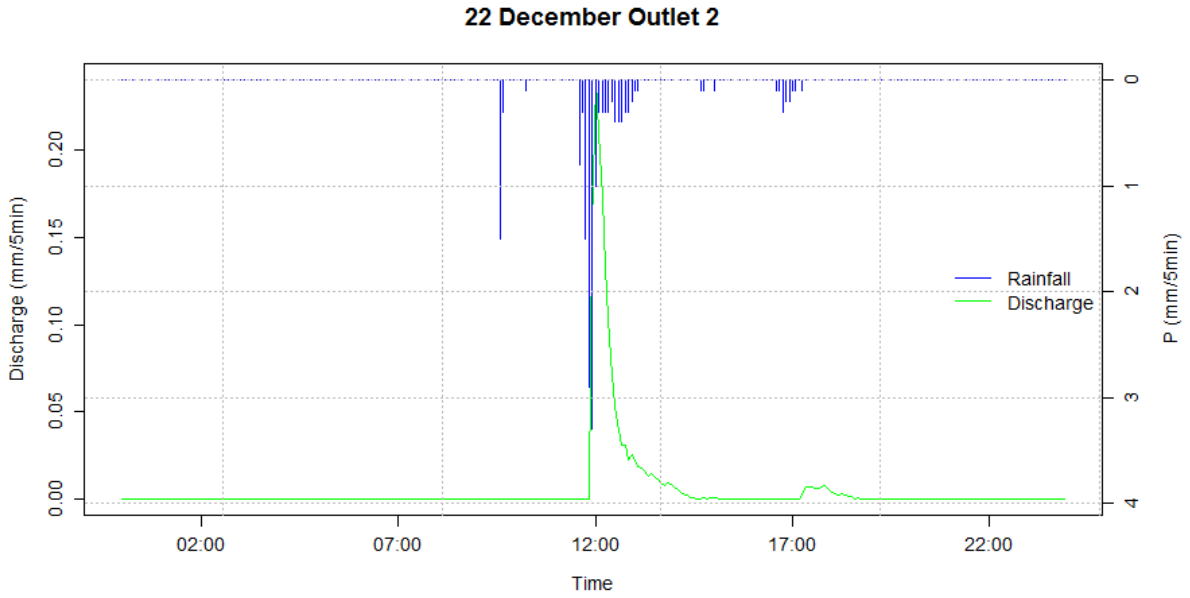

Figure VIII-13 *Unit hydrograph January 22nd at outlet 2. Total rainfall sum TB1 is 14.9 mm and total runoff is 1.5 mm.*

Appendix IX Sediment Load

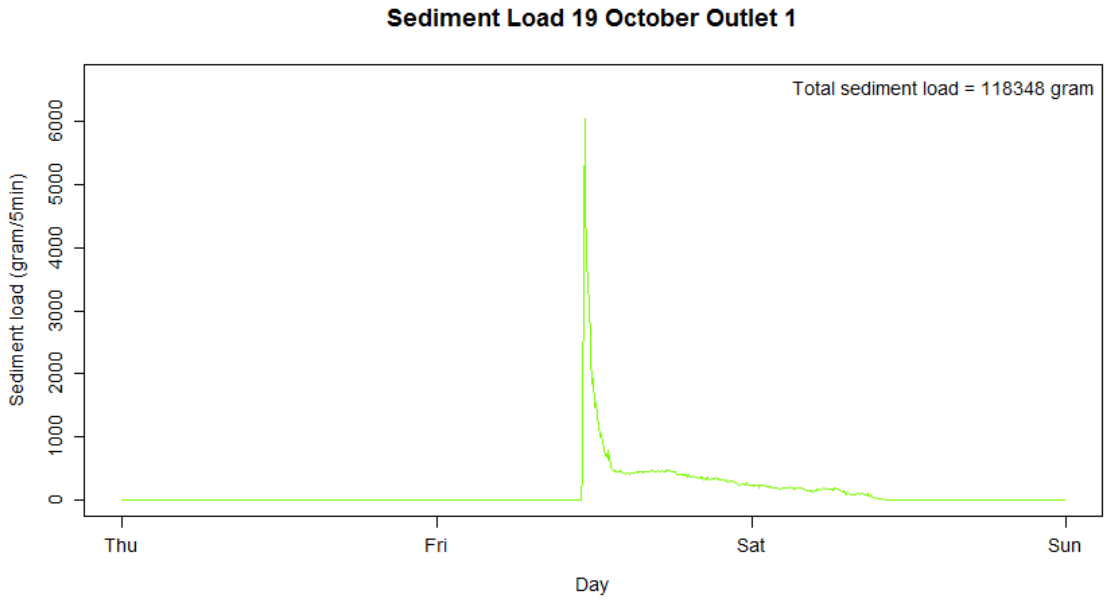

Figure IX-1 *Sediment Load 19 October outlet 1.*

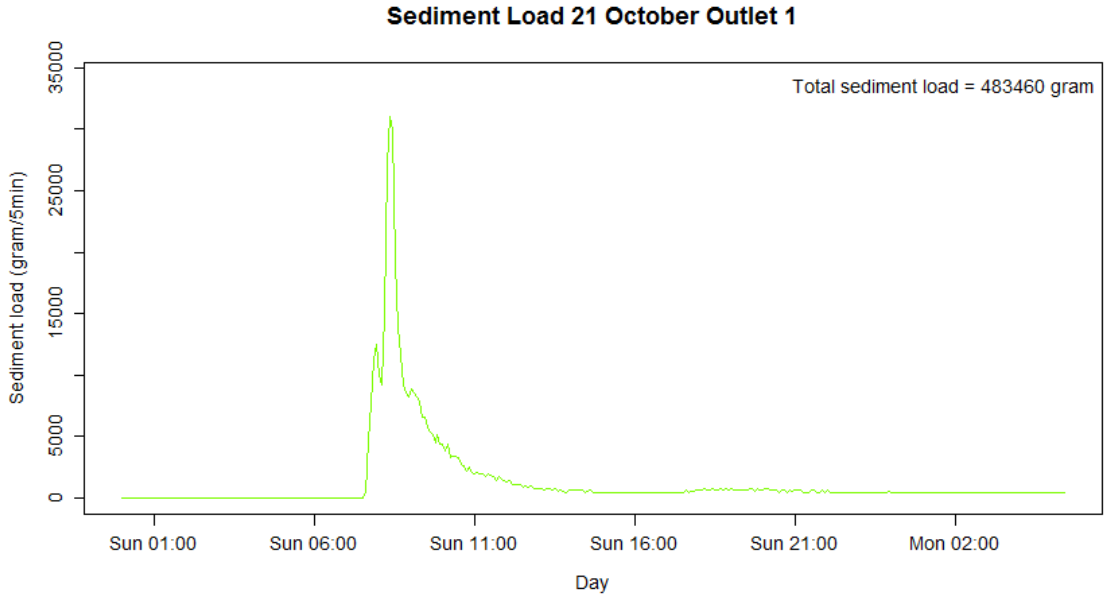

Figure IX-2 *Sediment Load 21 October outlet 1.*

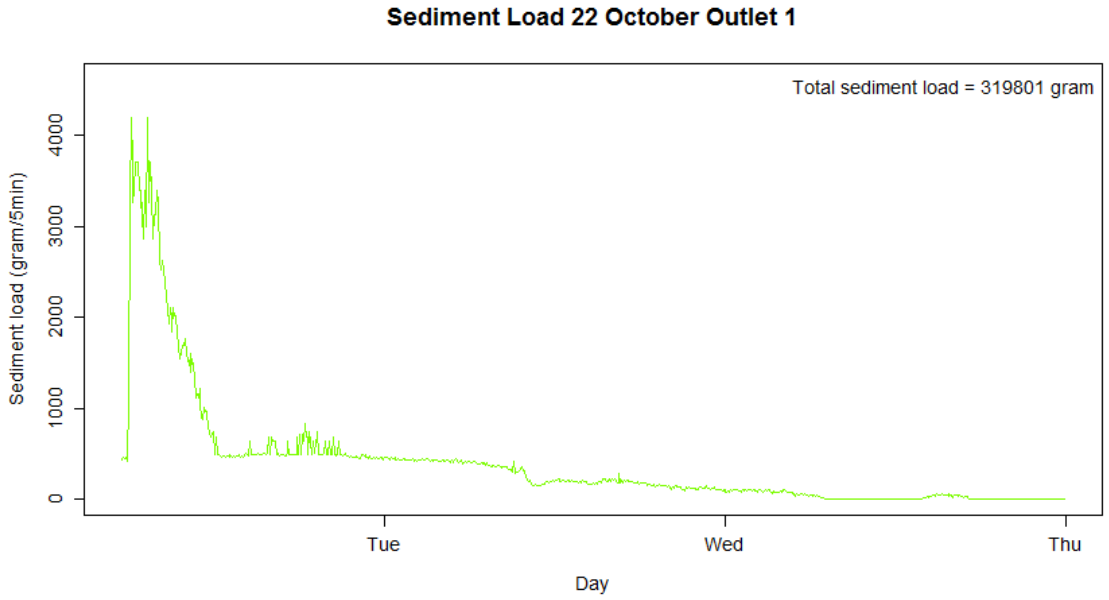

Figure IX-3 *Sediment Load 22 October outlet 1.*

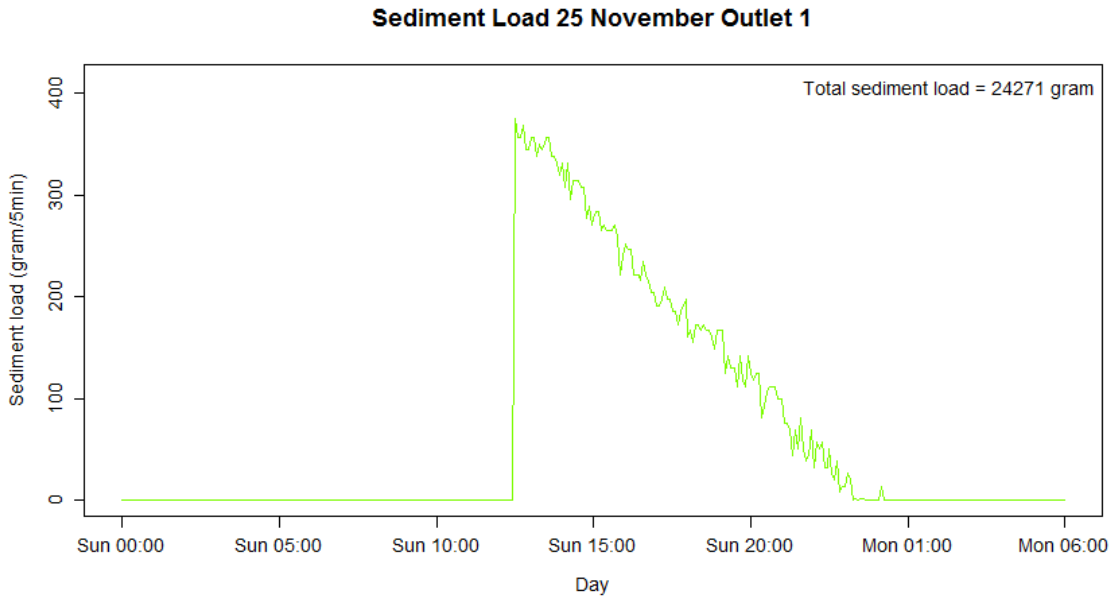

Figure IX-4 *Sediment Load 25 November outlet 1.*

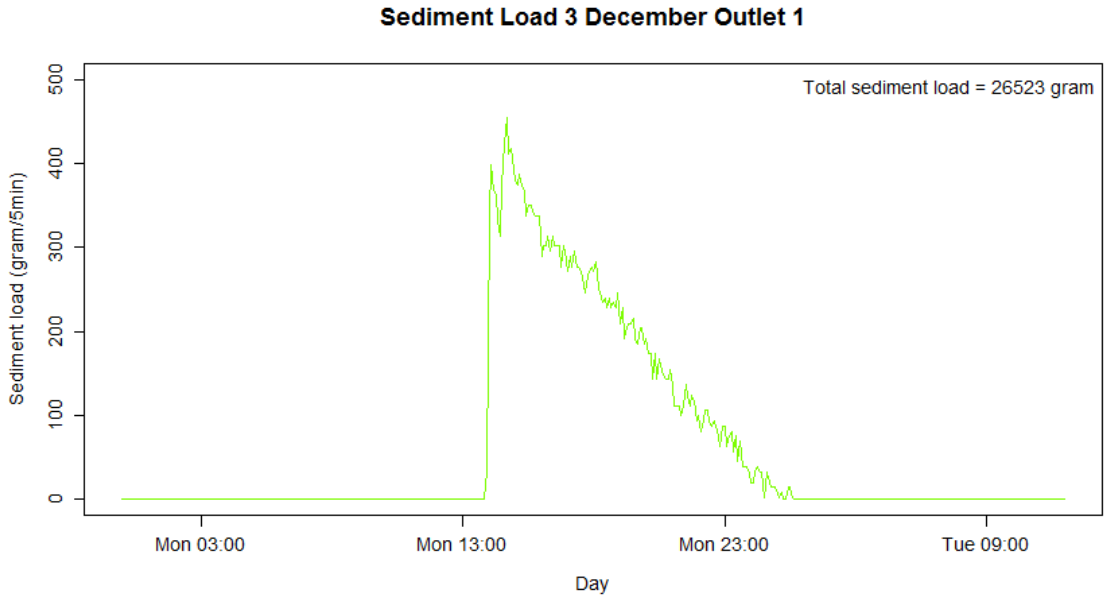

Figure IX-5 *Sediment Load 3 December outlet 1.*

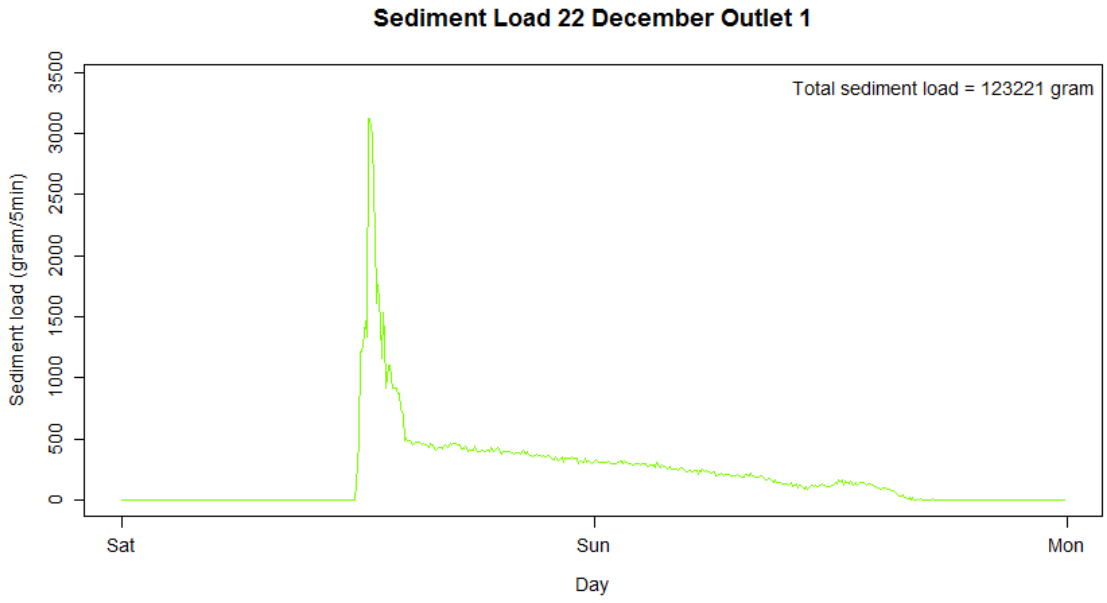

Figure IX-6 *Sediment Load 22 December outlet 1.*

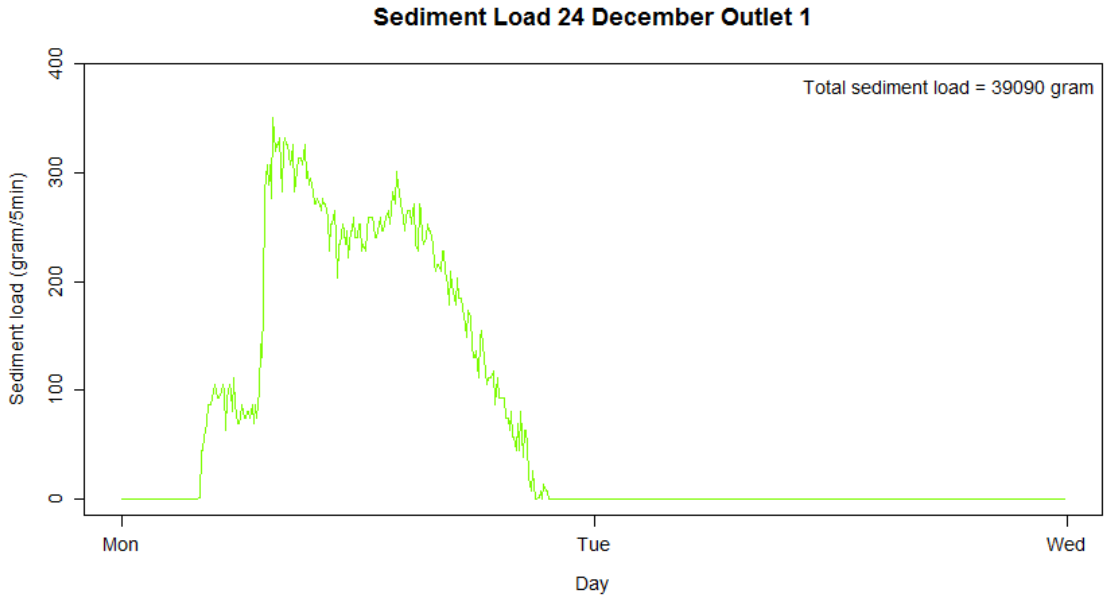

Figure IX-7 *Sediment Load 24 December outlet 1.*

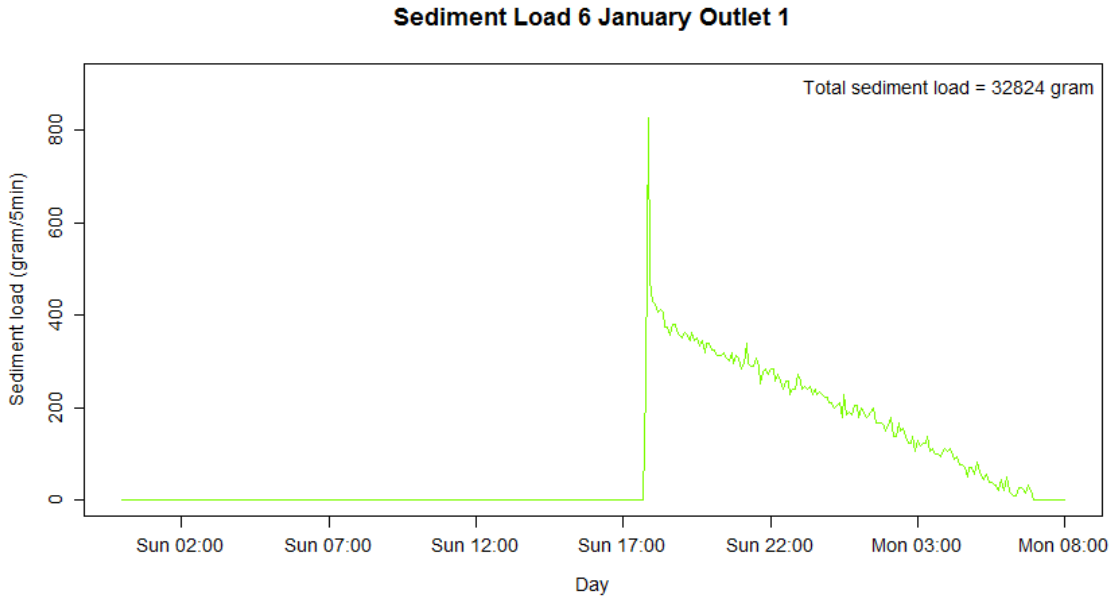

Figure IX-8 *Sediment Load 6 January outlet 1.*

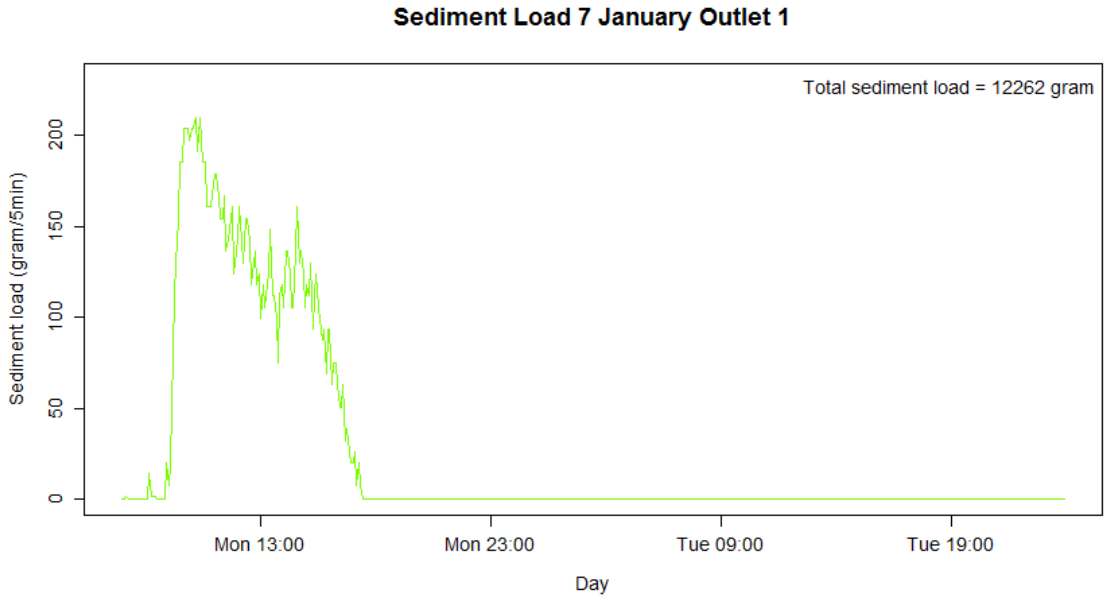

Figure IX-9 *Sediment Load 7 January outlet 1.*

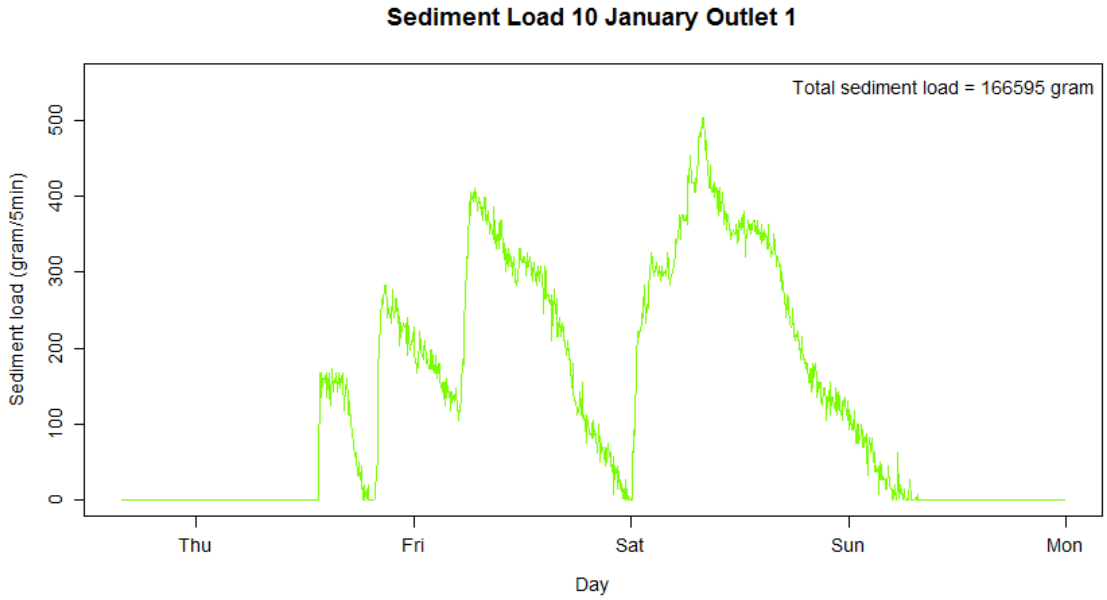

Figure IX-10 *Sediment Load 10 January outlet 1.*

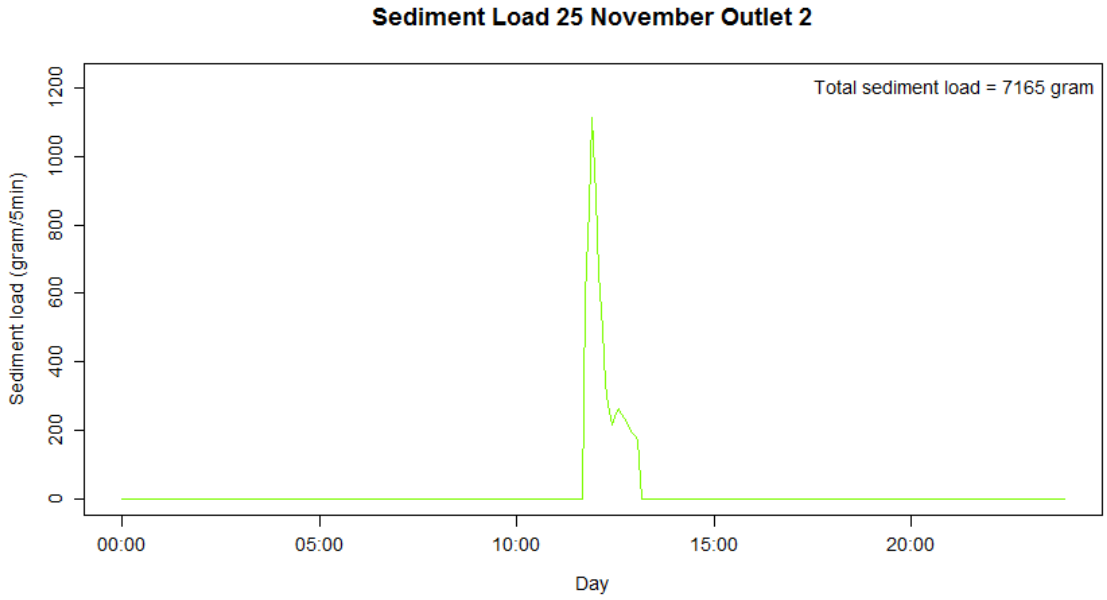

Figure IX-11 *Sediment Load 25 November outlet 2.*

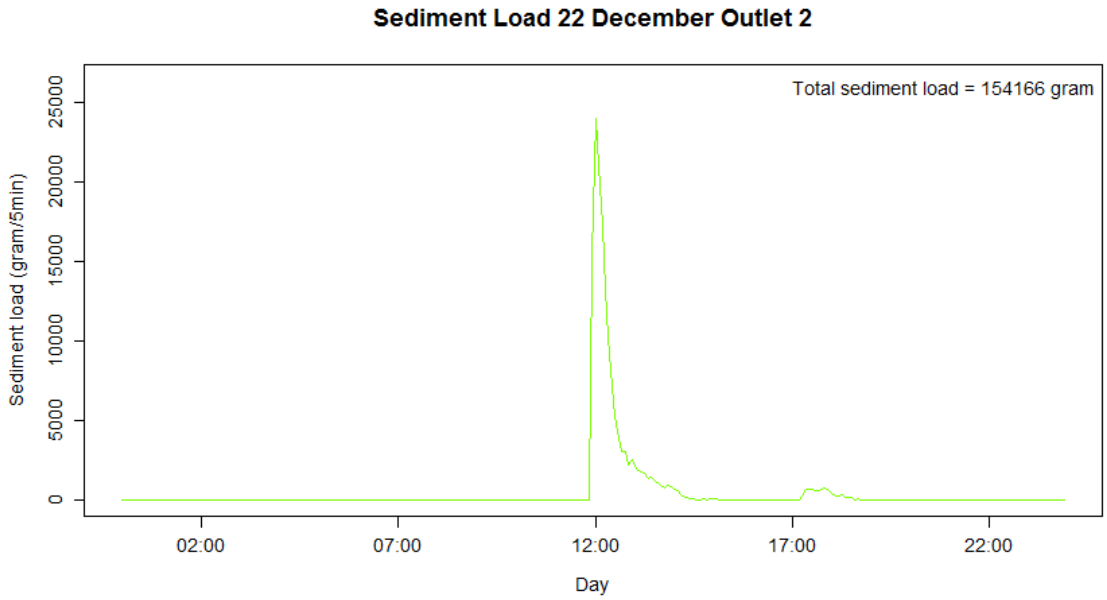

Figure IX-12 *Sediment Load 22 December outlet 2.*

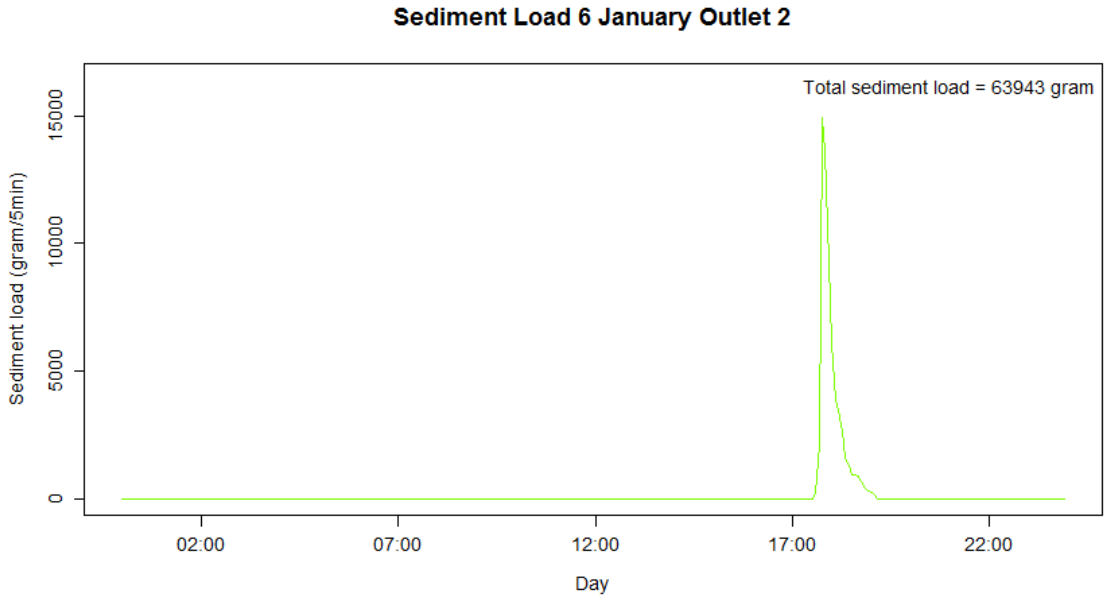

Figure IX-13 Sediment Load 6 January outlet 2.

Appendix X Interview

Kort interview Pedro de Jong

Inspecteur/controleur infrastructuur

Sinds 2005 werkt hij voor de overheid van Bonaire.

Vanaf het mangrove centrum wordt geen diabaas gebruikt, maar rotsen en zand vanuit de zee. Dit materiaal is beter bestand tegen het zoute water. En omdat de weg daar ook omringd word door zout water (mangrove, zee, zoutpannen) is dit nodig. Zout met ijzererst in het gesteente van het Diabaas zorgt voor een snellere verwering van het materiaal, waardoor je veel kleine deeltjes krijgt (stof) dat naar Lac stroomt en dat voor modderige wegen zorgt.

Diabaas = vulkanisch gesteente.

Minstens 1x per jaar wordt er aan de weg gewerkt richting Cai. Ongeveer 10 cm diabaas wordt dan op de weg gestort en aangedrukt. Hiervoor wordt ongeveer 2000 m3 diabaas gebruikt.

Eén keer in de vijf jaar wordt al het materiaal van de weg verwijderd en wordt er een gehele nieuwe laag gestort. Laatste keer dat dit gedaan is in de zomer van 2010.